EXPERIMENTAL INVESTIGATIONS OF NATURAL CONVECTION BOTH IN WATER AND IN MERCURY AT EXTREMELY LOW GRASHOF NUMBERS

by

SHU-CHEN YU
B. S., National Taiwan University, 1973

A MASTER'S THESIS

submitted in partial fulfillment of the

requirements for the degree

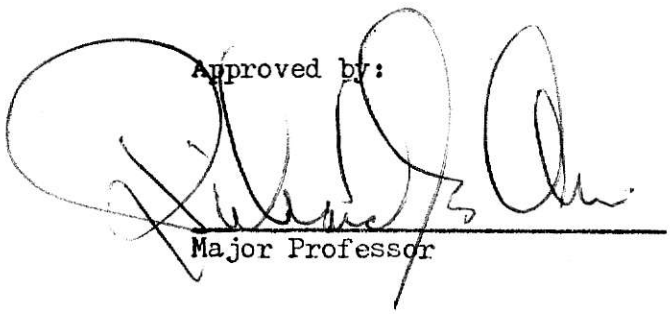
MASTER OF SCIENCE

Department of Chemical Engineering

KANSAS STATE UNIVERSITY
Manhattan, Kansas

1976

Approved by:



Major Professor

THIS BOOK
CONTAINS
NUMEROUS PAGES
WITH THE ORIGINAL
PRINTING BEING
SKEWED
DIFFERENTLY FROM
THE TOP OF THE
PAGE TO THE
BOTTOM.

THIS IS AS RECEIVED
FROM THE
CUSTOMER.

LD
2668
T4
1976
Y8
C.2
Document

TABLE OF CONTENTS

Title	Page
LIST OF FIGURES	iv
LIST OF TABLES	vi
1. INTRODUCTION	1
2. LITERATURE REVIEW	4
(2.1) Isothermal Plate	4
(2.2) Nonisorhermal Plate	13
(2.3) Uniform Heat Flux Plate	16
3. THEORETICAL ANALYSIS	20
(3.1) Boundary Layer Solution	23
(3.2) Perturbation Solution	28
4. EXPERIMENTAL APPARATUS AND PROCEDURE	38
(4.1) Apparatus	38
(4.2) Procedure	42
5. DATA ANALYSIS	46
(5.1) Data Treatment	46
(5.2) Data Error Source	48
6. RESULTS AND DISCUSSIONS	50
(6.1) Reproducibility and Stability of the Experimental Data	50
(6.2) Curve-Fitting Technique	57
(6.3) Dependence of Dimensionless Temperature Profiles on the Vertical Position up the Plate at a Constant Power Level	57
(6.4) Dependence of Dimensionless Temperature Profiles on the Grashof Number at Fixed Vertical Position up the Plate	64
(6.5) Dependence of Dimensionless Temperature Profiles on the Vertical Position up the Plate at Constant Gr_x^*	73
(6.6) Heat Transfer Correlation	80
7. CONCLUSIONS	83
NOMENCLATURE	85
BIBLIOGRAHPY	89

ACKNOWLEDGEMENTS 95

APPENDICES 96

Appendix A Computer Program for Data Reduction 96

Appendix B Copper-Constantan Thermocouple Calibration 100

Appendix C Sample Calculations 103

Appendix D Computer Program for Curve-Fitting 109

ABSTRACT 115

VITA 117

LIST OF FIGURES

	Title	Page
1.	Plate Coordinates	21
2.	Dimensionless Temperature Distributions for Various Prandtl Numbers	26
3.	Dimensionless Velocity Distributions for Various Prandtl Numbers.	27
4.	Comparison of Temperature Profiles for Pr=0.03 When $Gr_L^*=10^7$	35
5.	Comparison of Velocity Profiles for Pr=0.03 When $Gr_L^*=10^7$.	36
6.	Comparison of Temperature Profiles for Pr=0.03 When $Gr_L^*=10^9$	37
7.	Schematic Diagram of the Equipment.	39
8.	Vertical Plate and Thermocouple Probe	40
9.	Probe Driving Mechanism and Container in Constant Temperature Bath	43
10.	Duplicate Runs Made to Check the Reproducibility	51
11.	Duplicate Runs Made to Check the Reproducibility	52
12.	Duplicate Runs Made to Check the Reproducibility	53
13.	Comparison of the Profiles Toward and Away from the Plate	54
14.	Comparison of the Profiles Toward and Away from the Plate	55
15.	Comparison of the Profiles Toward and Away from the Plate	56
16.	Effect of Vertical Position on the Dimensionless Temperature Profiles of Water at $Gr_L^*=1.72\times10^6$	59
17.	Effect of Vertical Position on the Dimensionless Temperature Profiles of Water at $Gr_L^*=3.5\times10^7$	60
18.	Effect of Vertical Position on the Dimensionless Temperature Profiles of Mercury at $Gr_L^*=7.60\times10^6$	61
19.	Effect of Vertical Position on the Dimensionless Temperature Profiles of Mercury at $Gr_L^*=2.56\times10^7$	62
20.	Effect of Vertical Position on the Dimensionless Temperature Profiles of Mercury at $Gr_L^*=1.15\times10^8$	63
21.	Effect of Grashof Number on the Dimensionless Temperature Profiles of Water at x=3/8 inches	65
22.	Effect of Grashof Number on the Dimensionless Temperature Profiles of Water at x=1/4 inches	66
23.	Effect of Grashof Number on the Dimensionless Temperature Profiles of Water at x=1/8 inches	67
24.	Effect of Grashof Number on the Dimensionless Temperature Profiles of Mercury at x=1/4 inches	68
25.	Effect of Grashof Number on the Dimensionless Temperature Profiles of Mercury at x=1/8 inches	69
26.	Effect of Grashof Number on the Dimensionless Temperature Profiles of Mercury at x=1/16 inches	70

27. Effect of Grashof Number on the Dimensionless Temperature Profiles of Mercury at x=1/32 inches 71

28. Effect of Vertical Position on the Dimensionless Temperature Profiles of Water at Gr_x^* 100 74

29. Effect of Vertical Position on the Dimensionless Temperature Profiles of Water at Gr_x^* $2x10^3$ 75

30. Effect of Vertical Position on the Dimensionless Temperature Profiles of Mercury at Gr_x^* 20 76

31. Effect of Vertical Position on the Dimensionless Temperature Profiles of Mercury at Gr_x^* 100 77

32. Effect of Vertical Position on the Dimensionless Temperature Profiles of Mercury at Gr_x^* 400 78

33. Effect of Vertical Position on the Dimensionless Temperature Profiles of Mercury at Gr_x^* $6x10^3$ 79

34. Correlations of Nusselt and Grashof Numbers 82

35. Copper-Constantan Thermocouple (Reference Junction 0^oC) 102

LIST OF TABLES

Title — Page

1. Deviations of Curve-Fitting for Run Number 68 57

1. Introduction

The study of free convection has received much attention in recent heat transfer literature. This is due to the occurance of free convection in many circumstances and the utilization of this phenomenon in a large portion of the heat transfer. Therefore, it is important for an engineer to understand free convection, especially in the time of energy crisis, since by its use we have an efficient way to save energy.

Free Convection Phenomena

Exposing a heated plate to a fluid without any external source of motion results in a temperature gradient and, since the density of a fluid is temperature-depedent, density differences arise. In a gravitational field, such density differences are the cause of buoyancy forces which result in fluid motion. If the motion occurs purely as a result of the heat transport, the process is called "free" or "natural" convection.

In free convection, the fluid motion is governed by the process of heat transfer, and cannot exist independently. Hence, the temperature and velocity fields are a consequence of thermal and mechanical interaction, i.e., the equations of motion and energy are coupled. The interaction between heat transfer and fluid motion causes the free convection process to be more difficult to analyze than similar processes for forced convection.

Applications

Free convection has attracted wide attention due to its application in the design of many forms of industrial and commercial equipment. A hot radiator used for heating a room is one example of a practical device

in which a large portion of the heat is transferred by free convection.

In the fields of aeronautics, atomic power, electronic and chemical engineering, etc., free convection heat transfer has a great number of interesting engineering applications, such as heat transfer from heating and cooling coils, pipe bends, and electrical devices. Free convection flows produced by centrifugal forces are now of practical importance in aeronautics, because many aircraft propulsion systems contain components which rorate at high speed and in which heat is transferred by free convection. In many cases, microelectronic components are mounted on substrates that dissipate the generated energy primarily by free convection. Free convection also plays the chief role in the transfer of heat in air heaters, refrigerators, condensers, and in many forms of heat exchangers, whenever heat is added to or removed from air, water, brines or various other liquids or gases.

Recently, there has been a growing interest in the use of low-melting metals as heat transfer media. Liquid metals are useful high temperature coolants which allow very high heat transfer due to their high thermal conductivity. The theoretical and experimental investigations with mercury have been more extensive than those with other liquid metals, so the present experiment used mercury as one of the working fluids.

Objective of the Present Work

Free convection has developed rapidly within the last few decades. The progress has been most rapid in the analytic work owing to the development of computers. The considerable simplications displayed by early mathematicians have largely given way to solutions by computer, such as the numerical boundary-layer solutions for free convection at large Grashof numbers and

the perturbation solutions for free convection at small Grashof numbers.

Almost all of the free convection work until early 1960 were based on the boundary-layer solutions which represent the asymptotic solutions to the governing partial differential equations as the Grashof number tends to infinity. Free convection cannot be considered as completely understood without the corresponding physical knowledge in the range of moderate and small Grashof numbers. Experimental analyses of free convection in liquid metals and at small Grashof numbers are not numerous. Chang, et al. [7] in 1966 obtained a perturbation solution for laminar free convection along a uniformly heated plate, the first-order deviation from the classical boundary-layer solution was evaluated numerically.

The present work is concerned with laminar flow for the simplest case of a uniformly heated vertical plate immersed in an infinite fluid. The main objective of the experiment is to investigate free convection in water and in mercury at extremely low Grashof numbers and to compare the results with perturbation solutions [7] and Chang's results [6].

2. LITERATURE SURVEY

Natural convection heat transfer has been a quite popular topic since the nineteenth century. Thousands of articles in this field have been published. Although papers are still appearing, the rate of publication has slowed -- the subject has therefore reached a convinient stage for a general review. Chang [5] in his master's thesis has already surveyed most of the publications in natural convection heat transfer from a vertical plate through early 1970. Therefore, the present review will just confine its attention to some of the most important works before 1971 as well as all the recent works between 1971 and 1975. All the literature reviewed are pertinent to laminar free convection on a vertical flat plate under steady state conditions. They are divided into three catagories according to whether the vertical plate is isothermal, uniformly heated, or neither.

(2.1) Isothermal Plate

The earliest study in free convection from a heated vertical plate was by Lorenz [40] in 1881. He started the study by considering the simplest case -- that the surfaces of equal fluid velocity and temperature were parallel to the plate. Although inadequate assumptions were used, his results were in agreement with the then-existing experimental results.

In 1930, Schmidt and Beckmann [57] conducted experiments about three different sized plates. The velocity and temperature profiles were measured at various points along the isothermal plates. They concluded that Lorenz's assumptions were invalid. Later Pohlhausen applied the similarity method, which he had used in 1921 [46], to transform Prandtl's boundary layer equations into a set of ordinary differential equations. He then used the experimental measurements made by Schmidt and Beckmann [57] to obtain a numerical solution of these equations for a single value of the Prandtl

number, namely 0.733 (air). Schuh [58], in 1946, extended Pohlhausen's numerical calculations to higher Prandtl numbers of 10, 100, and 1000, and Sugawara and Michiyoshi [71] obtained the solutions for smaller Prandtl numbers of 0.03, 0.09, and 0.5.

In 1939, Saunders [50] gave a purely theoretical approximate solution for the temperature and velocity gradients near the surface, and compared his results for air with Pohlhausen's [57] and Squire's [68] solutions. Saunders also obtained some experimental data of heat loss from a vertical plate in water and in mercury. He was the first to study free convection in a liquid metal. In 1948, Eckert [15] performed similar experiments as those of Schmidt and Beckmann [57]. The results of both sets of experiments were in good agreement.

In 1953, Ostrach [45] analyzed the free convection flow about a flat plate oriented in a direction parallel to that of the generating body force. He found that the Grashof number was the principal factor of determining the type of flow and Pohlhausen's similarity equations were adequate to describe the boundary-layer type process. The temperature and velocity profiles for eight values of Prandtl numbers ranging from 0.01 to 1000 were computed numerically on the basis of constant body force and constant plate temperature by applying Pohlhausen's similarity equations. The agreement with the experiments using air by Schmidt and Beckmann [57] was, in general, good. Further calculations of the same type have been made by Sugawara and Michiyoshi [70], Sparrow, et al. [66], and Gebhart [23].

With publication of the work by Ostrach, the classical problem might be regarded as completely solved; however, there were other alternative methods proposed, in particular the integral equation method. Following the ideas of Von Karman [82], the usual boundary-layer equations were inte-

grated across the boundary layers, whose thicknesses were assumed to be the same for both velocity and temperature. The velocity and temperature were expressed as a simple polynomial functions of position in order to process further. This method was first used in free convection by Squire [68] in 1938. In 1954, Merk and Prins [42] used more complicated expressions for the velocity and temperature profiles to treat the free convection at the lower stagnant points of the horizontal cylinder. For the special case of vertical plate, they got the equations of Schmidt and Beckmann and showed that the mean Nusselt number was proportional to the one-fourth power of the Grashof and Prandtl numbers. They also compared this with Schmidt and Beckmann's experiments [57]. In 1959, Fujii [21] carried out both a mathematical analysis and an experimental study. In the theoretical analysis, he used the modified integral method to find the approximate solutions for a supplement to Squire's solutions [69]. The experimental results agreed well with Ostrach's theoretical calculations [45].

In 1962, Scherberg [52] investigated free convection in the neighborhood of several types of leading edges. For the isothermal case, the leading edge conditions only affected the relative vertical position of the boundary layers and not their thermal and velocity forms. In 1965, Scherberg [53] extended his previous work in 1962 intensively by determining the free convection from a thermal leading edge region and matching it with the known solutions immediately above the region.

Discrepancies between experimental results and theoretical predictions have already been observed and analyzed by several authors [45,57]. An important difference between theory and experiment is concerned with the temperature required for calculating the various physical properties. It is necessary to decide at what "reference" temperature the physical properties should be evaluated. In 1963, Eichhorn [17] made the measurements of

velocity profiles near a heated plate by particle trajectories. In comparing them with Pohlhausen's [57] and Ostrach's [45] solutions, he observed some disagreement. Eichhorn suggested three causes for the discrepancies. The first one was the inadequacy of the boundary layer discription and was partly explained later by the perturbation solution of Yang and Jerger [87]. The remaining two, namely the influence of the fluid motion inside the boundary layer and the geometry of the leading edge, were explained by Brodowicz [4] in 1968. After a detail discussion, Eichhorn concluded that the best reference temperature was 0.83 times of the surface temperature. In a theoretical paper, Sparrow and Gregg [65] advocated a corresponding figure of 0.62. In 1958, Sparrow in his Ph.D. thesis [61] recommended a weight of 70% of wall temperature and 30% of bulk temperature for free convection with a variable wall temperature.

In 1962, Gebhart [23] investigated the effect of viscous dissipation in the free convection boundary layer close to a vertical plate. He concluded that the effect was small for all Prandtl numbers where the buoyancy force was the only body force. Acrivos [1] in 1962 showed an approximate, but accurate, expression could be obtained for the rate of heat transfer in laminar boundary-layer flows by piecing together certain asymptotic solutions.

One of the important factors affecting the heat transfer rate of free convection is the temperature-density relationship of the convecting fluid, especially if the medium has a maximum density. In 1958, Schechter and Isbin [51] presented both theoretical and experimental analyses of natural convection from an isothermal vertical plate in water at $4^{\circ}C$. A set of similarity, ordinary, differential equations was solved using an analog computer to establish theoretical values, which agreed reasonably well with

the measured values. Goren [26] in 1966 also used the analog computer to solve the same problem as Schechter and Isbin [51]. The results indicated that the magnitudes of the convective currents and heat transfer rate in water were significantly reduced from those at $20^{\circ}C$.

Another important factor in natural convection is the occurance of a phase change (such as melting) at the solid-liquid interface. The change of phase induces an interfacial velocity which may distort the flow field and therby affect the heat transfer rate. In 1967, Vanier and Tien [80] extended Goren's work [26] to cover the effects of maximum density and melting on natural convection heat transfer from a vertical plate. The digital computer was used to give the solutions. The boundary-layer equations were solved for the range of temperature $0^{\circ}C \leq T_w \leq 35^{\circ}C$, $0^{\circ}C \leq T_{\infty} \leq 20^{\circ}C$ in a consistent manner. They showed that the heat transfer coefficients obtained by Goren [26] were too low.

So far most of the laminar free convection work has been based on Prandtl's boundary layer equations which are valid only at large Grashof numbers. The boundary layer equations are the asymptotic representations of the Navier-Stokes, energy, and continuity equations as the Grashof number approaches infinity. In 1964, Yang and Jerger [87] first suggested applying the perturbation technique to laminar natural convection in the range of moderate Grashof numbers. This approach had already been utilized by Kuo [38] in 1953 in dealing with incompressible forced convection past a horizontal plate at moderate Reynolds numbers.

In 1964, Yang and Jerger [87] used Pohlhausen's classical boundary-layer solutions as the zero-order approximations for the laminar natural convection from an isothermal plate, and calculated the first-order perturbations for Prandtl numbers of 0.72 and 10. Their theoretical results predicted local velocity and temperature profiles which agreed better with

the experimental data of Schmidt and Beckmann [57] than those of the pure boundary layer solutions. In 1965, Suriano, Yang, and Donlon [72] studied the laminar free convection along an isothermal vertical plate at extremely small Grashof numbers by the perturbation series expansion with the Grashof number itself as the perturbation parameter. The perturbation functions up to second-order approximations were calculated numerically for Prandtl numbers of 0.72 and 10. It was found that the leading edge effect became more and more significant as the Grashof number decreased. In 1968, Suriano and Yang [73] extended their previous work in 1965 to small and moderate Grashof numbers.

Cheesewright [8] in 1966 did an experimental investigation, and found that the existing similarity solutions for free convection from a vertical plate in isothermal surroundings did not provide a satisfactory description for nonisothermal conditions. In 1967, Cheesewright [9] presented a theoretical analysis of free convection in nonisothermal surroundings. Yang's procedures [85] were followed to derive the necessary conditions for the existence of a similarity transformation. The numerical solutions of the ordinary equations were obtained for the special case of isothermal plate. The results indicated that some variations in surrounding temperature might lead to reversal flow because the temperature in part of the boundary layer was less than outside the boundary layer. This phenomena could explain the unusual results of Tritton [78].

In 1967, Tien [76] used the integral method to study the laminar free convection from both isothermal and nonisothermal plates to a power-law fluid. In 1969, Tien and Tsuei [77] obtained an approximate solution for laminar free convection heat transfer between an isothermal plate and a fluid whose rheological behavior was characterized by Ellis' model. The results were compared with the available experimental data.

In 1968, Sparrow and Guinle [67] investigated the deviations from classical boundary layer theory at small Prandtl numbers. It was shown that for very low Prandtl numbers, the Grashof number should be quite large in order for the classical boundary layer results to be applicable. In the same year, Cygan and Richardson [13] applied a transcendental approximation to the velocity and temperature profiles to obtain integral solutions of free convection at small Prandtl numbers.

Nishikawa and Ito [44] in 1969 theoretically studied the laminar free convection from an isothermal plate to fluids at supercritical pressures, and they also took account of the temperature dependence of all the physical properties. Yung and Oetting [89] in 1969 investigated the effects of angular position on the free convection from an isothermal plate moved from the vertical through three inclined positions to the horizontal. Results of these tests showed good agreement with previous investigations [9,49,57].

Kuiken [36] in 1969 developed a method, using the singular perturbation technique described in the book of Van Dyke [79], to solve the first- and second-order perturbation equations by matching the inner flow (boundary-layer flow) to the outer flow (inviscid flow).

After 1971, most of the papers in laminar free convection from a vertical plate were about the correlations of the Grashof, Nusselt, and Prandtl numbers. Gryzagoridis [27] in 1971 carried out an experimental investigation of free convection in the low Grashof number ranges. The results suggested that the empirical power law, $Nu=0.555(GrPr)^{\frac{1}{4}}$, recommended by Schlichting [56] for the Grashof number ranges of 10^5-10^8 could be used with sufficient accuracy in the laminar ranges of 10^1-10^8. In 1973, Gryzagoridis [28] experimentally studied the leading edge effects on Nusselt number. The local heat transfer rates showed excellent agreement with those obtained by Eckert and Drake [16] for $Gr > 10^4$, and the departure at small Grashof numbers was

due to the fact that they did not account for the flow that started ahead of the plate. In 1975, Grazagoridis [29] investigated laminar free convection from a vertical plate with external assisting flow. First, he used hot wire anemometry to obtain velocity and temperature profiles, and the heat transfer rates were deduced from temperature profiles. The experimental data for the purely free convection case were compared with Ostrach's theoretical values [45]. Second, he used interferometer to obtain local heat transfer rates. For the purely free convection case, the local Nusselt numbers were compared with his previous data [28]. Both comparisons showed good agreement.

In 1971, Bottemanne [3] extended the results of Schmidt and Beckmann [57] for thermal free convection in air to the case of thermal free convection in air simultaneously with evaporation of water. Theoretical results were given for the case of Pr=0.71, Sc=0.63, and equal directed body force. His experimental data showed close agreement. Therefore, he concluded that the theory, based on a simple physical model that treated the two buoyancy effects as mutually indenpendent and additional forces, was sufficient to describe simultaneously heat and mass transfers.

In 1972, Lienhard, Eichhorn, and Dhir analyzed laminar free convection[39] for cases in which gravity varied with the distance from the leading edge of an isothermal plate. By extending the Squire-Eckert integral method, they developed a general integral method to account for arbitrary position-dependence of gravity. The series solutions they obtained provided a method for predicting the velocity and temperature distributions on a plate subject to a general variation of gravity $g=g(x)$. In the same year, Prasad and Ramanathan [47] investigated experimentally the effect of longitudinal oscillations on free convection heat transfer from a heated vertical plate. The results were presented in terms of the local Nusselt number, Grashof number, and vibrational Reynolds number. Their results lay in the steady combined forced and free

convection regime.

In 1973, Churchill and Ozoe [11] constructed a correlation of local Nusselt, Prandtl, and Rayleigh numbers. The correlations were identical for the cases of uniformly heated and uniform wall temperature plates except for different constant coefficients. In 1973, Hardwick and Levy [30] did, both theoretically and experimentally, the same study as Yang [86] except they used an isothermal plate rather than a uniform-heat-flux plate. In the theoretical analysis, they formulated the equations of motion and heat transfer in the near weak region and solved them by finite difference technique. Numerical results were obtained for a Prandtl number of 0.72 and five different values of Grashof numbers ranging from 10^6 to 10^8. The temperature and velocity profiles were also measured experimentally. The theoretical and experimental results indicated that the influence of the wake caused the velocity profiles near the top of the plate to be different from those obtained by the boundary-layer equations.

On the basis of the first two terms in the boundary layer expansion, Hieber [32] in 1974 found the leading edge effect upon the total heat transfer rate was given by $0.625k(T_w-T_\infty)$, and the average Nusselt number for the semi-infinite plate was given by $Nu=0.476Gr_x^{\frac{1}{4}}+0.625+O(Gr_x^{\frac{1}{12}})$ at a Prandtl number of 0.72. On the basis of recent analyses of the trailing edge region for the forced-flow problem, he expected the finite-plate effects contributed a term of $O(Gr_x^{1/16})$ to the average Nusselt number. In 1973, Wilks [83] solved numerically the similarity equations for Prandtl numbers of 0.1, 0.72, 1, 10, 100, and a range encompassing the transition from a purely forced convection to a purely free convection. The numerical solutions of temperature and velocity profiles were represented graphically. The results indicated that as the Prandtl number decreased buoyancy effects were increased in velocity profiles and there was a overshot at the lower end of the range. Vibrations in temper-

ature profiles were far less pronounced over the range of Prandtl numbers.

In 1975, Churchill and Chu [10] developed a simple expression for the mean Nusselt number for all Rayleigh and Prandtl numbers in terms of the model of Churchill and Usagi [12]. The expression was applicable to uniform heating as well as to uniform wall temperature, and for mass transfer and simultaneously heat and mass transfer. This correlation provided a basis for estimating transfer rate for non-Newtonian fluids and for inclined plates.

(2.2) Nonisothermal Plate

Up to 1955, all the work presented were concerned with the isothermal plate. Sparrow in 1955 [62] formulated the boundary layer equations for laminar free convection by the Von Karman-Pohlhausen integral method for some prescribed variations of wall heat flux and wall temperature. The approximate solutions were achieved by series expansion in the range of 0.01 to 1000 for the Prandtl number. In 1958, Sparrow and Gregg [64] again presented an analysis of laminar free convection from a vertical plate having nonuniform surface temperature. Numerical solutions were carried out for Prandtl numbers of 0.7 and 1.0.

In 1956, Finston [19] observed that the transformation given by Pohlhausen for isothermal plate belonged to a family of similarity transformations, in which the plate temperature was a function of the distance along the plate. He also showed that under the boundary-layer theory assumptions, the problem of free convection past a vertical plate had an exact solution if the plate temperature was proportional to a power of the distance from the leading edge. The solutions for a Prandtl number of 0.733 were evaluated by Niuman and Pohlhausen [43] with the aid of a differential analyzer. In 1958, Foote [20] extended Finston's method by discussing the possibility of solving the general problem in series, and he obtained the second term of the asymptotic expansions.

Siegel [59] in 1958 employed the same approach as Schuh's [58] in investigating the problem by use of the Von Karman-Pohlhausen integral momentum method and obtaining the solutions by the method of characteristics. He studied transient free convection on a vertical plate with a step change in uniform plate temperature or uniform heat flux. In 1962, Menold and Yang [41] presented the asymptotic solutions for unsteady free convection on a vertical plate with an arbitrary surface temperature or heat flux variation. These unsteady temperature and velocity profiles were utilized later by Siegel [59] to check the accuracy of the integral method.

In 1964, for free convection from a vertical plate having suitable restricted variation in wall temperature, Scherberg [54] found the solutions by the integral method. His theoretical results led him to conclude that the leading edge conditions for the variable wall temperature case affected the boundary layer structure more than that for the isothermal case. In 1964, Schetz and Eichhorn [55] experimentally studied the temperature and velocity fields for natural convection adjacent to a vertical plate with a discontinuous wall temperature variation.

In 1967, Hayday, Bowlus, and McGraw [31] explored a numerical solution for the non-similar free convection from a plate with a step discontinuity in wall temperature. The results compared favorably with, and formed a theoretical basis for, the experiments of Schetz and Eichhorn [55]. In 1968, Takhar [75] presented a numerical solution of free convection from a semi-infinite vertical plate which was uniformly heated up to a certain distance from the leading edge and insulated for the rest of the length. He pointed out that the velocity accelerated more rapidly and the temperature decayed more slowly for the insulated plate than those for the uniformly heated plate.

In 1971, Kelleher [34] analyzed the same problem as Hayday, et al. [31] by using asymptotic series expansion. Expansions for velocity and temperature

profiles were obtained in the region immediately above the discontinuity. Calculations of the wall heat flux were made for Prandtl numbers of 0.72 and 10, and for various wall temperature ratios. His solutions were in good agreement with the experimental results of Schetz and Eichhorn [55] and the numerical works of Hayday, et al. [31].

In 1969, Kuiken [37] theoretically studied the free convection past a vertical plate having a general class of nonlinear wall temperature distributions. He developed a method to find two series solutions; one for a small distance up the plate and the other for large distances. And an overall valid solution was obtained by graphically joining the two solutions.

In 1972, Kelleher and Yang [35] extended the well known Görtler series for forced flow over arbitrary cylinder to laminar free convection along a heated vertical plate with arbitrary surface-temperature variations. The leading edge term in the series was identical to the known similarity solution. Universal functions associated with the first five terms in the series were calculated for a Prandtl number of 0.72. A numerical example was shown for a specific surface-temperature variation, and the results were compared to that of an approximate integral solution by Sparrow [62] for the same case. The comparison showed a significant advantage of the Görtler's series over the integral solution.

In 1972, Yang, Novotny, and Cheng [88] studied the natural convection heat transfer from a non-isothermal vertical plate immersed in a temperature stratified enviroment. Numerical solutions were carried out for a wide range of surface and ambinent temperature distributions for Prandtl numbers between 0.1 and 20. They discussed the relative effects of the variable temperature distributions on the surface heat transfer, examined the flow reversal and temperature defect found in other investigations [9,18], and concluded that approximate solutions based on the local temperature difference were not

adequate to quantitatively predict the correct surface heat flux.

Fujii and Imura [22] in 1972 used two different sized plates to study experimentally natural convection heat transfer from a plate with arbitrary inclination. The results of heat transfer coefficients were presented in the relation of average Nusselt number versus Rayleigh number for the cases of vertical plate, inclined plate, and horizonal plate both facing downward and upward. The heat was transferred from one side surface of the plate.

In 1973, Soundalgekar [60] obtained the similarity approximate solutions for free convection flow of water at $4^{o}C$ by Karman-Pohlhausen's integral method when the wall temperature varied as a power n of distance along the plate. The approximate solutions for velocity and temperature were derived and the similarity parameter was obtained as $y/[Bx(\frac{1-2n}{4})]$, B was a constant.

(2.3) Uniform Heat Flux Plate

Sparrow and Gregg [63] in 1956 first analyzed the laminar free convection from a uniformly heated vertical plate. They also reduced the boundary layer equations to a set of ordinary differential equations by a similarity transformation, as Pohlhausen had done for the isothermal plate case. The solutions of the equations were obtained numerically for Prandtl numbers of 0.1, 1, 10, and 100. Results for the case of uniform surface heat flux by the approximate integral method [64] were in good agreement with the solutions obtained by the similarity transformation method. Dotson's experimental data [14] for air were used to verify this analysis. The experimental points reported by Dotson [14] as well as the theoretical line obtained by Sparrow and Gregg [63] were plotted together for comparison — the agreement was good over the entire range of $10^{5} < Gr_{x}^{*} < 10^{11}$.

In 1960, Goldstein and Eckert [25] used a Zehnder-Mach interferometer to make detailed observations of temperature profiles in water. The results

were compared with the results of Sparrow and Gregg's analysis [63] for the appropriate Prandtl number. A very satisfactory agreement was obtained. Szewczyk [74] in 1964 measured the temperature distributions in water by means of a thermocouple, and also obtained excellent agreement with Sparrow and Gregg's analytical solutions [63].

In 1964, Yang [86] analytically studied the laminar free convection wake above a uniformly heated plate. Under the assumption that the streamlines leaving the trailing edge of the plate were all parallel to the plate, he solved the equations by an asymptotic series expansion technique for some distance into the wake, the results were then continued to rest of the wake region by an integral solution. He found the spreading of the boundary layer in the wake was rather gradual, so that the assumption of streamlines parallel to the plate was valid.

In 1966, Chang, Akins, and Bankoff [7]extended Yang and Jerger's [87] first-order perturbation analysis of natural convection from an isothermal plate to the case of uniform heat flux plate. The zero-order solution satisfied the Sparrow and Gregg's boundary layer equations, and a first-order perturbation correction was constructed by finding the outer potential flow which matched the zero-order inner flow. They gave the numerical solutions for Prandtl numbers of 0.01, 0.03, and 0.1.

In 1969, Julian and Akins [33] undertook an experimental investigation of free convection in mercury in the range of moderate Grashof numbers ($10^4 < Gr_x^* < 10^9$). The results agreed well with the similarity and integral solutions of the boundary layer equations. In 1972, Chang and Akins [6] extended Julian's experiment to low Grashof numbers ($10 < Gr_x^* < 10^8$). They found that at the same Grashof numbers, increasing vertical distance up the plate shifted the temperature profile toward the boundary-layer solution, and at the same vertical distance up the plate, the temperature profile was

longer as the Grashof number increased. These results tended to verify the perturbation predictions, which said the temperature profiles depended upon the vertical distance up the plate as well as the Grashof number.

Vliet [81] in 1969 presented the experimental measurements of local heat transfer on a constant heat flux, inclined plate. The data covered angles from vertical to thirty degrees, and included laminar, transient, and turbulent regimes. In 1971, Rajan and Picot [48] carried out an experimental study of natural convection from a vertical plate with uniform heat flux. The solution of Sparrow and Gregg by Von Karman-Pohlhausen integral method [64] was applied to his steady state results to correlate the Prandtl, Grashof, and Nusselt numbers. The results were compared with the value obtained by Sparrow and Gregg [64].

In 1974, Godaux and Gebhart [24] experimentally studied the transition of natural convection flow adjacent to a vertical surface which dissipated a uniform heat flux. The region of transition was divided into two subregions. They found that, in the first, the velocity lost its laminar form on the way to turbulence, the second subregion began when the total amount of converted thermal energy had reached some particular value.

In 1974, Wilks [84] investigated the effect of buoyancy forces on the boundary layer flow over a semi-infinite vertical plate. The interaction of buoyancy force with the boundary-layer flow associated with a uniform stream was examined. Two solutions were obtained, one valid near the leading edge and the other downstream. An accurate numerical method was used to describe the flow in the region where the series were not valid. Comparison of the series expansions and the correct solutions led to some confidence that straightforward extrapolations linking these series representations were sufficiently well for practical purpose. Also the agreement between a local similarity analysis and the results of his investigation was good.

Chang and Akins [6] in 1972 found there were temperature profile dependences on the vertical distance up the plate and the Grashof number in their experimental investigation of natural convection in mercury at low Grashof numbers. The present research extends Chang's work [6] to free convection at extremely small Grashof numbers ($10^{-1} < Gr_x^* < 10^5$) both in water and in mercury, and also examines the dependences of the dimensionless temperature profiles on these parameters.

3. Theoretical Analysis

Laminar natural convection from a vertical flat plate with uniform heat flux is analyzed below, investigating the effects of changing Grashof number and Prandtl number on the thermal boundary layer in the range of small Grashof number. The plate is semi-infinite in z direction. The coordinate system is displayed in Figure 1. The origin of the rectangular axes is located at the leading edge of the plate. The plate has the coordinates of $0 \leq x \leq L$ and $y = 0$, and is supplied with a direct current power to generate uniform heat flux.

The complete equations of continuity, motion, and thermal energy, written in tensor forms are [2]:

Continuity:

$$\frac{\partial \rho}{\partial t} + \bar{\nabla} \cdot \rho \bar{v} = 0 \quad * \tag{1}$$

Motion:

$$\rho \left(\frac{D\bar{v}}{Dt}\right) = -\bar{\nabla} \cdot \bar{\bar{\tau}} - \bar{\nabla} p + \rho \bar{g} \tag{2}$$

Energy:

$$\rho C_v \left(\frac{Dt}{Dt}\right) = -\bar{\nabla} \cdot \bar{q} - T\left(\frac{\partial \rho}{\partial t}\right)_v (\bar{\nabla} \cdot \bar{v}) - \bar{\bar{\tau}} : \bar{\nabla} \bar{v} \tag{3}$$

The density is an important factor in natural convection heat transfer, but its change is considered to be sufficiently small so that it can be taken as constant except in the buoyancy term which provides the driving force for natural convection. A Taylor series expansion of the density at a reference temperature up to the first derivative is used to formulate the density in buoyancy term:

---

*A complete list of nomenclature is shown on page 85.

THIS BOOK CONTAINS NUMEROUS PAGES WITH DIAGRAMS THAT ARE CROOKED COMPARED TO THE REST OF THE INFORMATION ON THE PAGE.

THIS IS AS RECEIVED FROM CUSTOMER.

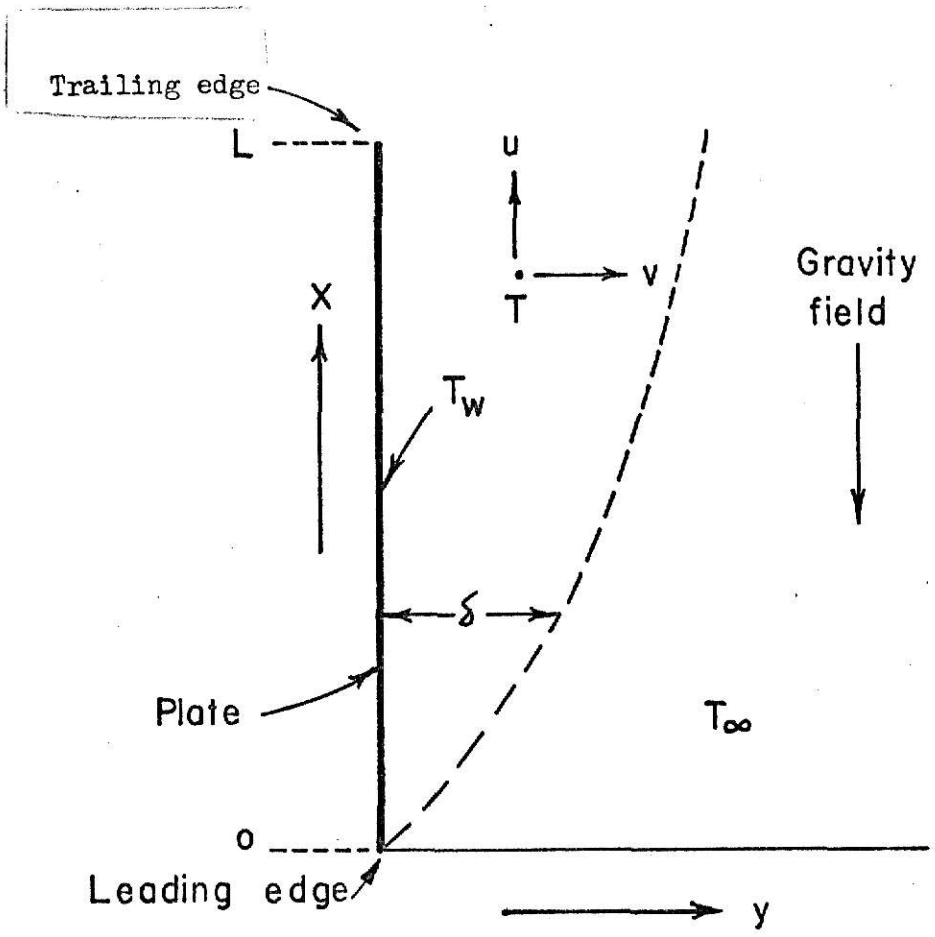


Plate is infinite in z direction.

Figure 1. Plate Coordinates.

$$\rho = \rho_{T_R} + \left(\frac{\partial \rho}{\partial T}\right)_{T_R} (T-T_R)$$

$$= \rho_{T_R} - \rho\beta\big|_{T_R} (T-T_R) \tag{4}$$

where β is the coefficient of volume expansion and $\beta = -\frac{1}{\rho}\left(\frac{\partial \rho}{\partial T}\right)_p$.

With the following assumptions,

(1) Steady state

(2) Laminar and two-dimensional flow

(3) Incompressible Newtonian fluid

(4) No sources of heat within the fluid

(5) Negligible viscous dissipation

(6) Constant physical properties except for the density in buoyancy term as expressed by equation (4)

(7) Gravity is the only body force and is opposite to the x-coordinate, i.e. $g_x = -g$; $g_y = 0$,

the equations (1), (2), and (3) can be reduced to:

Continuity

$$\frac{\partial u}{\partial x} + \frac{\partial v}{\partial y} = 0 \tag{5}$$

Motion

$$u\frac{\partial u}{\partial x} + v\frac{\partial u}{\partial y} = \nu\left(\frac{\partial^2 u}{\partial x^2} + \frac{\partial^2 u}{\partial y^2}\right) - \frac{1}{\rho}\frac{\partial p}{\partial x} - g + g\beta(T-T_R) \tag{6}$$

$$u\frac{\partial v}{\partial x} + v\frac{\partial v}{\partial y} = \nu\left(\frac{\partial^2 v}{\partial x^2}\right) - \frac{1}{\rho}\frac{\partial p}{\partial y} \tag{7}$$

Energy

$$u\frac{\partial T}{\partial x} + v\frac{\partial T}{\partial y} = \alpha\left(\frac{\partial^2 T}{\partial x^2} + \frac{\partial^2 T}{\partial y^2}\right) \tag{8}$$

where $\alpha = \frac{k}{\rho C_p}$ is the thermal diffusivity, ν is the kinematic viscosity, and the subscript T_R to ρ and β has been dropped. All the analyses of free convection are based on this set of equations which represent the

conservation of mass, momemtum, and energy in a fluid moving under the influence of a body force. The boundary conditions for this problem are:

$$
\begin{aligned}
&u = 0 \text{ (no slip at the plate)} && \text{at } y = 0,\ 0 \le x \le L \\
&v = 0 \text{ (no suction or injection)} && \text{at } y = 0,\ 0 \le x \le L \\
&q = -k\left.\frac{\partial T}{\partial y}\right|_{y=0} \text{ (constant heat flux)} && \text{at } y = 0,\ 0 \le x \le L \\
&u \to 0 \text{ (no bulk motion)} && \text{at } y \to \infty, \text{ all } x \\
&v \to 0 \text{ (no bulk motion)} && \text{at } y \to \infty, \text{ all } x \\
&T \to T_\infty \text{ (constant bulk temperature)} && \text{at } y \to \infty, \text{ all } x
\end{aligned}
\tag{9}
$$

The boundary conditions on velocity in free convection differ from those in forced convection and have the effect of changing the shape of the velocity and temperature profiles. The velocity changes from zero through a maximum to zero again, while temperature varies monotonically from a maximum at the plate to zero.

The present work was to obtain experimental measurements of temperature profiles for natural convection from a vertical plate at extremely small Grashof numbers for water and mercury. The experimental results were compared with the boundary-layer solution by Sparrow and Gregg [63] as well as the perturbation solutions by Chang, Akins, and Bankoff [7], therefore, these two theoretical analyses follow here.

(3.1) Boundary-layer Solution

Sparrow and Gregg [63] used Prandtl's boundary-layer assumptions to simplify equations of motion and energy. That is, $\frac{\partial^2 u}{\partial x^2}$ was neglected in equation (6); $\frac{\partial^2 T}{\partial x^2}$ in equation (8); and the equation of horizontal motion (7) was ignored. They also considered that, in natural convection, there was no external force so that the pressure at any point in

the fluid was only the hydrostatic pressure calculated for the fluid outside the boundary layer, i.e. $\frac{\partial p}{\partial x} = -\rho g$. Choosing the bulk temperature as the reference temperature T_R, the governing differential equations may be reduced to:

Continuity

$$\frac{\partial u}{\partial x} + \frac{\partial v}{\partial y} = 0 \tag{10}$$

Motion

$$u\frac{\partial u}{\partial x} + v\frac{\partial u}{\partial y} = \nu\frac{\partial^2 u}{\partial y^2} + g\beta(T-T_\infty) \tag{11}$$

Energy

$$u\frac{\partial T}{\partial x} + v\frac{\partial T}{\partial y} = \alpha \quad \frac{\partial^2 T}{\partial y^2} \tag{12}$$

The stream function ψ, which satisfies the continuity equation (10), and the similarity variables η, $F(\eta)$, and $\bar{\Theta}(\eta)$ are introduced in the following ways:

$$\frac{\partial \psi}{\partial y} = u \ , \qquad \frac{\partial \psi}{\partial x} = -v \tag{13}$$

$$\eta = \left(\frac{Gr_x^*}{5}\right)^{1/5} \frac{y}{x} \tag{14}$$

$$F(\eta) = \left(\frac{Gr_x^*}{5}\right)^{-1/5} \frac{\psi}{5\nu} \tag{15}$$

$$\bar{\Theta}(\eta) = \left(\frac{Gr_x^*}{5}\right)^{1/5} \frac{k(T-T_\infty)}{qx} \tag{16}**$$

$$Gr_x^* = \frac{g\beta x^4 q}{k\nu^2} \tag{17}$$

where Gr_x^* is called the modified Grashof number. Equations (11) and (12) can be transformed into a set of ordinary differential equations:

$$F''' - 3(F')^2 + 4FF'' + \bar{\Theta} = 0 \tag{18}$$

**In Sparrow and Gregg's nomenclature, $-\Theta$ equals to the present $\bar{\Theta}$.

$$\bar{\theta}'' + Pr[4\bar{\theta}'F - \bar{\theta}F'] = 0 \tag{19}$$

subject to the following boundary conditions:

$$F(0) = F'(0) = 0$$

$$\bar{\theta}'(0) = 1 \tag{20}$$

$$F'(\infty) = \bar{\theta}(\infty) = 0$$

The primes denote differentiation with respect to η. Now the only parameter in the equations is the Prandtl number, $Pr = \frac{\nu}{\alpha}$.

The velocity components can be derived from Equations (13), (14), and (15) and the temperature is obtained by rearranging Equation (16),

$$u = \frac{5\nu}{x}\left(\frac{Gr_x^*}{5}\right)^{2/5} F''(\eta) \tag{21}$$

$$v = \frac{\nu}{x}\left(\frac{Gr_x^*}{5}\right)^{1/5} [\eta F''(\eta) - 4F(\eta)] \tag{22}$$

$$T = T_\infty + \left(\frac{Gr_x^*}{5}\right)^{-1/5} \frac{qx}{k}\,\bar{\theta}(\eta). \tag{23}$$

Or, in dimensionless form:

$$\frac{\frac{x}{\nu}}{5\left(\frac{Gr_x^*}{5}\right)^{2/5}} u = F'|(\eta) \tag{24}$$

$$\frac{T - T_\infty}{T_w - T_\infty} = \frac{\bar{\theta}(\eta)}{\bar{\theta}(0)}\,. \tag{25}$$

The solutions to the differential equations (18) and (19) have been obtained numerically by digital computer by Sparrow and Gregg [63]. Results were carried out for Prandtl numbers of 0.1, 1, 10 and 100. Chang, et al. [7] extended the solutions to Prandtl numbers of 0.01 and 0.03. Figures 2 and 3 present their numerical results—the dimensionless temperature and velocity profiles for various Prandtl numbers.

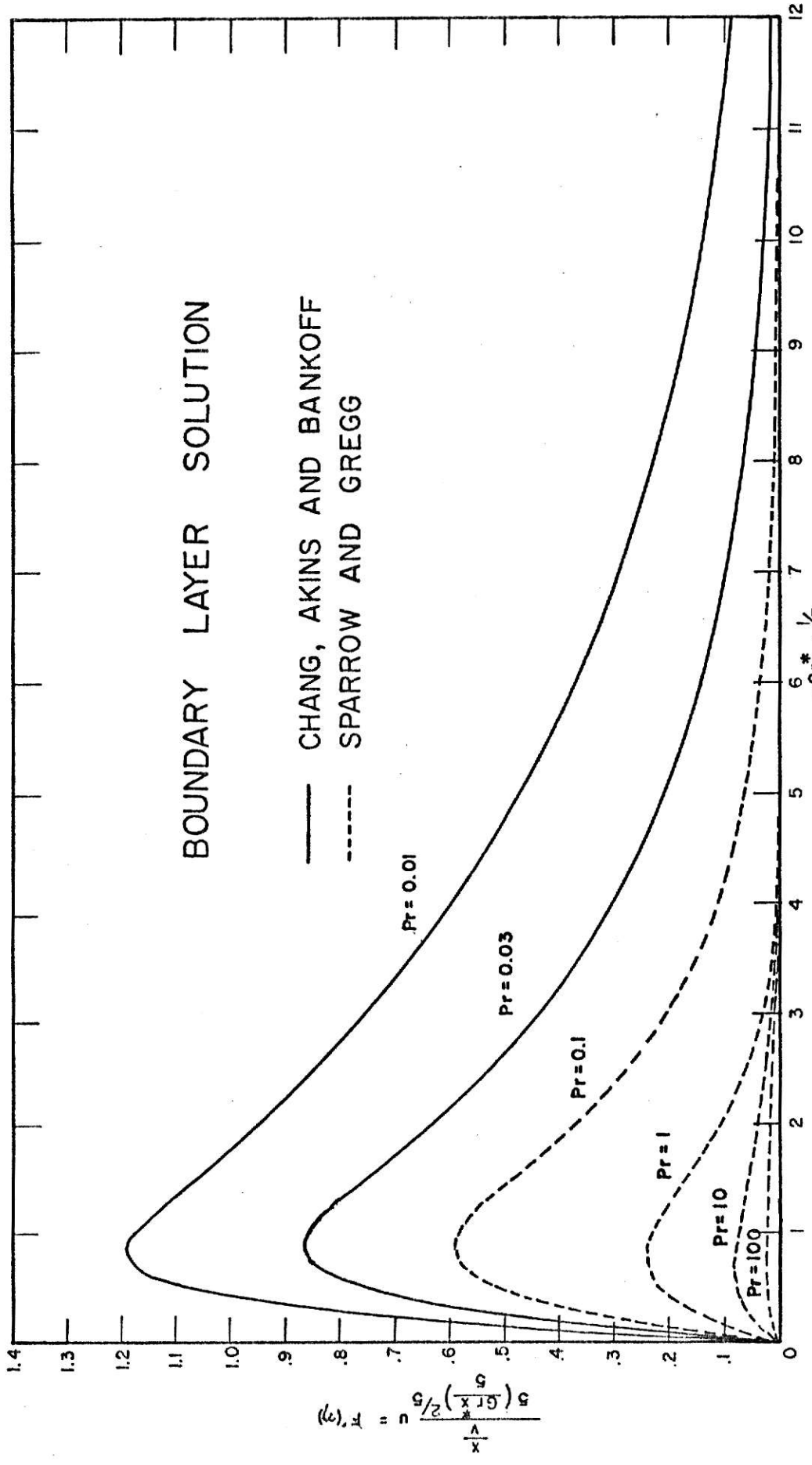


Figure 2. Dimensionless Velocity Distribution for Various Prandtl Numbers.

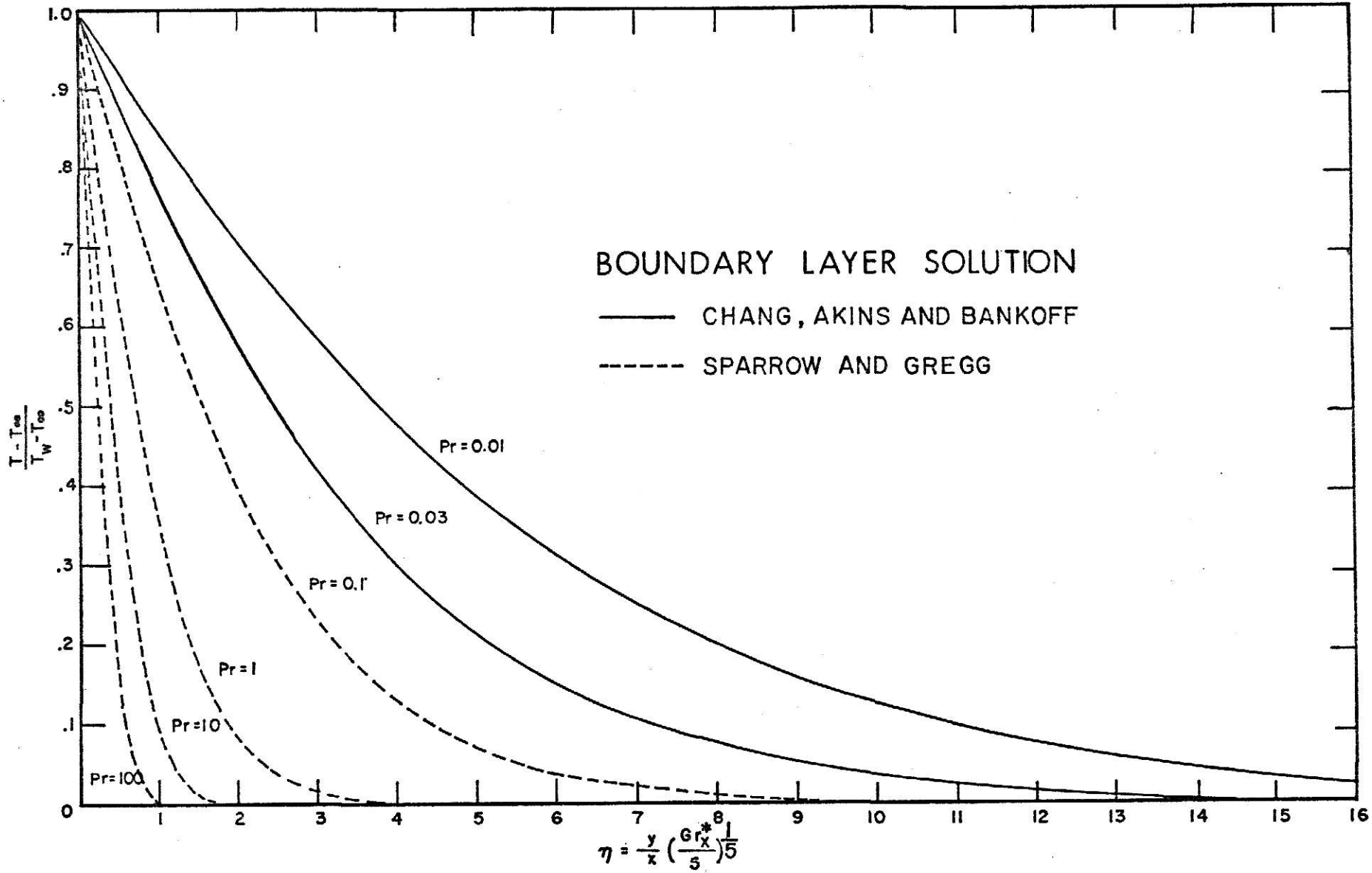


Figure 3. Dimensionless Temperature Distribution for Various Prandtl Numbers.

(3.2) Perturbation Solution

In the boundary-layer solution, Prandtl's boundary-layer equations were applied. That is, they neglected heat conduction in the vertical direction. This is not permissible when the thermal boundary-layer thickness along the vertical distance is no longer negligible in comparison with the height of the plate. One such situation occurs when the fluid, having high thermal conductivity (or low Prandtl number), flows slowly -- for example, natural convection of mercury at low Grashof numbers.

In order to avoid the simplification due to the boundary-layer assumptions, Chang, et al. [7] applied the perturbation technique to solve equations (5), (6), (7), and (8) with the boundary conditions (9). They first introduced the following dimensionless quantities:

$$\bar{x} = \frac{x}{L} , \qquad \bar{y} = \frac{y}{L} ; \tag{26}$$

$$\bar{\Psi} = \frac{\Psi}{Gr_L^{*}\upsilon} ; \tag{27}$$

$$\theta = \frac{(T - T_\infty)k}{qL} Gr_L^{*1/5} ; \tag{28}$$

$$P = \frac{(p - p_\infty)L^2}{\rho\upsilon^2 Gr_L^{*4/5}} ; \tag{29}$$

$$G = \frac{gL^3}{\upsilon^2 Gr_L^{*4/5}} ; \tag{30}$$

$$\bar{u} = \frac{\delta\bar{\Psi}}{\delta\bar{y}} = \frac{uL}{\upsilon Gr_L^{*}} , \qquad \bar{v} = -\frac{\delta\bar{\Psi}}{\delta\bar{x}} = \frac{vL}{\upsilon Gr_L^{*}} ; \tag{31}$$

$$X = \bar{x} , \qquad Y = Gr_L^{*1/5}\,\bar{y} ; \tag{32}$$

$$\Psi = Gr_L^{*4/5}\,\bar{\Psi} ; \tag{33}$$

where Ψ has already been defined in equation (13), $\bar{\Psi}$ is dimensionless stream function, G is dimensionless gravitational acceleration, θ is dimensionless

temperature, and $\bar{u}$ and $\bar{v}$ are the dimensionless velocities. From Sparrow and Gregg's boundary layer solutions [63], it is known that $\bar{y}/\bar{x}$ is of the order $Gr_L^{*1/5}$. Therefore, a second transformation of the $\bar{x}$, $\bar{y}$ system to the X, Y system is introduced to bring order of magnitude of Y to that of X, and the second dimensionless stream function is also introduced in such a manner that

$$\Psi_Y/-\Psi_X = \bar{u}/(\bar{v}Gr_L^{*1/5}) \quad ; \tag{34}$$

then equations (6), (7), and (8) are transformed to:

$$\Psi_Y\Psi_{XY} - \Psi_X\Psi_{YY} = -P_X + Gr_L^{*-2/5}\Psi_{XXY} + \Psi_{YYY} - G + \theta \quad ; \tag{35}$$

$$Gr_L^{*-2/5}(-\Psi_Y\Psi_{XX} + \Psi_X\Psi_{XY}) = -P_Y - Gr_L^{*-4/5}\Psi_{XXX} - Gr_L^{*-2/5}\Psi_{XXY} \quad ; \tag{36}$$

$$\Psi_Y\theta_X - \Psi_X\theta_Y = Pr^{-1}(Gr_L^{*-2/5}\theta_{XX} + \theta_{YY}) \quad . \tag{37}$$

To solve equations (35), (36), and (37) by perturbation method, it is assumed that the stream function Ψ, the pressure P, and the temperature θ can be expanded in terms of a small constant parameter ϵ:

$$\Psi = \Psi^{(0)} + \epsilon\Psi^{(1)} + \epsilon^2\Psi^{(2)} + \ldots \quad ; \tag{38}$$

$$P = P^{(0)} + \epsilon P^{(1)} + \epsilon^2 P^{(2)} + \ldots \quad ; \tag{39}$$

$$\theta = \theta^{(0)} + \epsilon\theta^{(1)} + \epsilon^2\theta^{(2)} + \ldots \quad . \tag{40}$$

The boundary-layer theory assumed the velocity and temperature effects occurs only inside a very thin layer along the plate. In Sparrow and Gregg's analysis [63], they found that the horizontal velocity at the edge of the boundary layer does not vanish ($v \to -4Gr_L^{*-1/5}(5x)^{-1/5}F(\infty)$); which means flow does exist outside the boundary layer. Therefore, the flow field was divided into two regions : one is the boundary layer next to the plate -- the boundary limit problem, and the other is a potential flow region outside

the boundary layer—the interior limit problem. The boundary-layer solution and the potential flow solution can be taken as zero- and first-order approximations, respectively, but the two fields must join smoothly. This means that the horizontal velocity in the potential flow field, which is $0(\varepsilon)$ according to series expansion in the parameter ε, must equal to that of the viscous flow field at the edge of the boundary layer, which is $0(Gr_L{}^{*-1/5})$. Therefore, $Gr_L{}^{*-1/5}$ is taken as the series expansion parameter ε.

Substituting equations (38), (39), (40), and the definition of ε into equations (35), (36), and (37), then equating the coefficients of like powers of ϵ, we get the following zero- and first-order perturbation equations.

The zero-order perturbation equations are:

$$\Psi_Y{}^{(0)}\Psi_{XY}{}^{(0)} - \Psi_X{}^{(0)}\Psi_{YY}{}^{(0)} = -P_X{}^{(0)} + \Psi_{YYY}{}^{(0)} - G + \Theta^{(0)} \quad ; \tag{41}$$

$$-P_Y{}^{(0)} = 0 \quad ; \tag{42}$$

$$\Psi_Y{}^{(0)}\Theta_X{}^{(0)} - \Psi_X{}^{(0)}\Theta_Y{}^{(0)} = \frac{1}{Pr}\,\Theta_{YY}{}^{(0)} \quad . \tag{43}$$

Equation (42) implies the zero-order pressure gradient exists only in the x-direction and for a vertical plate, $P_X{}^{(0)} = -G$; i.e., the zero-order pressure in the x-direction is due solely to the weight of the fluid. With the following new similarity variables being introduced:

$$\eta = Y/(5X)^{1/5} \quad ; \tag{44}$$

$$\Psi^{(0)} = (5X)^{4/5} F(\eta) \quad ; \tag{45}$$

$$\Theta^{(0)} = (5X)^{1/5}\,\bar{\Theta}(\eta) \quad ; \tag{46}$$

where η is the similarity variable and the same as equation (14), $F(\eta)$ and $\bar{\Theta}(\eta)$ are also defined in equations (15) and (16), the zero-order

equations (41) and (43) can be reduced to a pair of ordinary differential equations:

$$F''' - 3(F')^2 + 4FF'' + \bar{\theta} = 0 \quad ; \tag{47}$$

$$\bar{\theta}'' + Pr[4F\bar{\theta}' - F'\bar{\theta}] = 0 \quad . \tag{48}$$

The boundary conditions given in equation (9) become:

$$\begin{aligned} &F(0) = F'(0) = 0 \quad , \\ &\bar{\theta}'(0) = 1 \quad , \\ &F'(\infty) = \bar{\theta}(\infty) = 0 \quad . \end{aligned} \tag{49}$$

Equations (47) and (48) are evidently the same as equations (18), (19), which were derived directly from boundary layer equations by the similarity transformation method. The numerical solutions for these equations are already available for Prandtl numbers of 0.01, 0.03, 0.1, 1, 10 and 100.

The first-order perturbation equations are:

$$\Psi_y^{(0)}\Psi_{XY}^{(1)} + \Psi_Y^{(1)}\Psi_{XY}^{(0)} - \Psi_X^{(0)}\Psi_{YY}^{(1)} - \Psi_X^{(1)}\Psi_{YY}^{(0)}$$

$$= - P_X^{(1)} + \Psi_{YYY}^{(1)} + \theta^{(1)} \quad ; \tag{50}$$

$$-P_Y^{(1)} = 0 \quad ; \tag{51}$$

$$\Psi_Y^{(0)}\theta_X^{(1)} + \Psi_Y^{(1)}\theta_X^{(0)} - \Psi_X^{(0)}\theta_Y^{(1)} - \Psi_X^{(1)}\theta_Y^{(0)} = \frac{1}{Pr}\theta_{YY}^{(1)} \quad . \tag{52}$$

Now the functions $P^{(1)}$, $\Psi^{(1)}$ and $\theta^{(1)}$ need to be solved. The first-order perturbation solutions are determined on the basis of potential flow theory. Chang, et al. [7] showed that the first-order pressure $P^{(1)}$ is one order higher, with respect to the parameter ε, than the corresponding velocity field. Therefore, $P^{(1)}$ could be deleted from the first-order perturbation equations. They also showed that the first-order variables could be expanded as follows:

$$\Psi^{(1)} = \frac{20F(\infty)}{\pi} \left[S f_{00}(\eta) - \sum_{m=0}^{\infty} \frac{X^{m+1/5}}{5m+1} f_m(\eta) \right] \quad ; \tag{53}$$

$$\Theta^{(1)} = \frac{20F(\infty)}{\pi} (5X)^{-3/5} \left[S\Theta_{00}(\eta) - \sum_{m=0}^{\infty} \frac{X^{m+1/5}}{5m+1} \Theta_m(\eta) \right] \quad ; \tag{54}$$

where f_{00}, f_m, Θ_{00}, and Θ_m are functions of η alone, η is the same as that defined in Equation (44) and

$$S = \sum_{m=0}^{\infty} \frac{3}{(5m+1)(5m+4)} = 0.864806 \ldots . \quad ; \tag{55}$$

Substituting equations (53) and (54) into the first-order perturbation equations, gives the following two sets of ordinary differential equations:

$$\begin{aligned} &f_{00}''' + 4Ff_{00}'' - 2F'f_{00}' + \Theta_{00} = 0 \quad , \\ &\frac{1}{Pr}\Theta_{00}'' + 4F\Theta_{00}' + 3F'\Theta_{00} - \bar{\Theta}f_{00}' = 0 \quad ; \end{aligned} \tag{56}$$

$$\begin{aligned} &f_m''' + 4Ff_m'' - (5m+3)F'f_m + (5m+1)F''f_m + \Theta_m = 0 \quad , \\ &\frac{1}{Pr}\Theta_m'' + 4F\Theta_m' - (5m-2)F'\Theta_m - \bar{\Theta}f_m' + (5m+1)\bar{\Theta}'f_m = 0 \quad ; \end{aligned} \tag{57}$$

where $m = 0, 1, 2, \ldots .$ The boundary conditions are:

$$\begin{aligned} &f_{00}(0) = f_{00}'(0) = \Theta_{00}'(0) = 0 \quad , \\ &f_{00}'(\infty) = 1 \quad , \qquad \Theta_{00}(\infty) = 0 \quad ; \end{aligned} \tag{58}$$

and

$$\begin{aligned} &f_m(0) = f_m'(0) = \Theta_m'(0) = 0 \quad , \\ &f_m'(\infty) = 1 \quad , \qquad \Theta_m(\infty) = 0 \quad . \end{aligned} \tag{59}$$

The solutions for equations (56) and (57) have been obtained numerically by Chang, et al. [7] for Prandtl numbers of 0.1 and 0.03. The values of m were taken from zero to ten inclusive. No further calculations were carried out for m larger than 10 since sufficiently accurate results were determined by the first 11 terms in the series. Equations

(56) and (57) are strongly dependent on the zero-order solutions since the zero-order functions appear as the variable coefficients in these equations. Therefore, the first-order perturbation equations had to be solved with the zero-order perturbation equations simultaneously.

Finally, the velocity and temperature distributions of perturbation solutions up to first-order can be calculated. From equations (33), (38), (45), and (53), we get

$$\Psi = Gr_L^{*4/5}\,\bar{\psi}$$

$$= (5X)^{4/5}F(\eta) + \varepsilon\frac{20F(\infty)}{\pi}\left[Sf_{00}(\eta) - \sum_{m=0}^{\infty}\frac{X^{m+1/5}}{5m+1}f_m(\eta)\right] \tag{60}$$

Substituting $\bar{\psi}$ into equation (29) and rearranging yields the dimensionless velocity distribution

$$\frac{\frac{x}{\nu}}{5\left(\frac{Gr_x^*}{5}\right)^{2/5}}u = F'(\eta) + \varepsilon\frac{20F(\infty)}{\pi(5X)^{4/5}}\left[Sf_{00}'(\eta) - \sum_{m=0}^{\infty}\frac{X^{m+1/5}}{5m+1}f_m'(\eta)\right] \tag{61}$$

Similarly, from equations (28), (40), (46), and (54), the following equation is obtained,

$$\frac{(T-T_\infty)k}{qL}\left(\frac{Gr_L^*}{5X}\right)^{1/5} = \bar{\theta}(\eta) + \varepsilon\frac{20F(\infty)}{\pi(5X)^{4/5}}\left[S\theta_{00}(\eta) - \sum_{m=0}^{\infty}\frac{X^{m+1/5}}{5m+1}\theta_m(\eta)\right] \tag{62}$$

or dividing equation (62) by the value at the wall, we get

$$\frac{T-T_\infty}{T_w-T_\infty} = \frac{\bar{\theta}(\eta) + \varepsilon\frac{20F(\infty)}{\pi(5X)^{4/5}}\left[S\theta_{00}(\eta) - \sum_{m=0}^{\infty}\frac{X^{m+1/5}}{5m+1}\theta_m(\eta)\right]}{\bar{\theta}(0) + \varepsilon\frac{20F(\infty)}{\pi(5X)^{4/5}}\left[S\theta_{00}(0) - \sum_{m=0}^{\infty}\frac{X^{m+1/5}}{5m+1}\theta_m(0)\right]} \tag{63}$$

Comparing equations (61) and (63) with equations (24) and (25), it is noted that the second terms in equations (61) and (63) are additional terms to the zero-order solution. These additional terms are both functions of Gr_L^* and X. This indicates that the dimensionless velocity and

temperature depend on the modified Grashof number, Gr_L^*, and the distance up the plate, X. These profiles have been calculated numerically for Prandtl numbers of 0.1 and 0.03 at different distances up the plate with various values of Gr_L^* by Chang, et al. [7]. Figures 4, 5, and 6, are some of their results. From the results, they pointed out that for Prandtl number of 0.03 all the effects seen for Prandtl number of 0.1 are magnified.

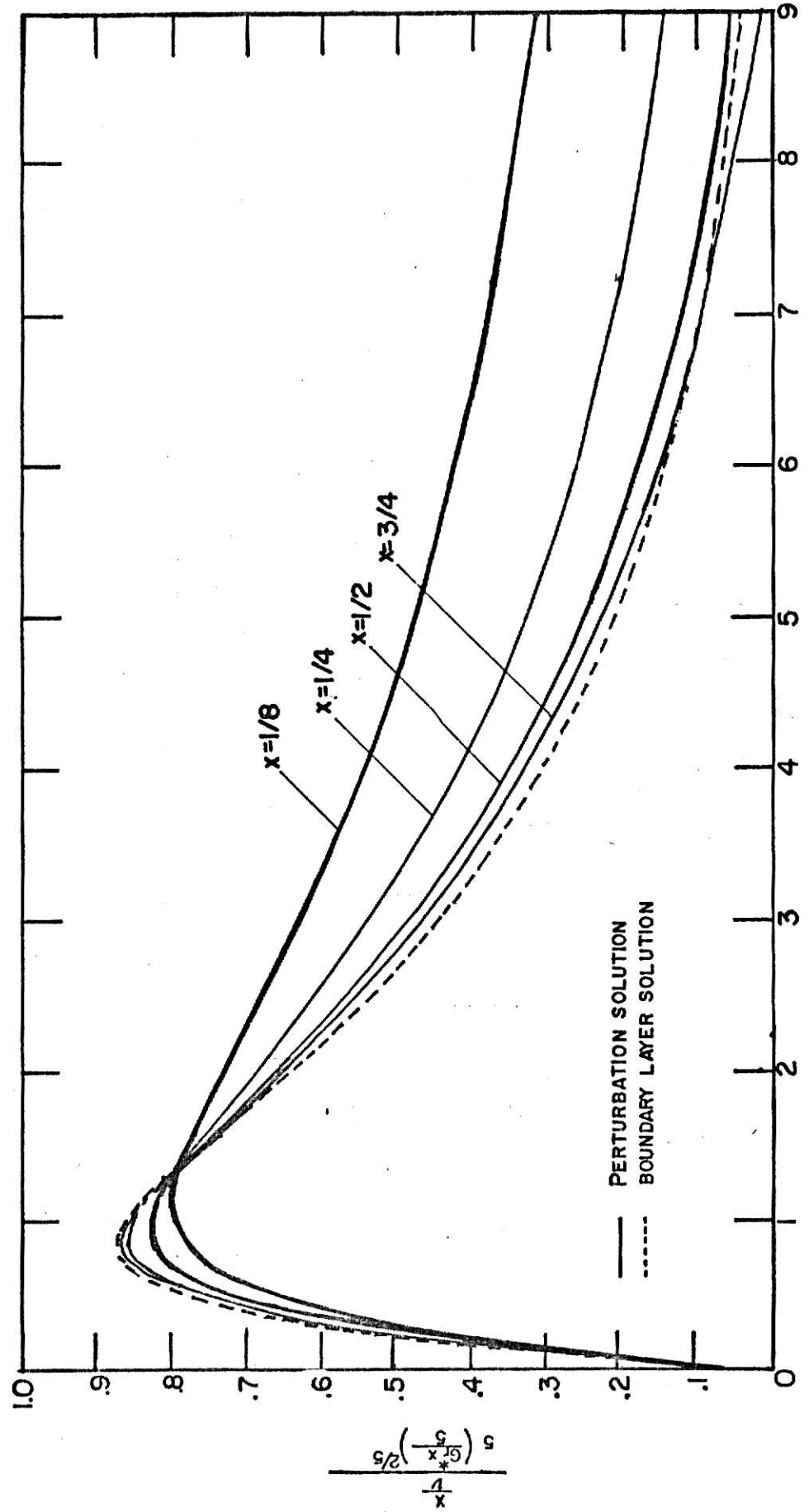


Figure 4. Comparison of velocity profiles for Pr=0.03 when $Gr^*_L=10^7$

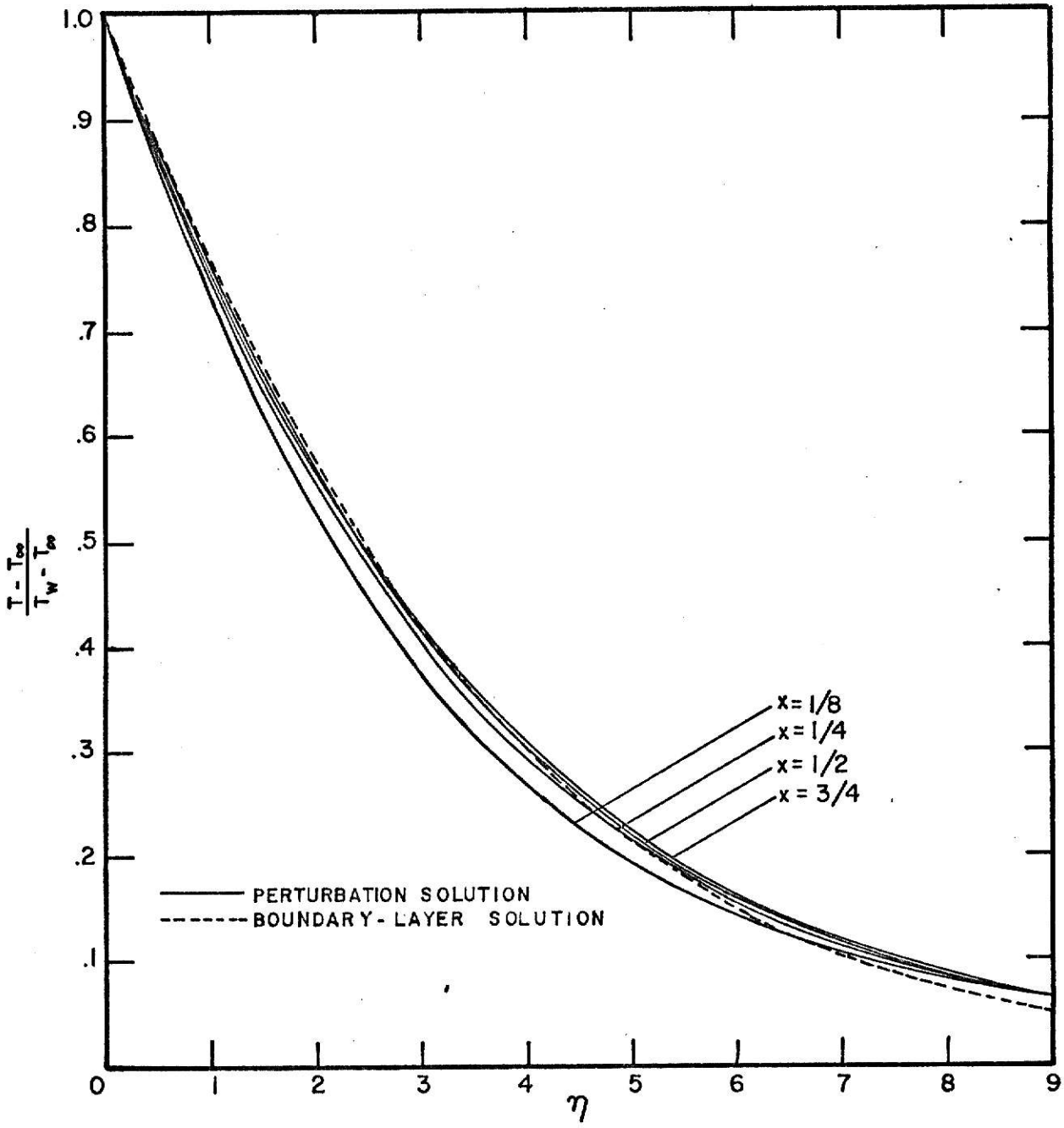


Figure 5. Comparison of Temperature Profiles for $Pr = 0.03$ When $Gr^*_L = 10^7$

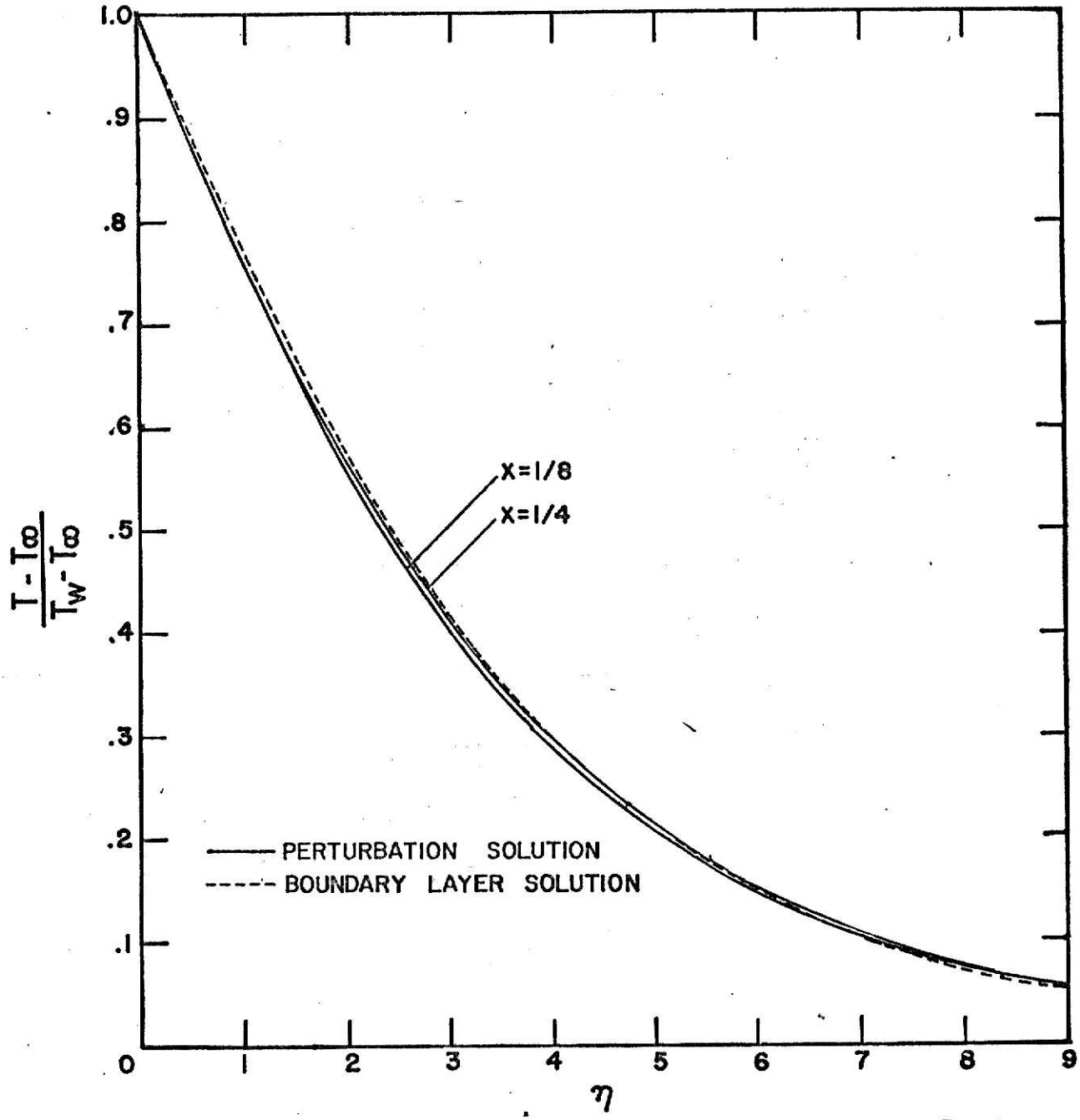


Figure 6. Comparison of Temperature Profiles for Pr=0.03 When $Gr_L^* = 10$.

4. Experimental Apparatus and Procedure

(4.1) Apparatus

The experimental equipment was essentially the same as that used by Chang [6]. The only modification was that an additional "Nanovoltmeter" was used to measure the E.M.F. of the thermocouple junction. The nanovoltmeter measured the temperature difference to 0.0025°C, but the Sanborn recorder, used by Chang [6], allowed a temperature difference measurement of only 0.03°C.

Figure 7 is a schematic diagram of the apparatus used to measure the temperature profiles. The apparatus consisted mainly of a heated vertical plate, a thermocouple, a probe driving mechanism for positioning the thermocouple, a container for the working fluid, a constant temperature bath, a nanovoltmeter, and a strip-chart recorder. Each piece of apparatus is described in detail in the following:

Plate:

The heated vertical plate shown in Figure 8 was 0.004-inch-thick, 2-inch-high, 4-inch-wide, and type 302 stainless steel with both trailing and leading edges. Both sides of the plate were coated with a plasticized acrylic resin, which served as an insulating material to minimize electrical leakage into the mercury. The plate was located in the center of the container and was connected to a D.C. power supply source to generate a constant surface heat flux, dissipated from both sides. The low electrical resistance and uniform thickness of the plate ensured the constant power dissipation and uniform generation over the plate. A voltmeter and an amperemeter were used to measure the voltage and current, respectively, for determining the power supplied.

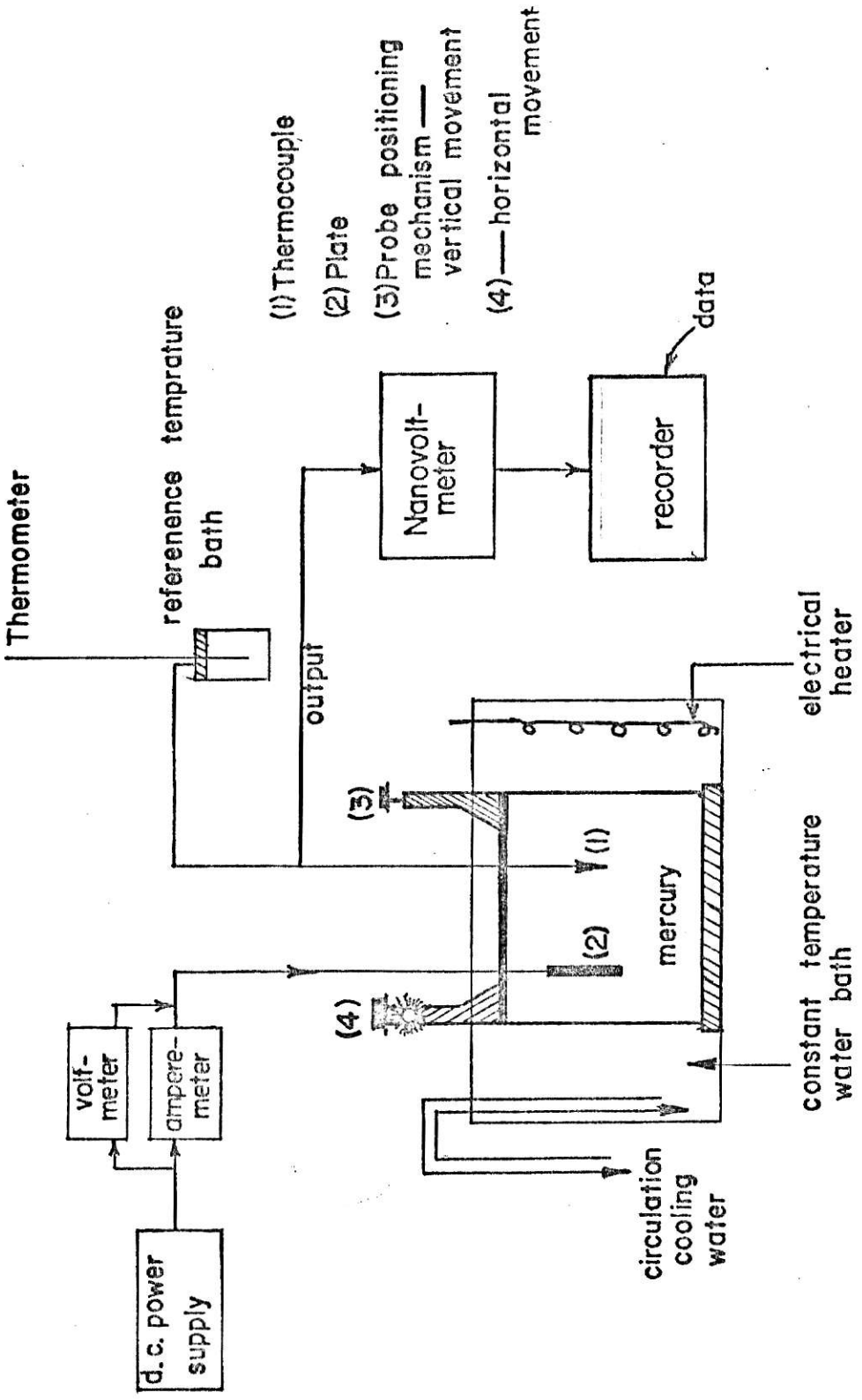


Figure 7. The schematic diagram of the equipment.

THIS BOOK CONTAINS SEVERAL DOCUMENTS THAT ARE OF POOR QUALITY DUE TO BEING A PHOTOCOPY OF A PHOTO.

THIS IS AS RECEIVED FROM CUSTOMER.

THIS BOOK CONTAINS NUMEROUS PICTURES THAT ARE ATTACHED TO DOCUMENTS CROOKED.

THIS IS AS RECEIVED FROM CUSTOMER.

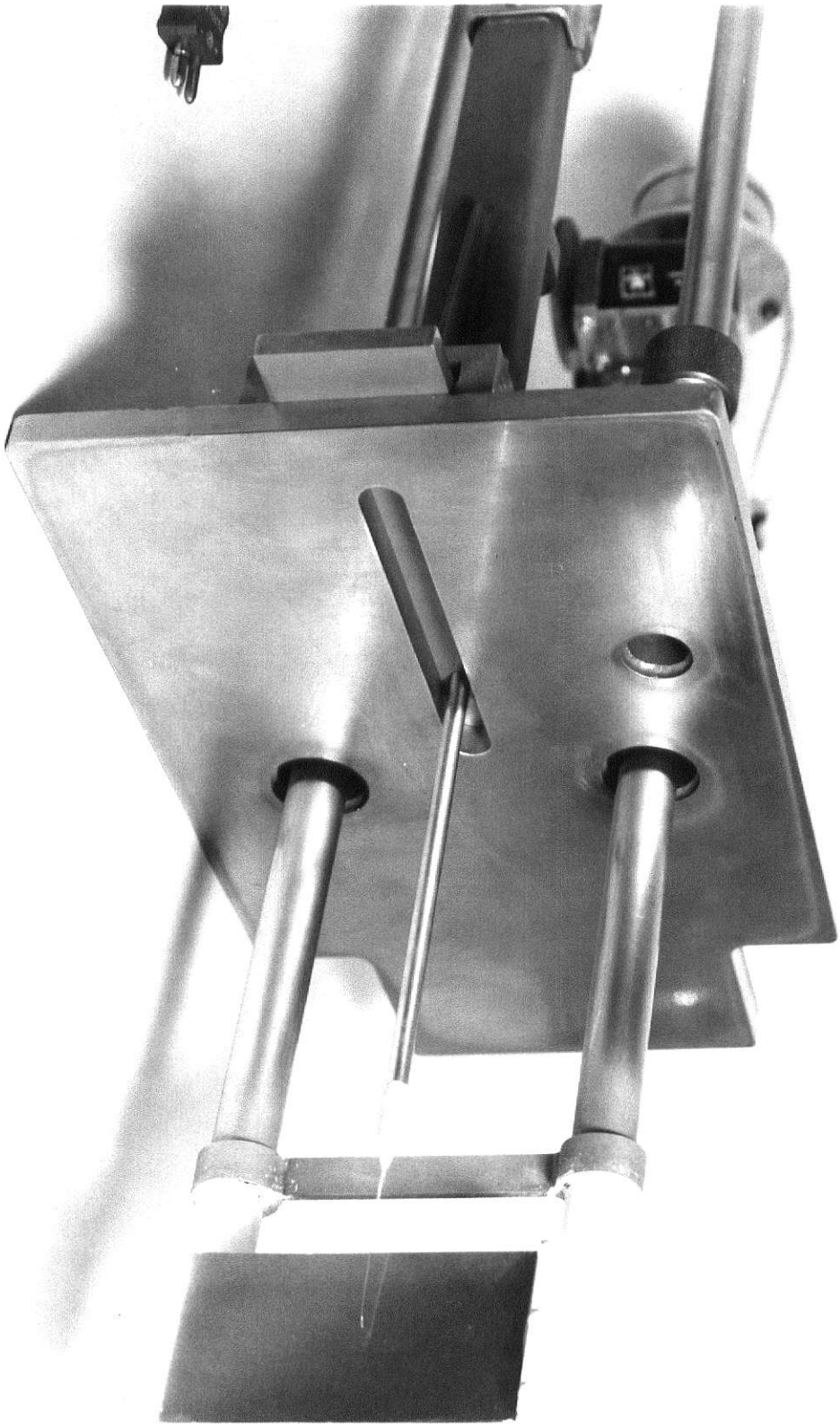


Figure 8. Vertical Plate and Thermocouple Probe.

Thermocouple:

The temperature of the fluids was measured by a copper-constantan-thermocouple, Robinson-Hanpern Model 302A-T300S-08L. The copper-constantan wires were enclosed in a 2-inch-long, 0.008-inch-diameter, stainless steel sheath. The hot junction was in water (or mercury) and the cold junction was in a reference bath of room temperature water. The end of the thermocouple was 0.004-inch-thick and had a time constant of approximately 0.02 seconds.

Probe Driving Mechanism:

The horizontal movement (toward or away from the plate) was accomplished by using a synchronous motor operated by a control switch. The driving mechanism was a 7/16-inch-thick, 8 by 13 inch base plate. A slot was cut in the base plate over which a slide moved. The slide was connected to a 2-RPM synchronous motor by a 1/2 - 32 precision pitch screw to move the probe toward or away from the plate continuously. The linear speed of the thermocouple was 1/16 of an inch per minute.

The vertical movement could be made manually by a knob with a counter and a vernier. Turning twenty units of counter in the counterclockwise direction equaled to moveing the thermocouple down 1/32 of an inch.

Container and Constant Temperature Bath:

The plate and thermocouple were both enclosed in a 7-inch-wide, 9-inch-long, and 13-inch-high stainless steel container which held the working fluid (water or mercury). The top of the container was covered with the stainless base plate which carried the plate supports and the probe driving mechanism. These were all put in a constant temperature bath used to keep the bulk temperature of the fluid inside the container constant.

Figure 9 is a photograph of the probe driving mechanism and container in the constant temperature bath. The bath was a twenty gallon stainless steel tank filled with rust inhibitor and water to a level which at least covered the base plate. The bath was equipped with cooling coils and electrical heating coils. With these coils the bath temperature could be controlled to within one degree centigrade, but this control was not precise enough for the experiments having small heat fluxes. Therefore, it was found that for the case of small power, simply allowing the bath to remain at room temperature without cooling or heating provided the most constant temperature.

Nanovoltmeter and Strip-Chart Recorder:

The output of the thermocouple was measured by a "Keithley 180 Digital Nanovoltmeter", then recorded on a "Sanborn 296 Recorder".

The nanovoltmeter, having the functions of zero suppression and range selection, could measure the E.M.F. of the thermocouple to the accuracy of 10 nanovolts, which is equivalent to approximately $0.0025^{\circ}C$. The Sanborn recorder, having the functions of pen position, standardization, calibration, zero suppression, and attenuation, could be adjusted to plot the temperature profiles. For a fixed vertical position of the thermocouple, the temperature versus horizontal distance was plotted in the Y-versus-X coordinates of the recorder paper.

(4.2) Procedure

Experimental Preparation:

The first step in the procedure was to set up the equipment, that included the following preparations: the container was immersed in the constant temperature bath and the working fluid was added into the container. The end of the thermocouple was located at the trailing edge of the plate

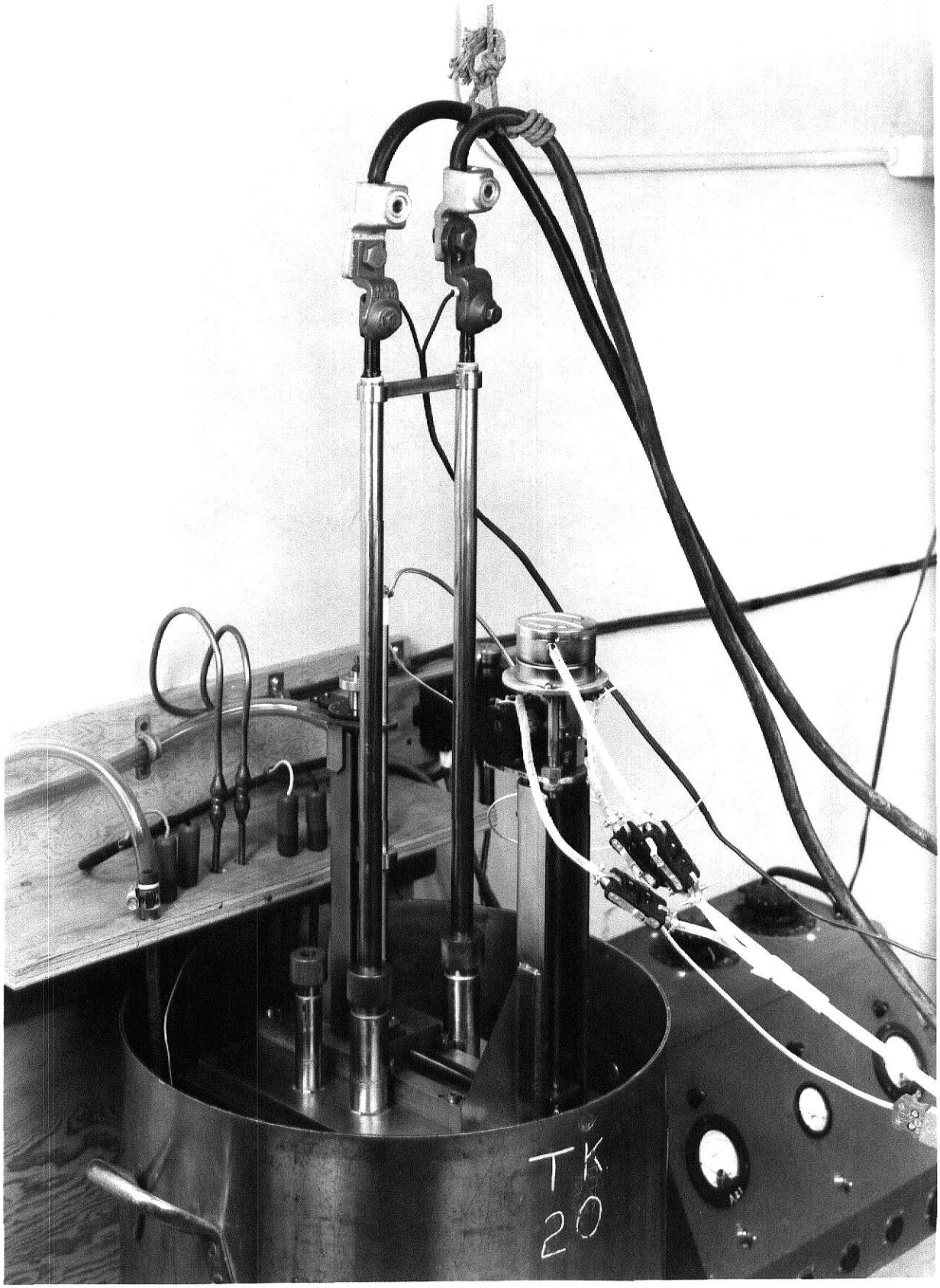


Figure 9. Probe Driving Mechanism and Container in Constant Temperature Bath.

and the base plate was clamped on the top of the container. Water and anti-rust were added to the constant temperature bath. A small Dewar flask was filled with water at room temperature to serve as the reference temperature of the thermocouple cold junction. The power lines were connected tightly and the proper amperemeter and voltmeter were installed.

Experimental Run:

The D.C. power supply was turned on, and the desired voltage was supplied to the plate. The circulation pump was turned on to maintain the uniform temperature throughout the constant tamperature bath. The thermocouple was moved to a distance far from the plate, then the knob of the vertical movement positioning mechanism was turned to set the thermocouple up or down at a desired vertical position. Before recording data, the Sanborn recorder was warmed up for about half an hour and the calibration and standardization were checked every time.

The equipment was allowed to run at least three hours for water to establish the steady state for the small power runs. Mercury is a good conducting material and it took a shorter time to reach steady state than water. Steady stste was assumed when the temperature at the plate was constant. After steady state was attained, the zero supression of the nanovoltmeter was set to zero when the thermocouple was located at the bulk. Hence, when the zero suppression switch of the nanovoltmeter was turned to "off", the value shown on the nanovoltmeter was the relative temperature of the bulk with respect to the reference temperature of the thermocouple cold junction. Also the zero suppression and attenuation of the Sanborn recorder were adjusted so that the profile would be plotted within the scale of the recorder paper.

"One millimeter per second" paper speed was used. All the profiles

were plotted from the bulk to the plate and then, by reversing the motor, from the plate to the bulk. In this manner, the effects of the increasing (or decreasing) of the bulk temperature could be minimized by taking the average value of two profiles for data analysis. When the thermocouple probe was turned to move toward the plate, the temperature remained at a constant value for awhile at the beginning (that meant the thermocouple was still in the bulk), then increased more and more rapidly as the probe approached the plate, and finally the temperature increase stopped. The point where the temperature stopped increasing was assumed to be the plate. After this, the positioning mechanism motor was reversed to bring the thermocouple probe from the plate back to the bulk.

The same procedure was repeated for many vertical positions up the plate and power levels.

As the profiles were recorded, the voltage, current, chart speed, vertical position up the plate, the temperature of the thermocouple cold junction, the temperature of thermocouple hot junction measured on the nanovoltmeter, and the zero suppression of the nanovoltmeter, were written down. The final dimensionless temperature and distance were calculated from these data and the recorded profiles.

The experimental runs for water and mercury were essentially the same except that the resistance was carefully checked in the mercury runs to detect any short circuiting through the mercury. If a short circuit occurred the resistance would drop, then the equipment had to be taken apart and the plate and its junction to the copper rods were sprayed with a very thin coat of paint. This coating could eliminate the short circuit.

5. Data Analysis

(5.1) Data Treatment

All the experimental data were plotted on the strip-chart recorder. A typical millivolt-versus-time plot (equivalent to temperature versus distance) contained two parts; first, a profile with the probe moving from the bulk to the plate and, second, one with the probe moving from the plate back to the bulk. For water both profiles were generally smooth. But for mercury the recorded curve had a peculiar shape. After the probe started moving away from the plate, the temperature response curve was constant for a short period, then showed a sudden drop. The explanation for this is that as the probe began to move away, it stuck to the plate for a short period before moving. This jump in the curve made the determination of the exact plate position difficult. Extrapolation of the second profile could be used, however, this procedure contained extrapolating errors. Therefore, if the jump was too sharp, it was most accurate to take the data points only from the first profile for analysis.

The temperature and distance at each point were calculated from the known bulk temperature, plate temperature, and the characteristics of the driving mechanism, then transformed into dimensionless variables. All the calculations were carried out on an IBM digital computer. The computer program is presented in Appendix A. The data reduction is described in detail on the following paragraphs.

First, the thermocouple E.M.F., in millivolts, at the plate and in the bulk were computed from the measured values together with the known temperature of the thermocouple cold junction and the zero suppression of nanovoltmeter. The E.M.F. of each data point was then calculated by

the linear interpolation of computed plate and bulk temperatures. The resulting voltages were converted into degrees centigrade by a least-square fit fourth-order polynomial of the copper-constantan thermocouple calibration (shown in Appendix B).

Next, all the physical properties were evaluated at a reference temperature which was based on a weighted average of 70% of the wall temperature and 30% of the bulk temperature [60]. The physical properties, including density, viscosity, thermal conductivity, coefficient of thermal expansion, and Prandtl number, were calculated at this reference temperature by fourth-order polynomial equations [33].

Then, the overall resistance of, and the total power dissipated at, the combination of the plate, copper rods, and contacts, were calculated from the measured voltage and current. The resistance of the plate was computed at the plate temperature by a second-order polynomial equation which was obtained from the characteristics of the plate. The heat flux at the plate was calculated from the surface area of the plate and the power consumed by the plate. The power consumed by the plate was determined from the total power multiplied by the ratio of the plate resistance to the overall resistance. The local Nusselt and modified Grashof numbers could be evaluated with the physical properties, heat flux, and the vertical position up the plate.

Then, the distance of the thermocouple horizontally away from the plate as measured in millimeters of chart scale was converted to centimeters of distance by means of the motor rotation speed, the pitch of screw, and the recording paper speed.

Finally, the temperatures in degrees centigrade and the distance in centimeters were transformed into dimensionless forms by dividing each

by a proper quantity.

Because the data points were taken from two profiles, these dimensionless data points did not constitute a smooth curve any more. Therefore, these dimensionless data points were fitted with a semi-logarithmetic, least-squares, polynomial equation to obtain a representative smooth profile. This curve fitting was done by an IBM scientific subroutine and the computer program is shown in Appendix D. The resulting curve was plotted with the data points on the Calcomp Digital Incremental Plotter, Model 665.

A sample calculation giving the detail of data analysis is shown in Appendix C.

(5.2) Data Error Source

In order to get small Grashof numbers, the power used was kept as small as possible, and the resulting temperature difference between the plate and the bulk was very small. Therefore, a little fluctuation from the steady state and slight inaccuracy of the instruments would cause a significant error in the final results. The following were the important sources of error:

1. The current was not constant due to the characteristics of the power supply, thus the resulting heat flux was not constant either. The fluctuation amplitude of the heat flux was about 0.1 Btu/hr-ft^2, which was less than 2% of the total heat flux.
2. The temperature of thermocouple cold junction increased slowly with time, hence the increasing temperature of the profile toward the plate contained the temperature increase of thermocouple itself. For example, in the smallest power case of 0.74 watts, the increase of thermocouple cold junction temperature was about 0.0004 mv, which was equal to 6% of the total temperature increase. But this error would

be canceled out if the data points for analysis were taken from both the toward and away profiles.

3. The constant temperature bath was used to keep the bulk temperature in the container constant, but the heat dissipated from the vertical plate would cause the bulk temperature to increase slightly. For example, in the longest run of mercury, the increase of bulk temperature during one run was about $0.01^{\circ}C$.

4. Taking temperature data from the X-Y Sanborn plot had an accuracy to within 0.5 mm on the chart scale, which was 2.5% of the smallest total temperature range (20 mm).

5. The estimation of distance away from the plate could be made to an accuracy of within 1 mm on the chart scale, which was less than 1.2% of the shortest total distance range (90 mm).

6. Results and Discussions

The temperature profiles for various power levels and vertical positions had been obtained with the equipment described in section 4, and were transformed into dimensionless plots with the data treatment procedures stated in section 5. The results are presented and discussed in the following sections. First, the reproducibility and stability of the experimental data are checked. Next, the curve fitting technique for this work is discussed. Then the dimensionless profiles obtained by curve fitting are plotted for several parameters -- namely, the power level, the vertical position up the plate, and the local Grashof number -- to examine the dependences of the profiles on these parameters. Finally, the heat transfer results are correlated in terms of the local Nusselt and Grashof numbers.

(6.1) Reproducibility and Stability of the Experimental Data

Some of the experiments at various power levels and vertical positions were rerun. The results are shown in Figures 10, 11, and 12. The data points of the initial and duplicated runs are denoted with different symbols. The solid line is the best curve fit for the two sets of data. From the figures, it is seen that the data sets of two separate runs are very agreeable. Some are even overlapped. These show the excellent reproducibility of the data.

In Figures 13, 14, and 15, two temperature profiles for mercury are given in each figure. One profile is the result of moving the probe toward the plate; the other is the result of moving the probe away from the plate. If the data were taken at steady state and if the probe movement had no effect, these two profiles would be identical. However, these figures show that the two profiles are not exactly identical in all the cases. The sudden drop in the curve as mentioned in the data treatment section

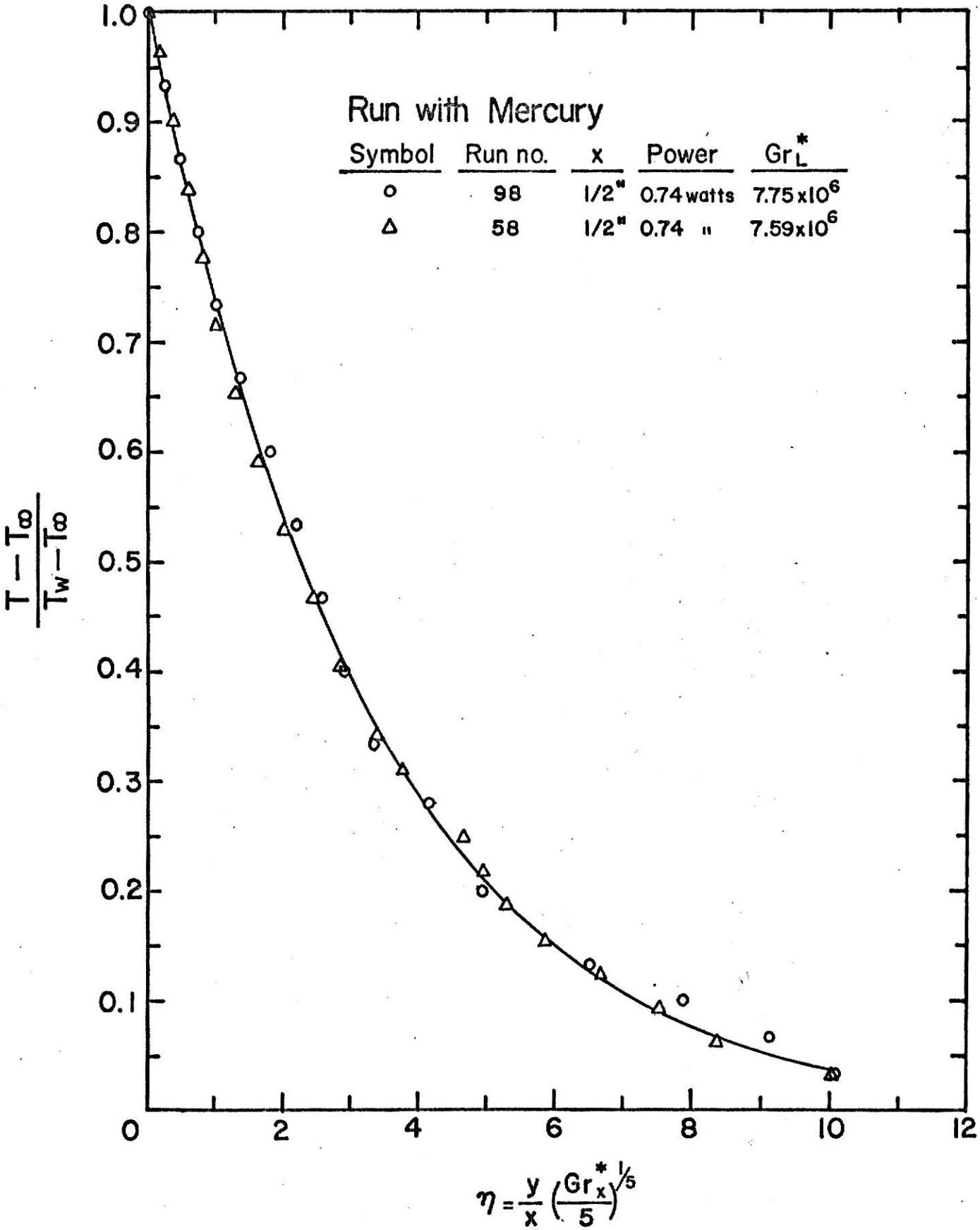


Figure 10. Duplicate Runs Made to Check Reproducibilit

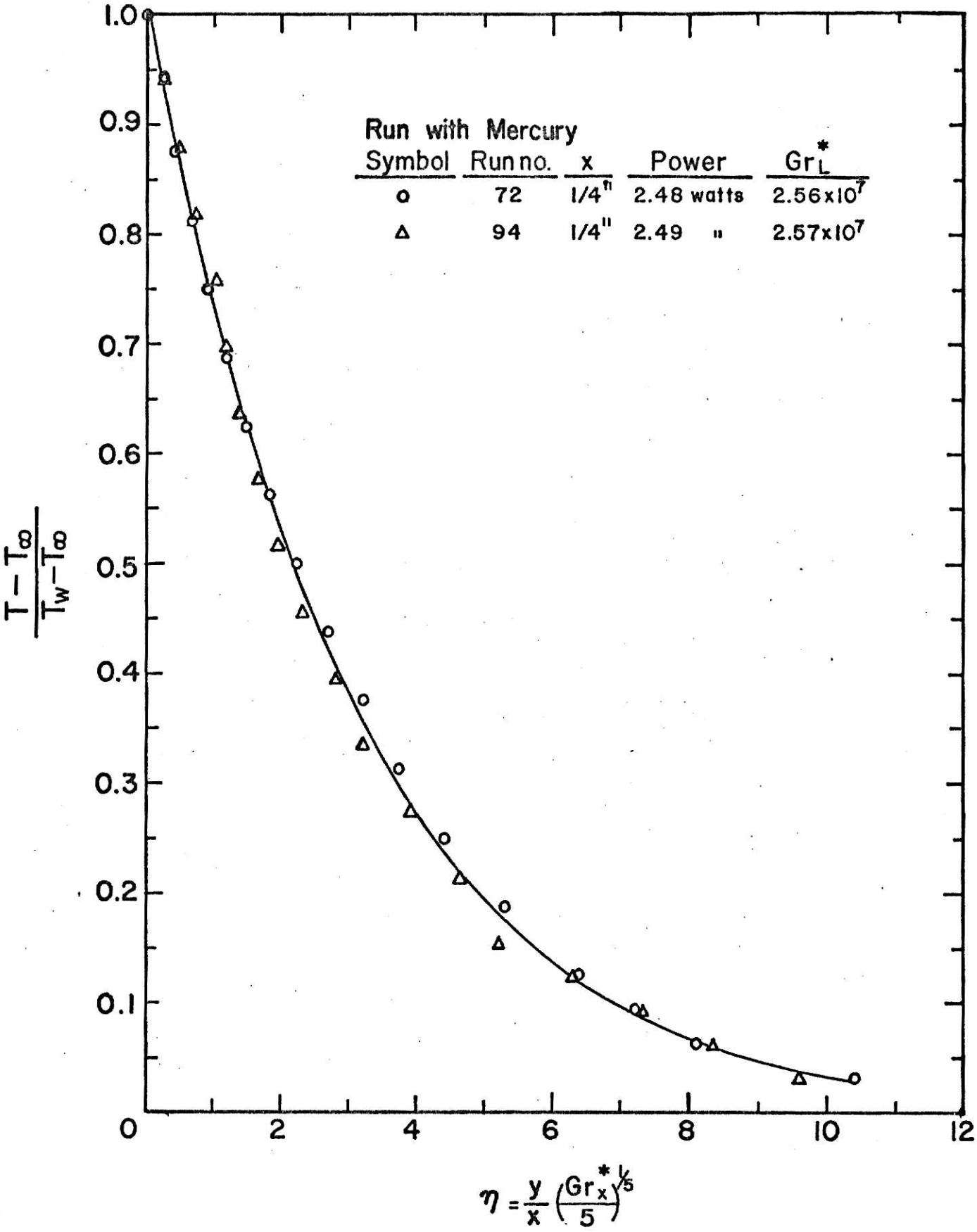


Figure 11. Duplicate Runs Made to Check Reproducibility

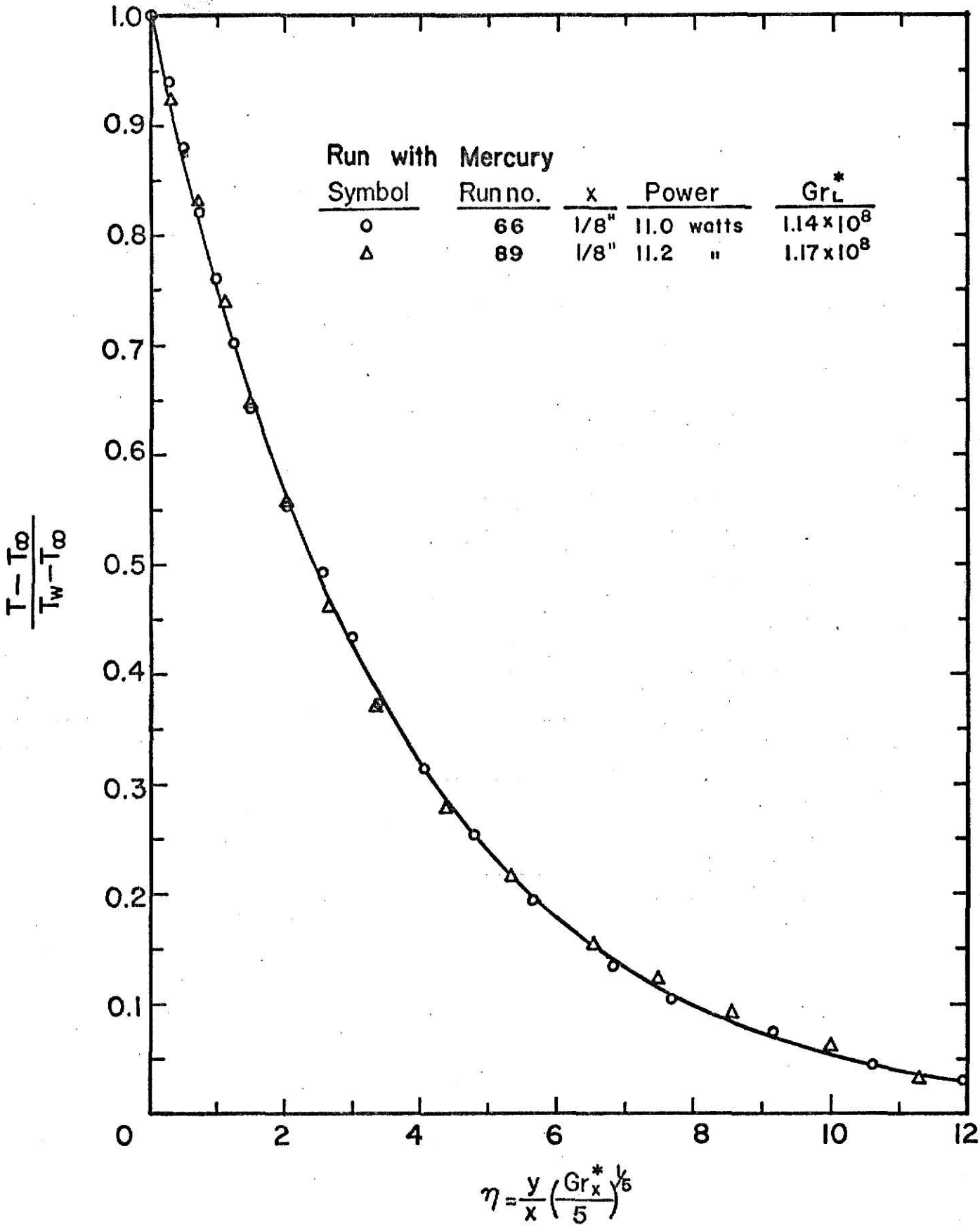


Figure 12. Duplicate Runs Made to Check Reproducibilit

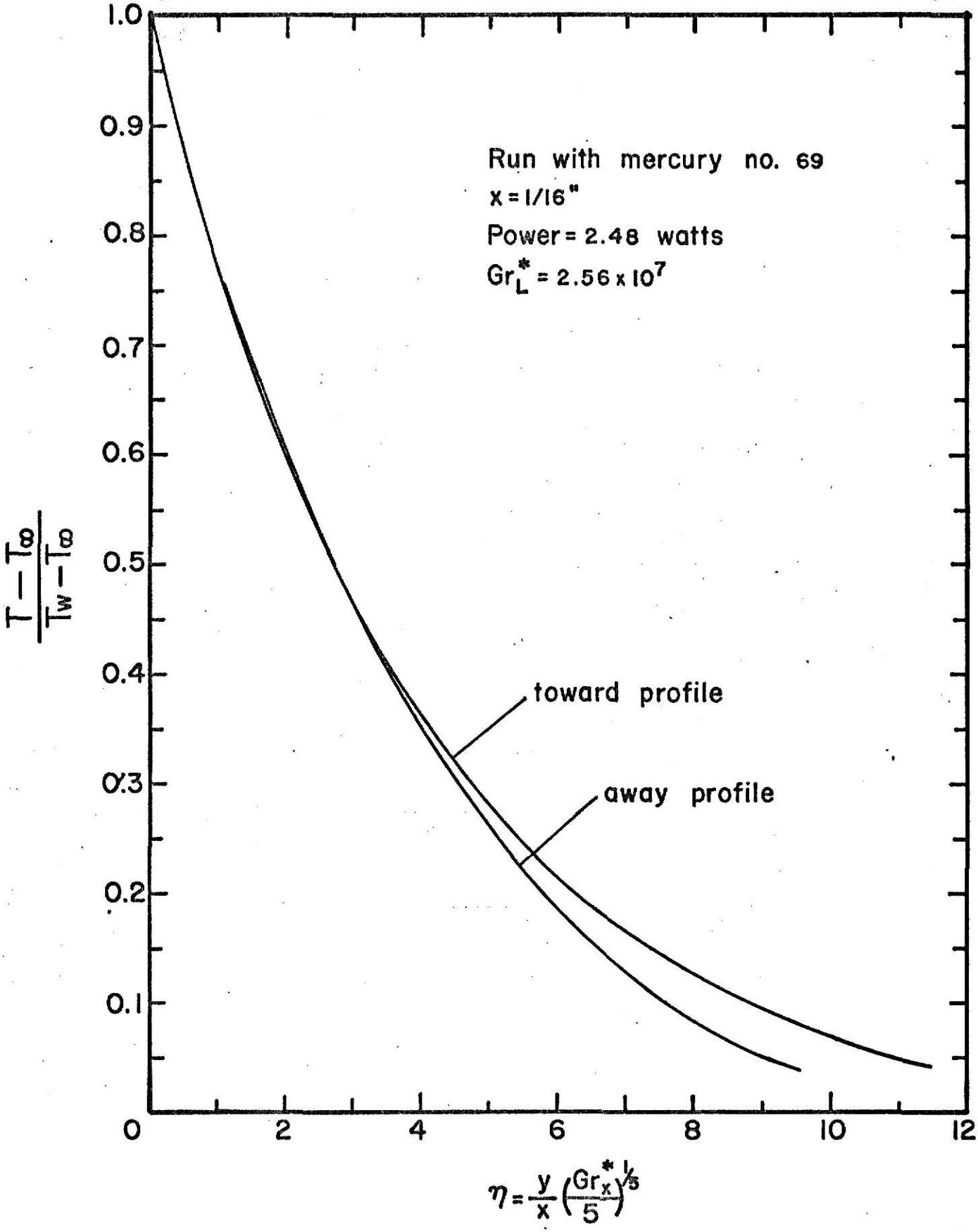


Figure 13. Comparison of the profiles toward and away from the plate.

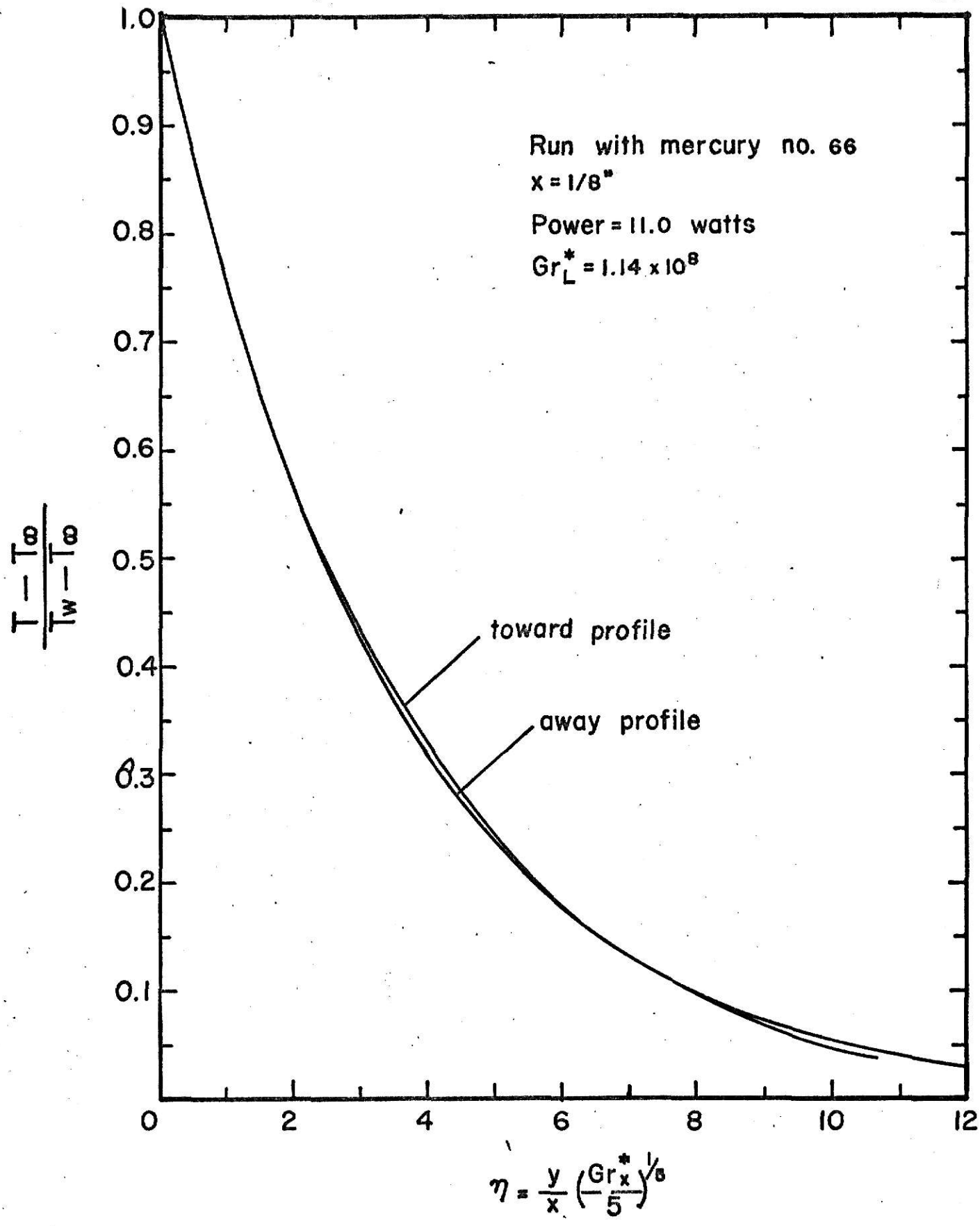


Figure 14. Comparison of the profiles toward and away from the plate.

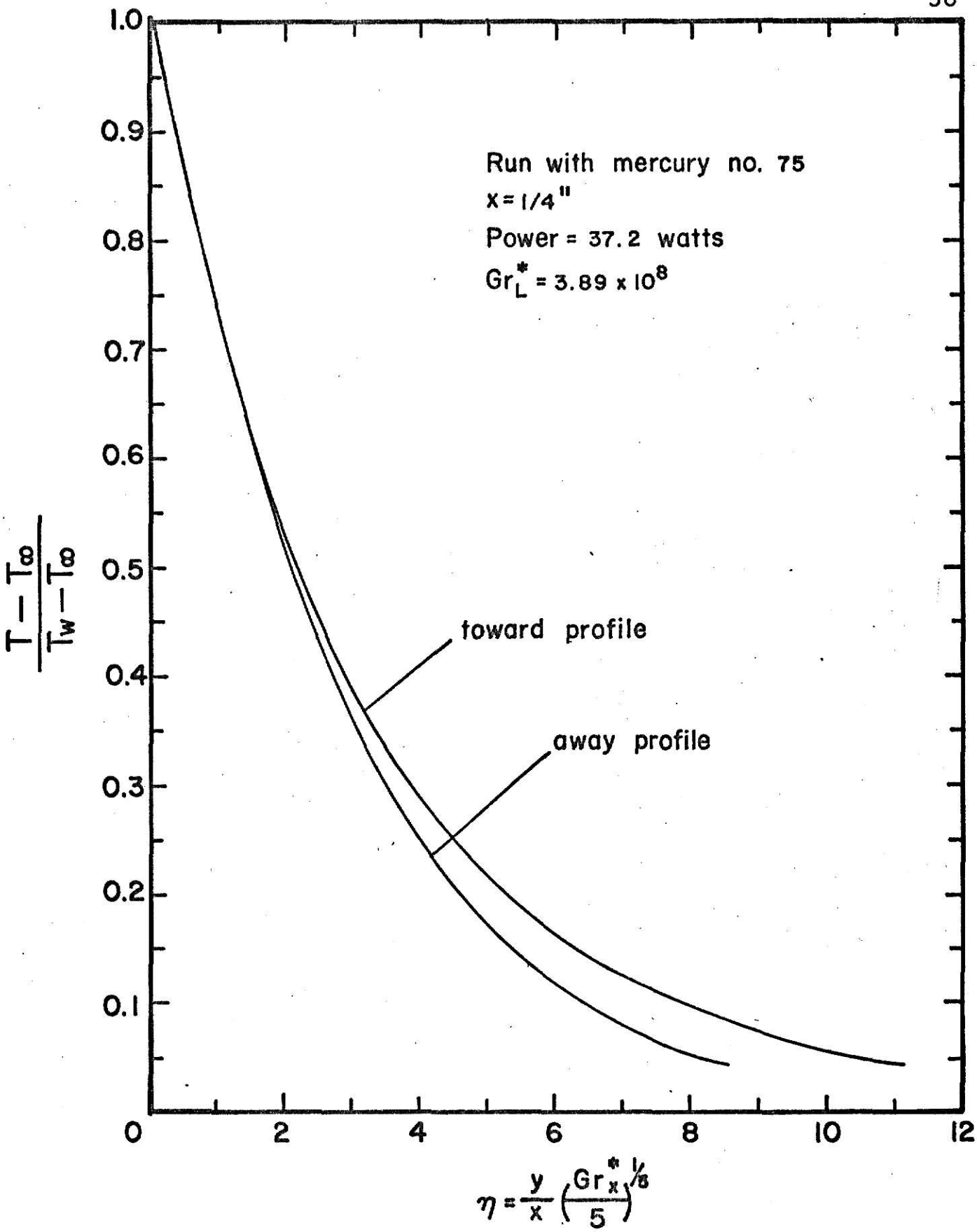


Figure 15. Comparison of the profiles toward and away from the plate.

makes the determination of the exact plate position very difficult. An extrapolated value for the plate position was used for the profile with the probe moving away. Even by extrapolation, the difference of the two dimensionless profiles was less than 8% of the total profile distance. Therefore, it is concluded that the experiments have a good stability. The dimensionless profiles generally were a result of fitting one curve to data points from both "toward" and "away" profiles.

(6.2) Curve-Fitting Technique

Occasional fluctuation of the power caused some scattering of the data. And data points for analysis were taken mostly from both the "toward" and "away" profiles; these points did not constitute a smooth curve. Therefore, a curve-fitting technique was needed to obtain a representative curve. Usually two sets of profile data were used for fitting. When duplication runs were made, four sets of profile data were used. A semi-logarithmetic, polynomial, least-squares curve fitting process was used with polynomials of one to six tried. The results are shown in Table 1 -- obviously the second-order polynomial, having the smallest deviation, fitted best and hence was chosen for the present purpose.

Order	Deviation
1	0.60
2	0.58
3	0.60
4	0.60
5	0.91
6	0.77

Table 1. Deviations of Curve-Fitting for Run Number 68.

(6.3) Dependence of Dimensionless Temperature Profiles on the Vertical Position up the Plate at a Constant Power Level (or a Constant Grashof Number)

Several sets of data at various positions up the plate, x, were plotted at a constant power level (i.e., constant heat flux or constant Gr_L^*). Figures 16 and 17 are the results of water at two power levels of 0.746 and 12.0 watts. The two dash lines are the Sparrow and Gregg's [63] numerical solutions. The figures show that there is a uniform dependence of the profiles on the vertical position such that the lower the position the higher the dimensionless profile is.

Figures 18, 19, and 20 are the same plots for mercury at power levels of 0.74, 2.48, snd 11.0 watts. The dash line represents the boundary-layer solution for Prandtl number of 0.024, which is obtained by the interpolation of the boundary-layer solutions for Prandtl numbers of 0.01 and 0.03 obtained by Chang, et al. [7]. The figures also show a uniform dependence of the profiles on the vertical position as was the case with water. But the dependence of the profiles for mercury is much more significant than that for water (although this fact is difficult to see because of the different scales in Figures 16 and 17 compared to Figures 18, 19, and 20). This is because the mercury is a much better conductor, the heat conduction through the leading edge goes much farther than that of water. Therefore, free convection of mercury starts at a lower position below the leading edge, so that the deviations from the boundary layer solution are much more appreciable.

The experimental results in Figures 18, 19, and 20 show a same profile tendency as that of the perturbation solutions. That is, as shown in Figure 5, profiles are located below the boundary-layer solution at small dimensionless distance, η, and are located above the boundary-layer solution at large η. However, the experimental profiles show a dependence on x contrary to that of the perturbation solutions. That is, a larger x gives

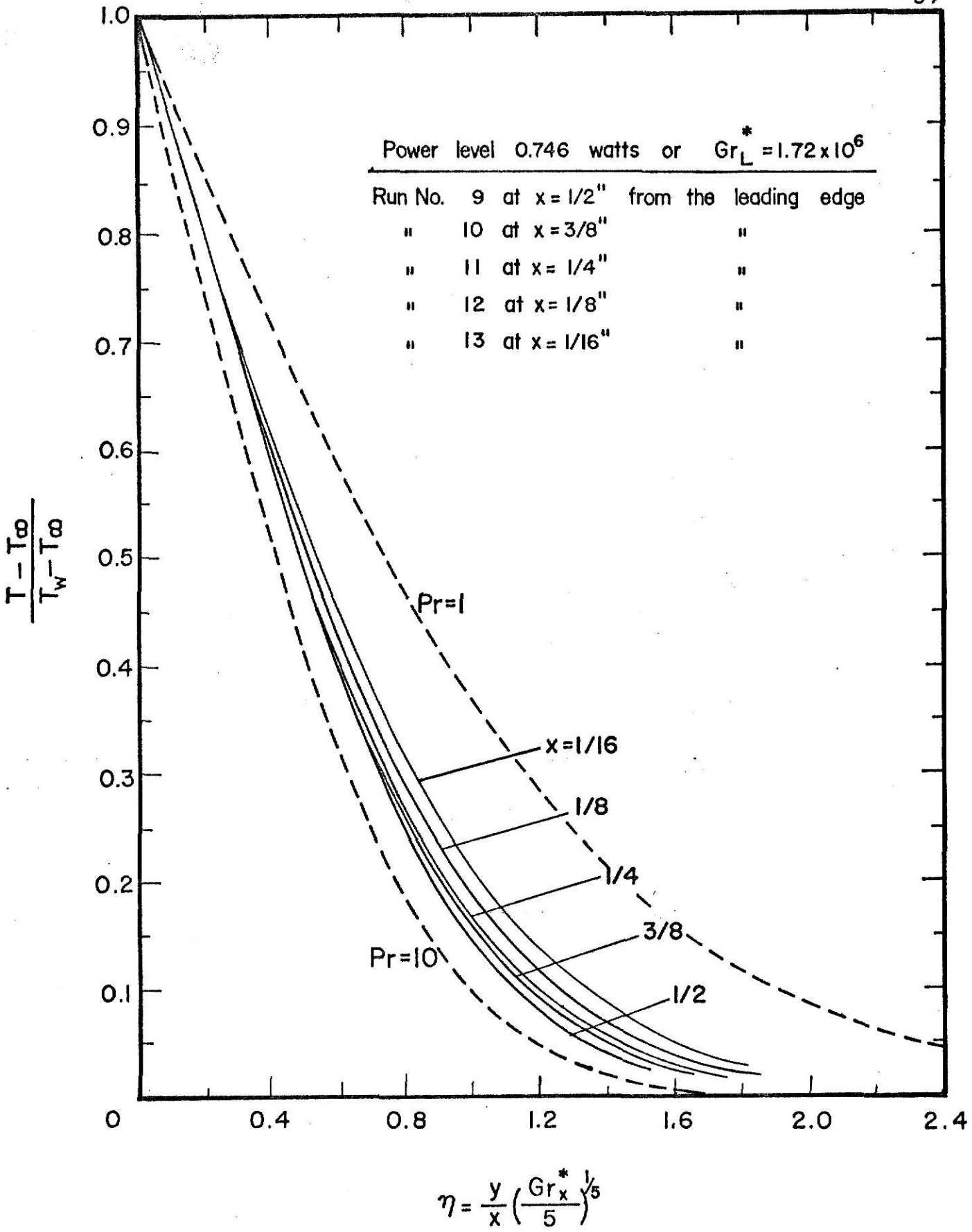


Figure 16. Effect of Vertical Position on the Dimensionless Temperature Profiles of Water at $Gr_L^* = 1.72 \times 10^6$.

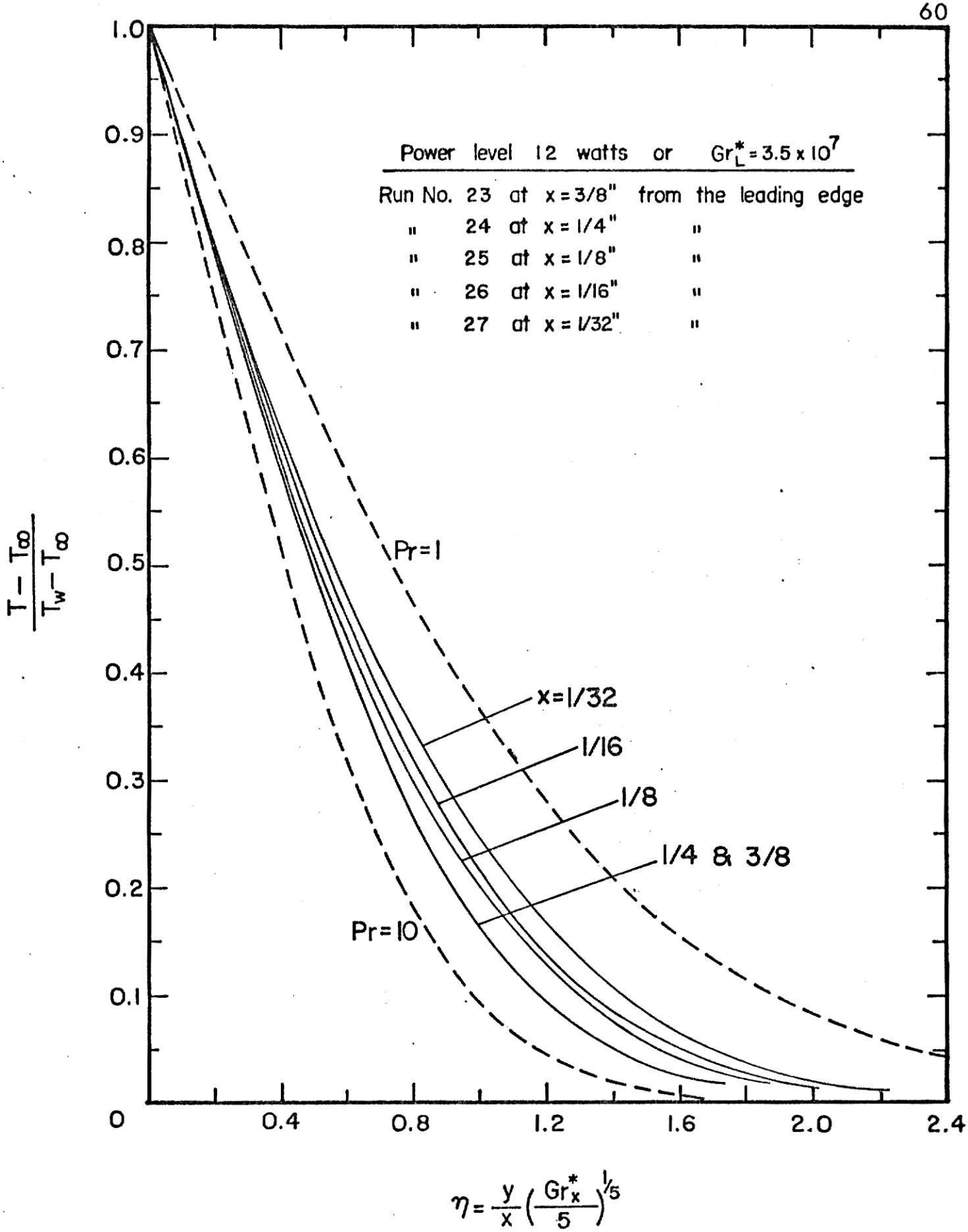


Figure 17. Effect of Vertical Position on the Dimensionless Temperature Profiles of Water at $Gr_L^* = 3.5 \times 10^7$.

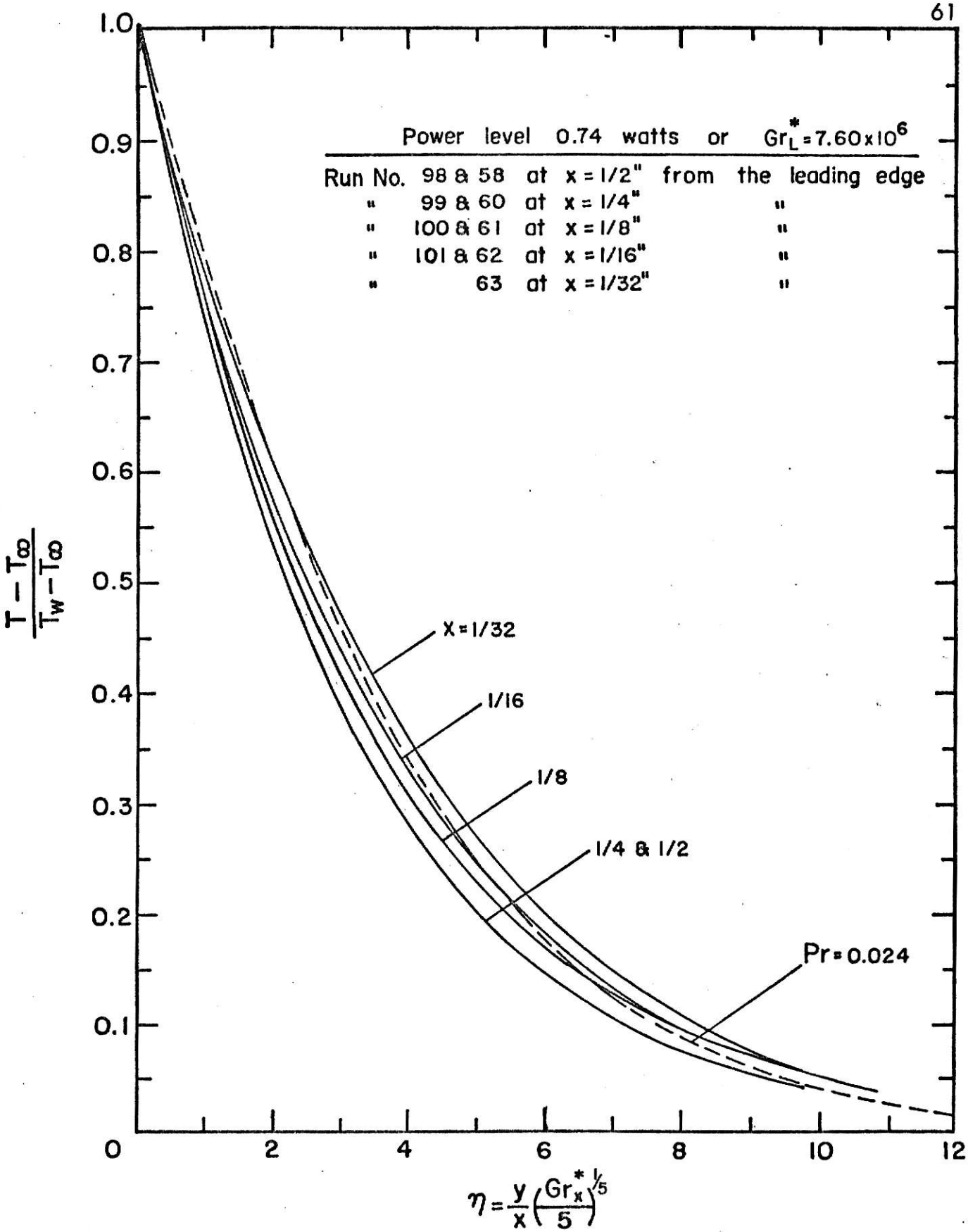


Figure 18. Effect of Vertical Position on the Dimensionless Temperature Profiles of Mercury at $Gr_L^* = 7.60 \times 10^6$.

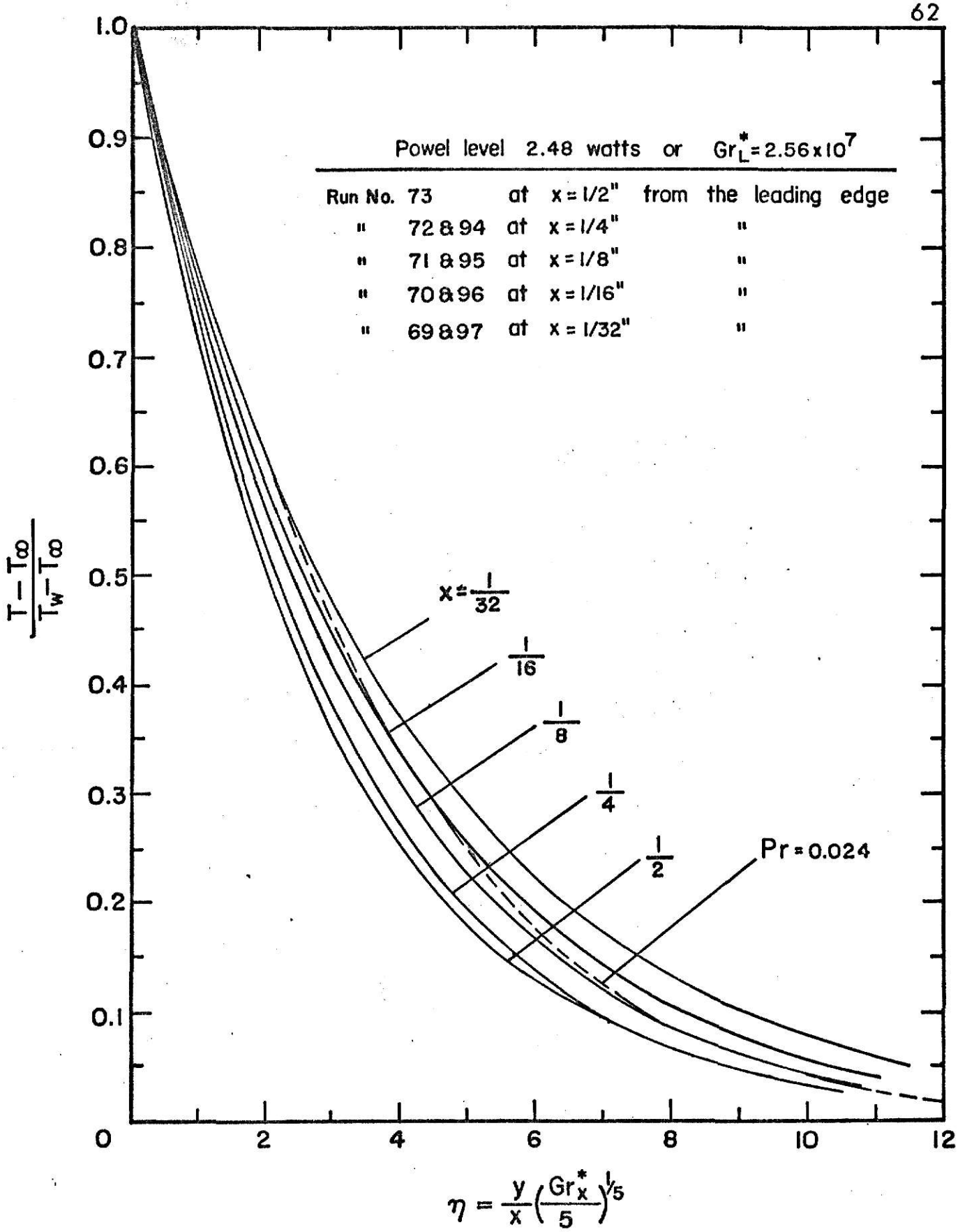


Figure 19. Effect of Vertical Position on the Dimensionless Temperature Profiles of Mercury at $Gr_L^* = 2.56 \times 10^7$.

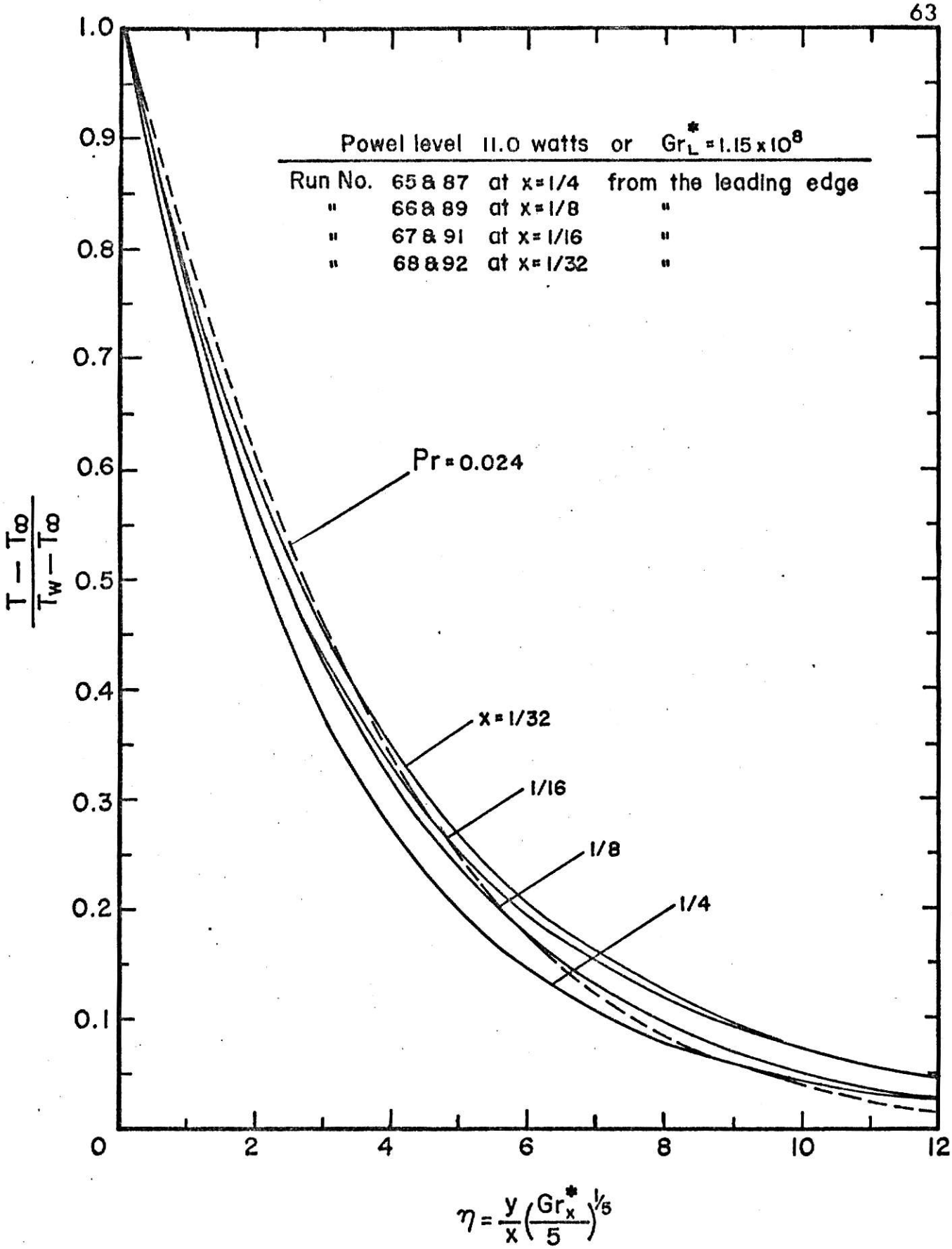


Figure 20. Effect of Vertical Position on the Dimensionless Temperature Profiles of Mercury at $Gr_L^* = 1.15 \times 10^8$

a farther downward shift from the dash line at small η.

The dependence of the profiles on x in Figures 18, 19, and 20 are the same as that in the upper part of the plate obtained by Chang [6]. In the lower part of the plate, the crossing of the profiles at small η occured in his results. This is absent in the present results -- namely, the present results are different from Chang's at small η and in the lower part of the plate, but both coincide in the other regions.

The present results are contrary to perturbation solutions, and Chang's results also partially disagreed with perturbation solutions. An explanation for this discrepancy may be the inaccurate approximation of the existing perturbation solutions. In perturbation solutions, Chang, et al. [7] considered only up to the first-order term and neglected the second- and higher-order terms. This neglection might have caused a significant error. The second- and higher-order terms might have negative effect and cause the direction of the dependence on x to reverse. Hence, it is recommended for further work to examine the effect by considering the second- and higher-order terms.

(6.4) Dependence of Dimensionless Temperature Profiles on the Grashof Number (or Power Level) at Fixed Vertical Position up the Plate

For a fixed vertical position on the plate, the dimensionless temperature profiles at several Grashof numbers (power levels) are plotted in Figures 21, 22, and 23 for water and Figures 24, 25, 26, and 27 for mercury.

Figures 21 through 23 show that there is, at most, a very small dependence of the profiles on the Grashof number. The small dependence of the profiles on the Grashof number is uniform such that a smaller Grashof number gives a lower dimensionless temperature profile.

Four groups of profiles at positions of 1/32, 1/16, 1/8, and 1/4 inches

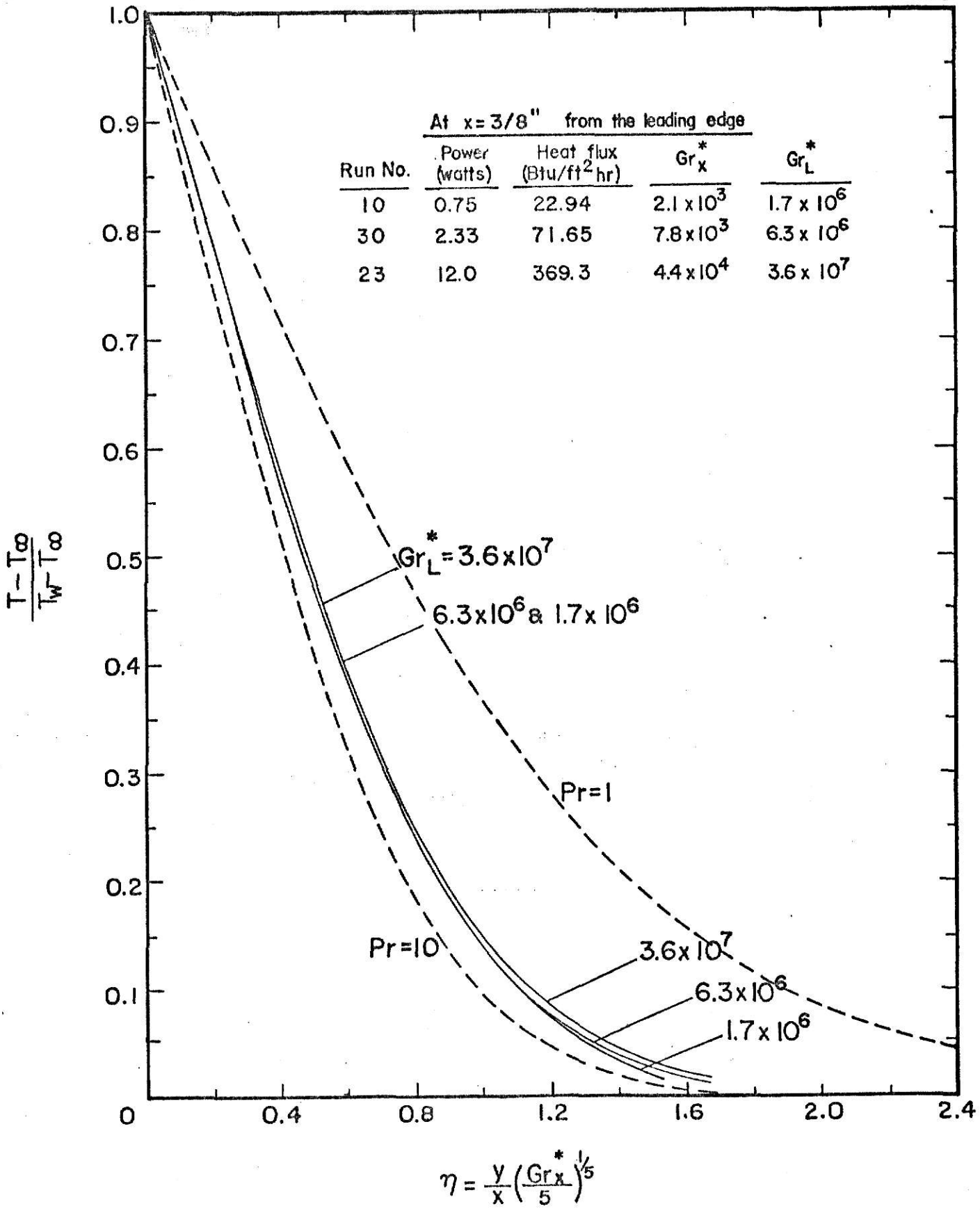


Figure 21. Effect of Grashof Number on the Dimensionless Temperature Profiles of Water at x = 3/8 inches.

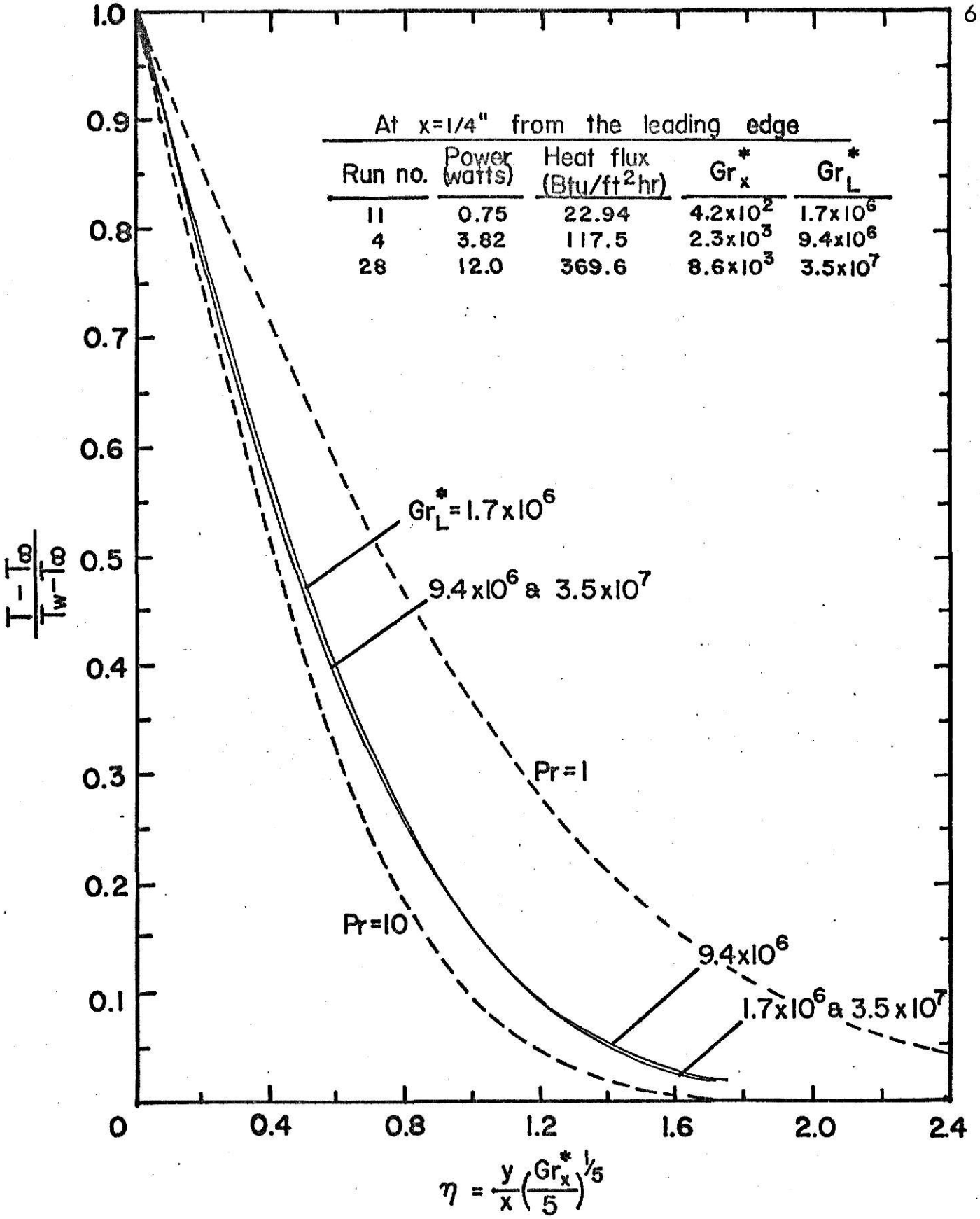


Figure 22. Effect of Grashof Number on the Dimensionless Temperature Profiles of Water at x=1/4 inches.

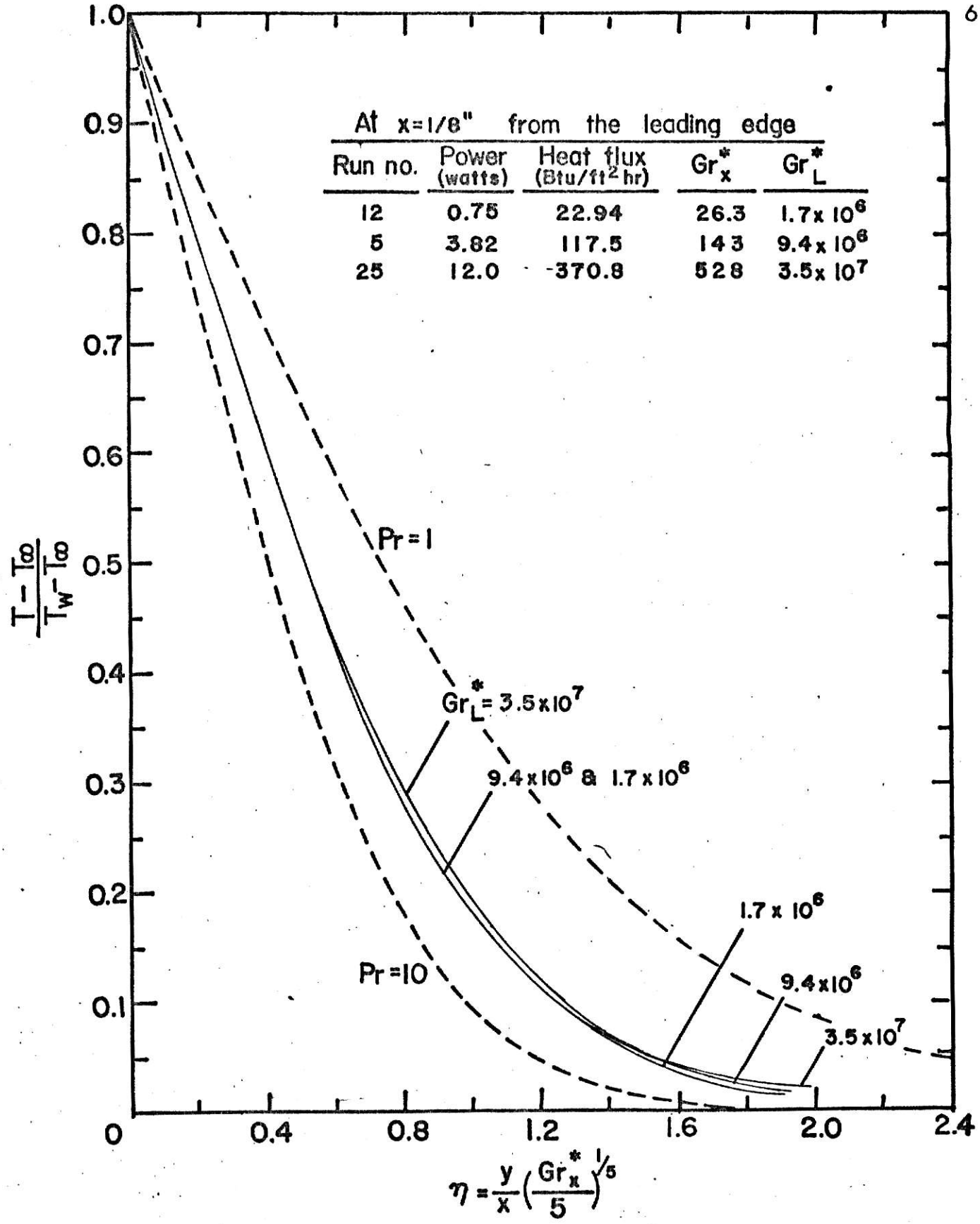


Figure 23. Effect of Grashof Number on the Dimensionless Temperature Profiles of Water at x=1/8 inches.

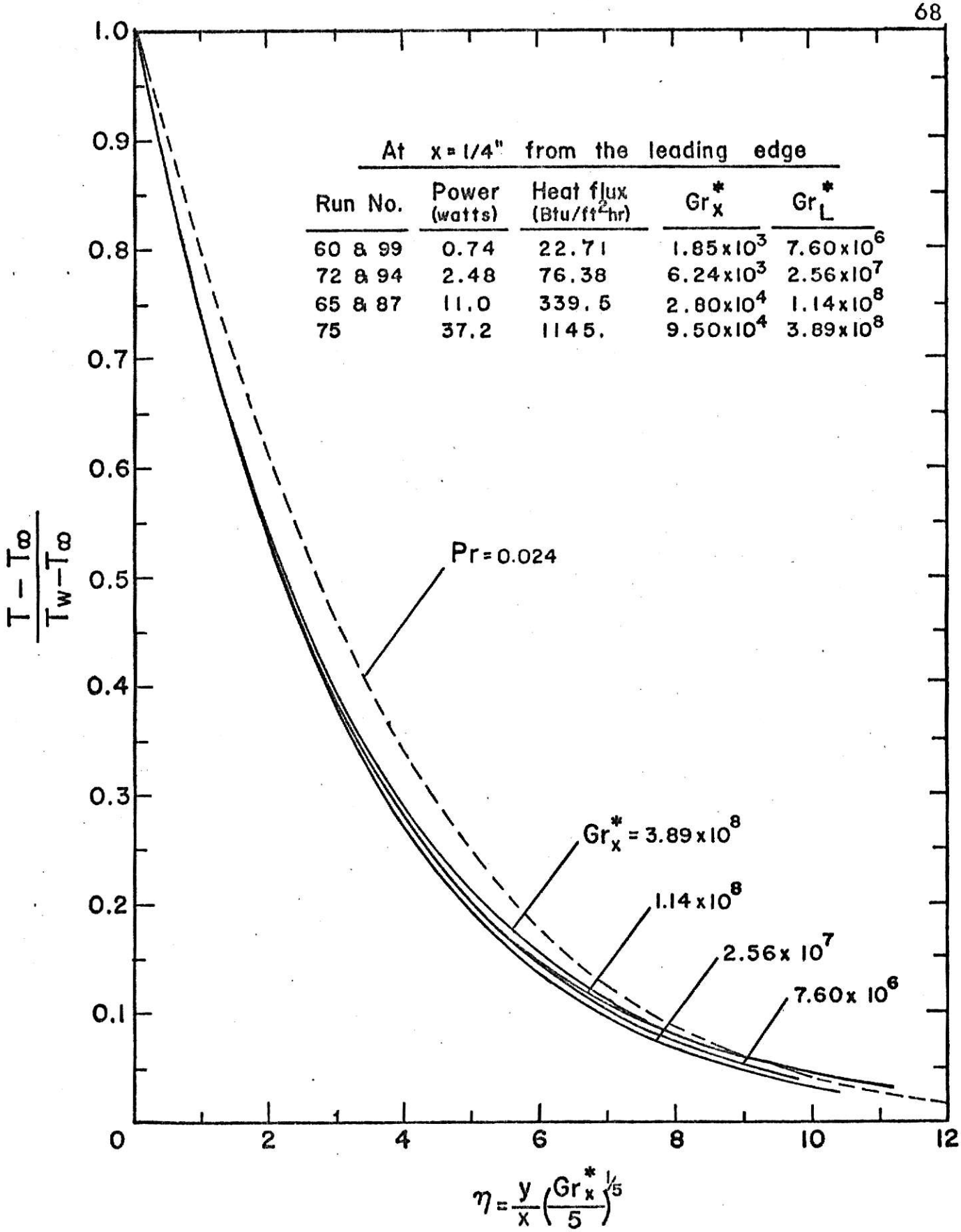


Figure 24. Effect of Grashof Number on the Dimensionless Temperature Profiles of Mercury at x=1/4 Inches.

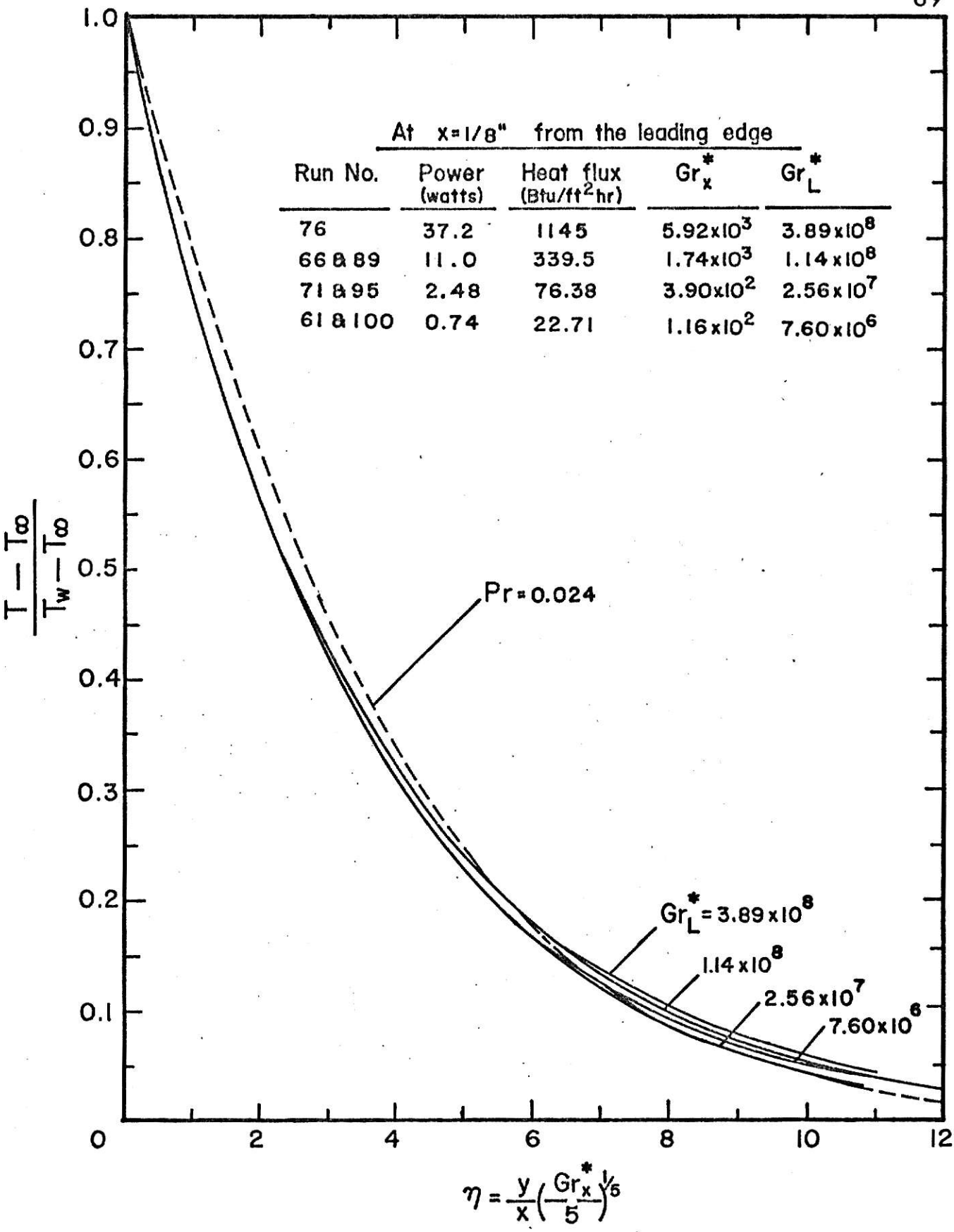


Figure 25. Effect of Grashof Number on the Dimensionless Temperature Profiles of Mercury at x = 1/8 inches.

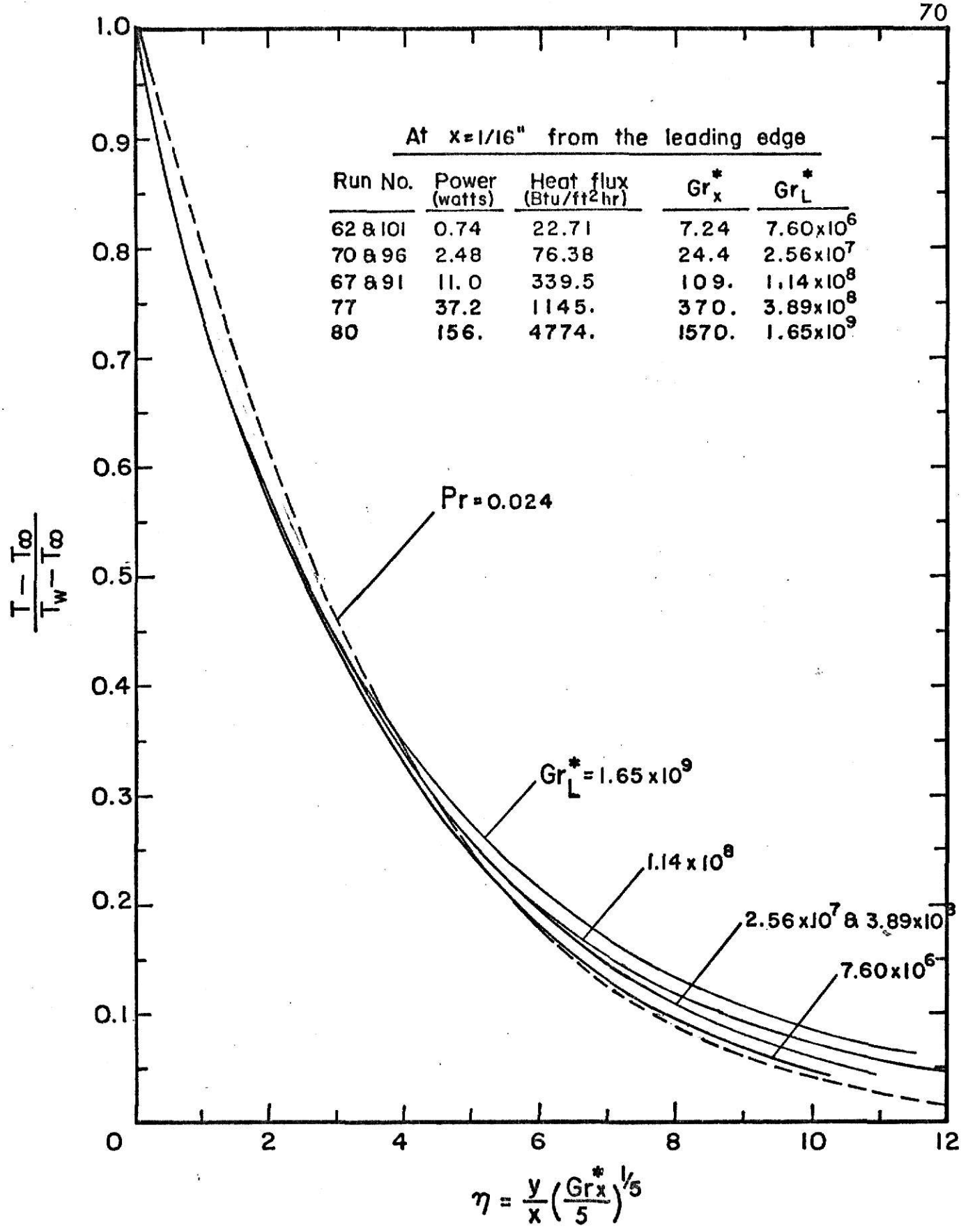


Figure 26. Effect of Grashof Number on the Dimensionless Temperature Profiles of Mercury at x=1/16 inches.

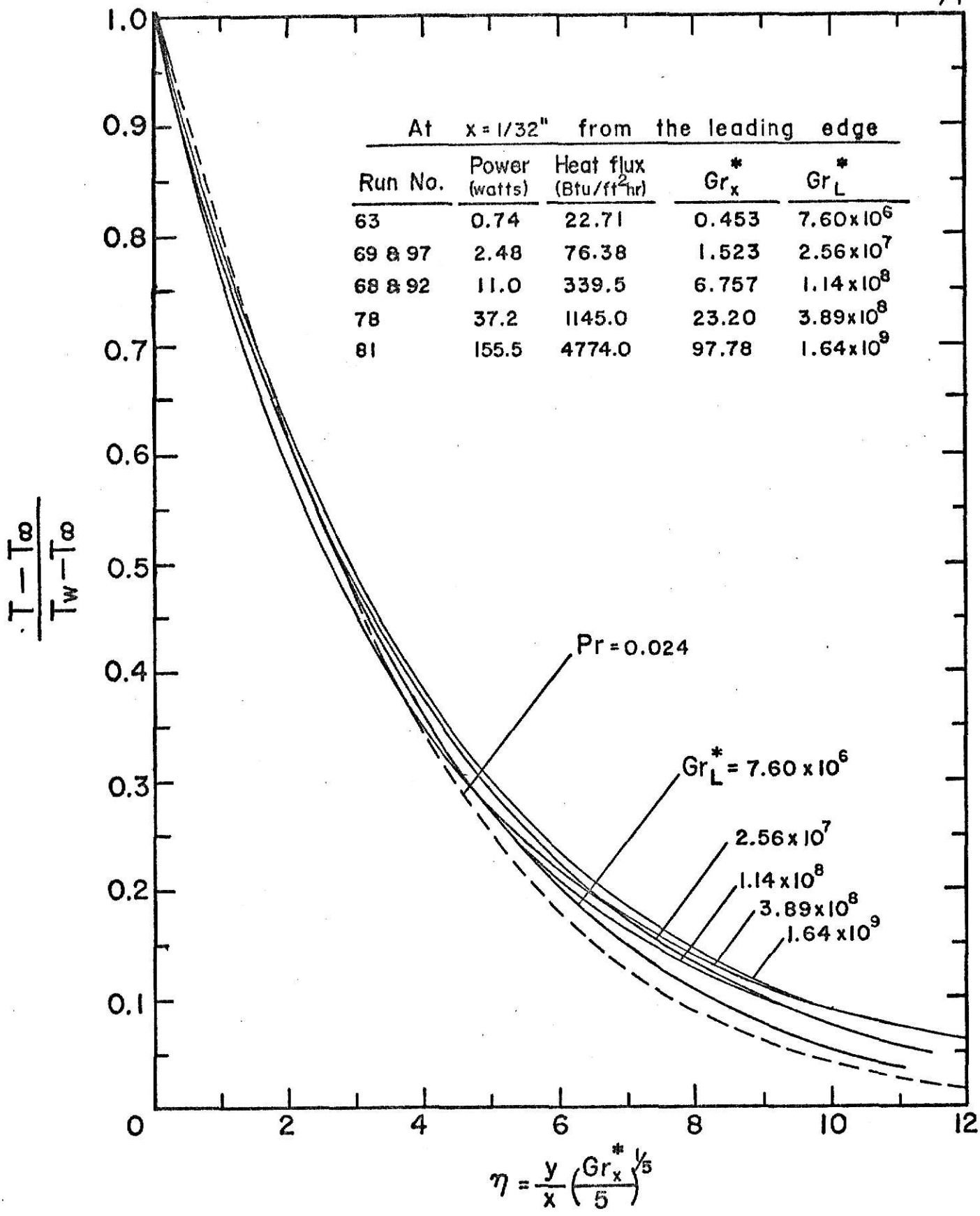


Figure 27. Effect of Grashof Number on the Dimensionless Temperature Profiles of Mercury at x = 1/32 inches.

from the leading edge are presented for mercury with the Grashof number as the parameter. These figures show that the dependence of the profiles on the Grashof number is more significant than that for water. This agrees with the theoretical prediction that the temperature profiles of the fluid with high conductivity is more dependent on the Grashof number than those of the fluid with low conductivity. The crossing of the profiles with the boundary-layer solution occurs. This is similar to the phenomenon in the previous plots of profiles at a constant power level (or Grashof number) with several positions up the plate. The trend of the dependence on the Grashof number for mercury is the same as that for water -- generally a smaller Grashof number causes a greater deviation from the boundary-layer solution at small η. In other words, the profile at small η tends to approach the boundary-layer solution by increasing the Grashof number. The distinction between the profiles at small η is clear in the 1/32 inch case and it diminishes gradually when the position gets higher and higher.

Because Chang [6] also had results for mercury at positions of 1/16, 1/8, and 1/4 inches from the leading edge, the present results are compared with his. The agreement in the dependence on the Grashof number is generally good except that his profiles are different at small η. The perturbation solutions of this kind are not available for comparison.

At a fixed vertical position, the higher the power the larger is the Grashof number hence the boundary-layer solution is more applicable. Consequently, the deviation from the boundary-layer solution becomes smaller when the Grashof number gets larger. The present results agree well with this prediction.

Comparison of the present results is also made with those shown in section (6.3). It is obvious that the dependence of the profiles on the

vertical position is much greater than the dependence on the Grashof number.

(6.5) Dependence of Dimensionless Temperature Profiles on the Vertical Position up the Plate (or on the Power Level) at Constant Gr_x^*

A set of dimensionless temperature profiles at a constant Gr_x^* could be obtained by increasing the position up the plate, x, and decreasing the power level, q, simultaneously and in the proper ratio. Because of the changes of the physical properties with the power used, it is not easy to get exactly the same Gr_x^*. Thus the same order of magnitude of Gr_x^* is regarded as constancy of Gr_x^*. Figures 28 and 29 are the dimensionless profiles in water at Gr_x^* equal to approximately 100 and 2×10^3, and Figures 30, 31, 32, and 33 for mercury at Gr_x^* equal to approximately 20, 100, 400, and 6×10^3.

For the temperature profiles at a constant Gr_x^*, both the position and power level can be the parameters, but the directions of dependence on x and q are reversed.

For water, the dependence of the profiles on the position, x, is that a smaller x gives a higher dimensionless profile. Same dependence on x for mercury in Figures 30 through 33 is obtained. That is, the profile at larger x (or smaller q) deviates much more from the boundary-layer solution. The dependence of the profiles on x at a constant Gr_x^* for water is smaller compared to that for mercury.

The dependence of the profiles on x at constant Gr_x^* agrees well with Chang's [6] results. In other words, both concluded that a smaller x (or a larger q) gave a higher dimensionless profile. This conclusion can also be drawn from the combined results of sections (6.3) and (6.4) -- the smaller the x is and the larger the q is; the higher the dimensionless profile is and the less the deviation is. Therefore, the results are very consistent.

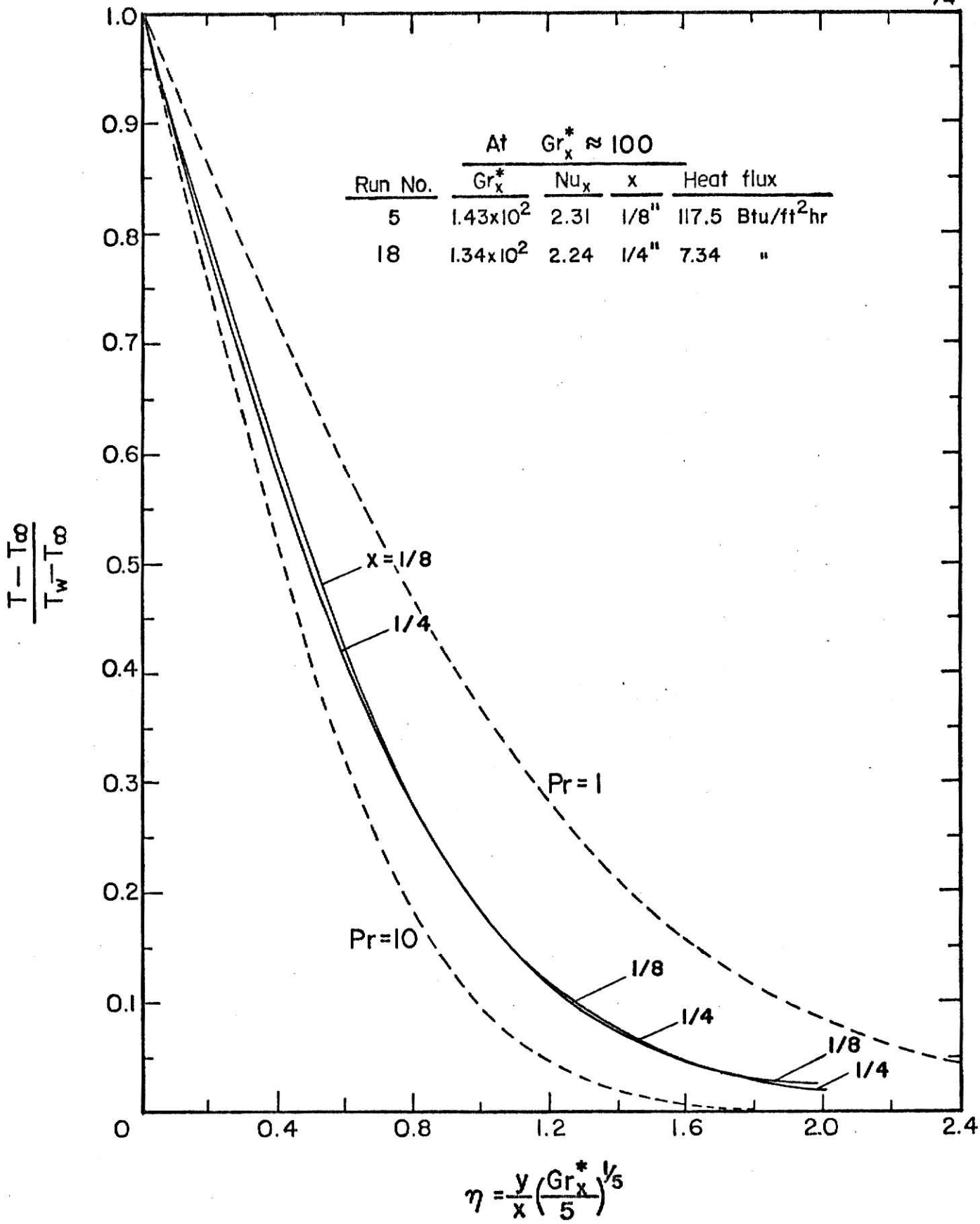


Figure 28. Effect of Vertical Position on the Dimensionless Temperature Profiles of Water at $Gr_x^* \approx 100$.

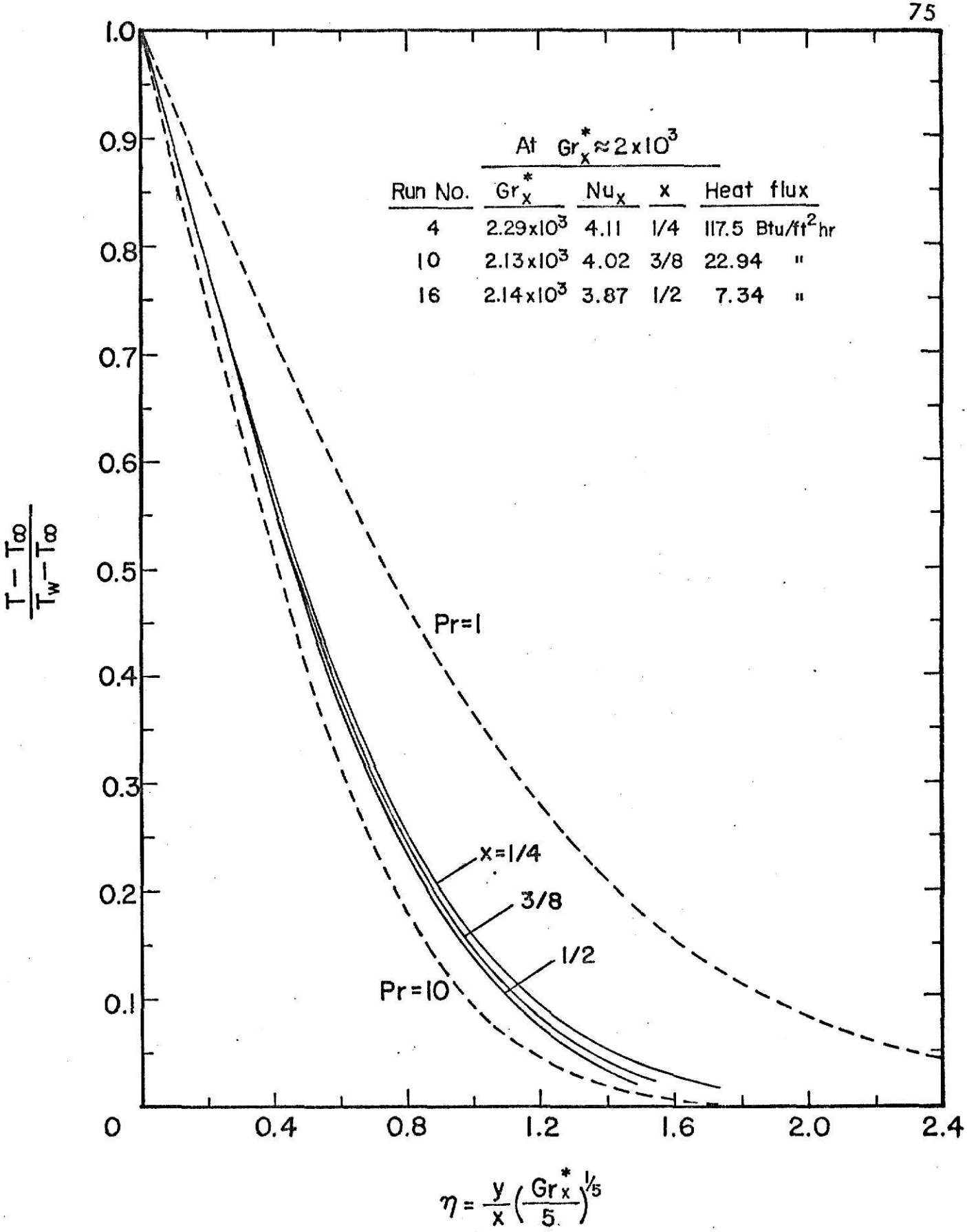


Figure 29. Effect of Vertical Position on the Dimensionless Temperature Profiles of Water at $Gr_x^* \approx 2 \times 10^3$.

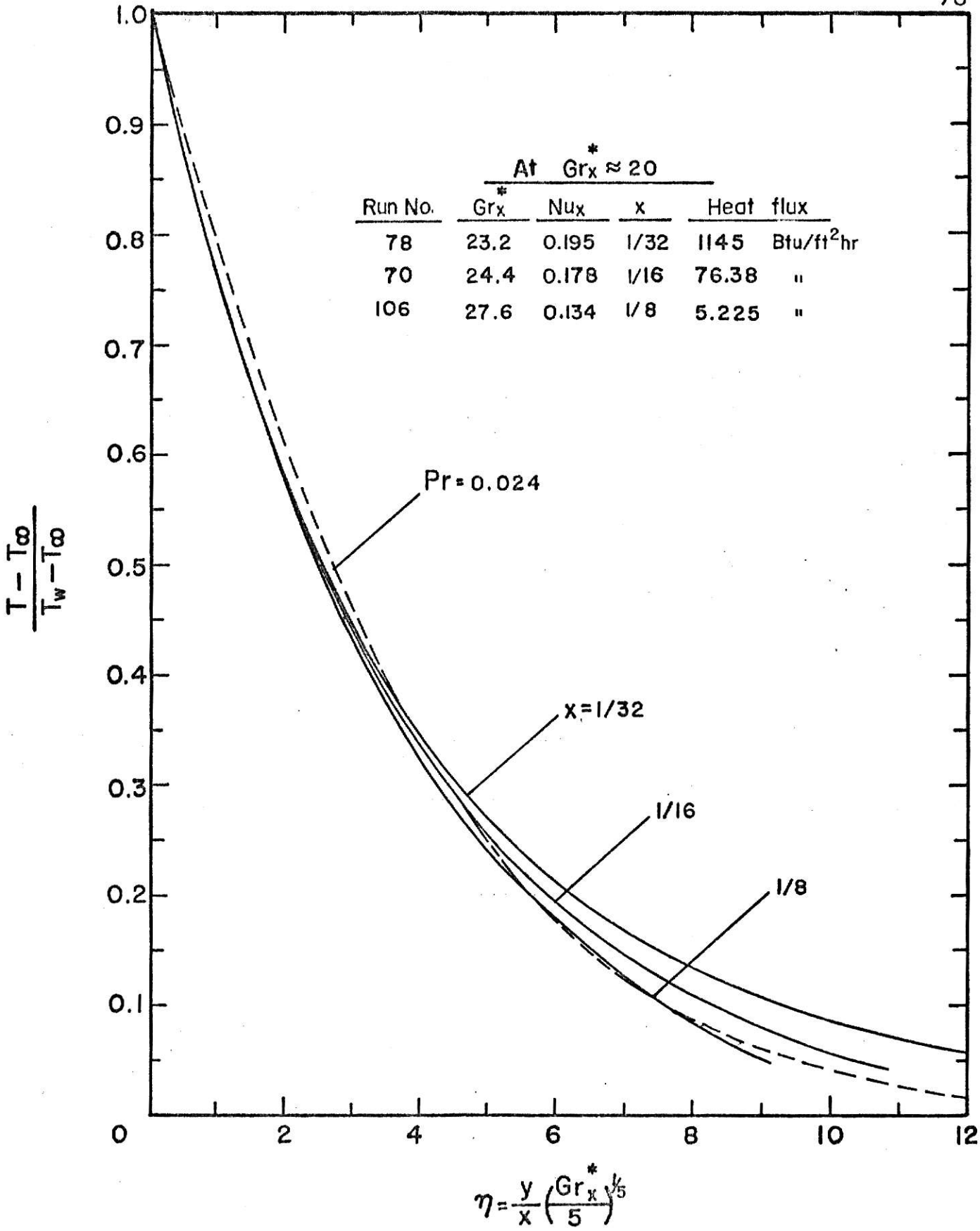


Figure 30. Effect of Vertical Position on the Dimensionless Temperature Profiles of Mercury at $Gr_x^* \approx 20$.

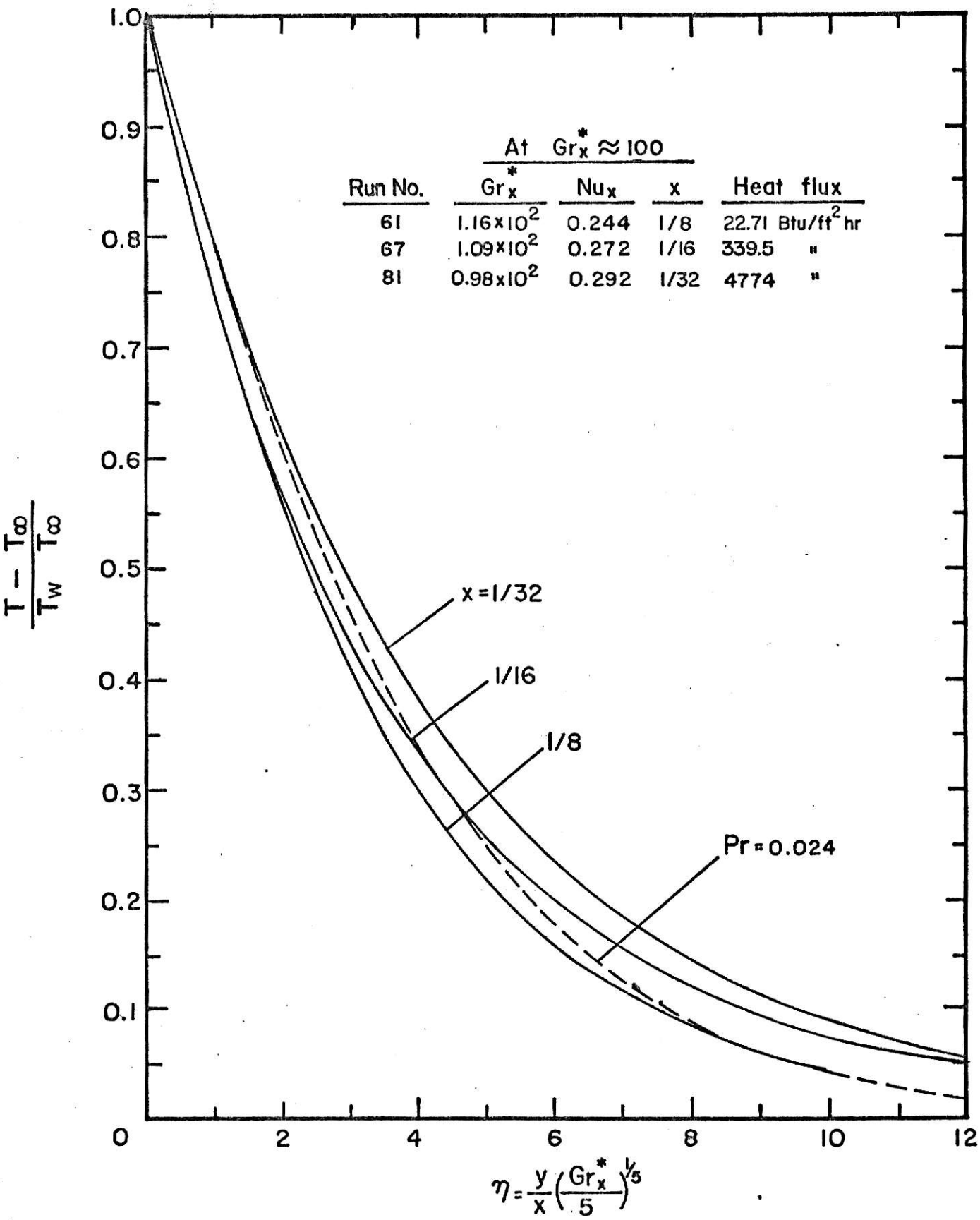


Figure 31. Effect of Vertical Position on the Dimensionless Temperature Profiles of Mercury at $Gr_x \approx 100$.

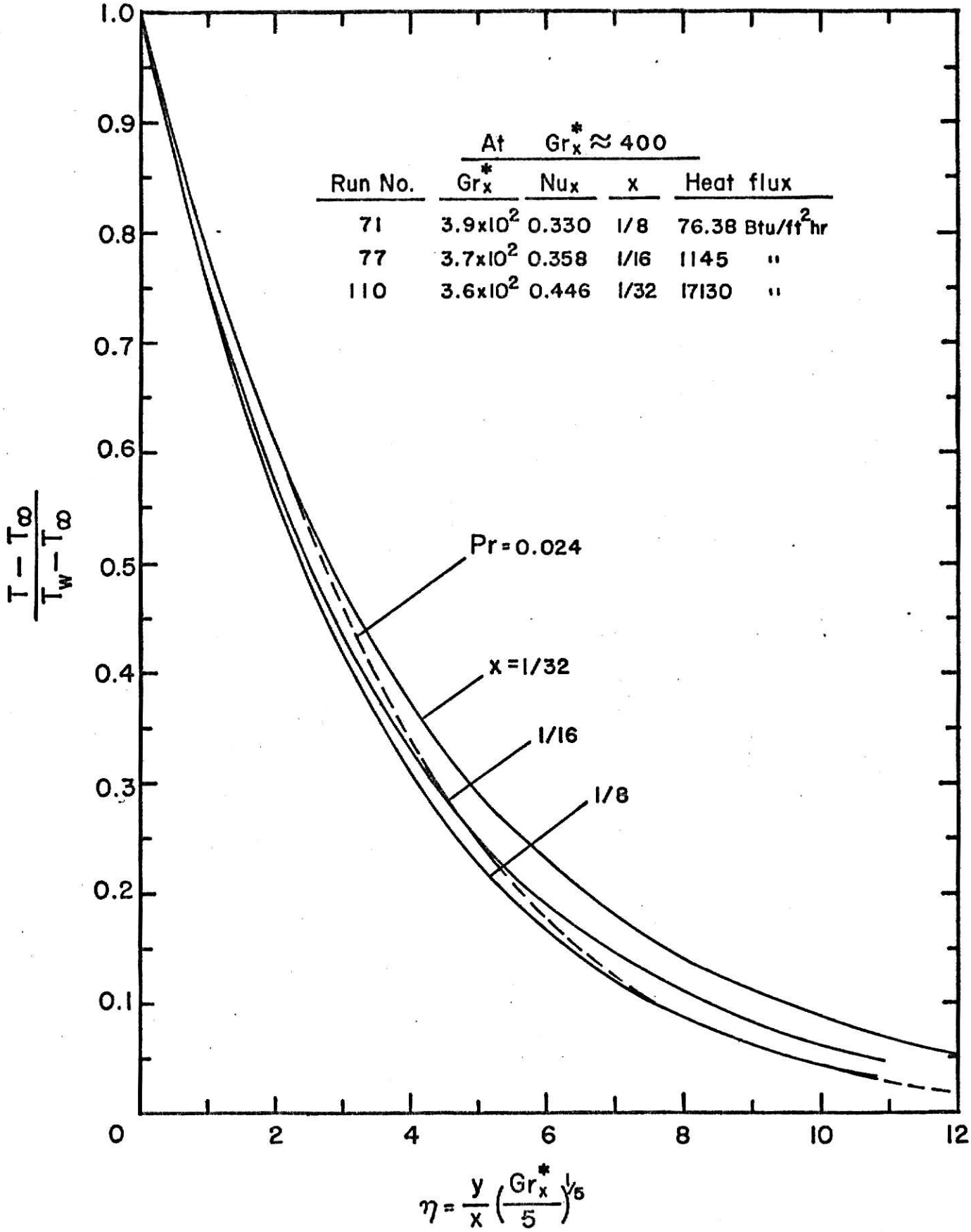


Figure 32. Effect of Vertical Position on the Dimensionless Temperature Profiles of Mercury at $Gr_x^* \approx 400$.

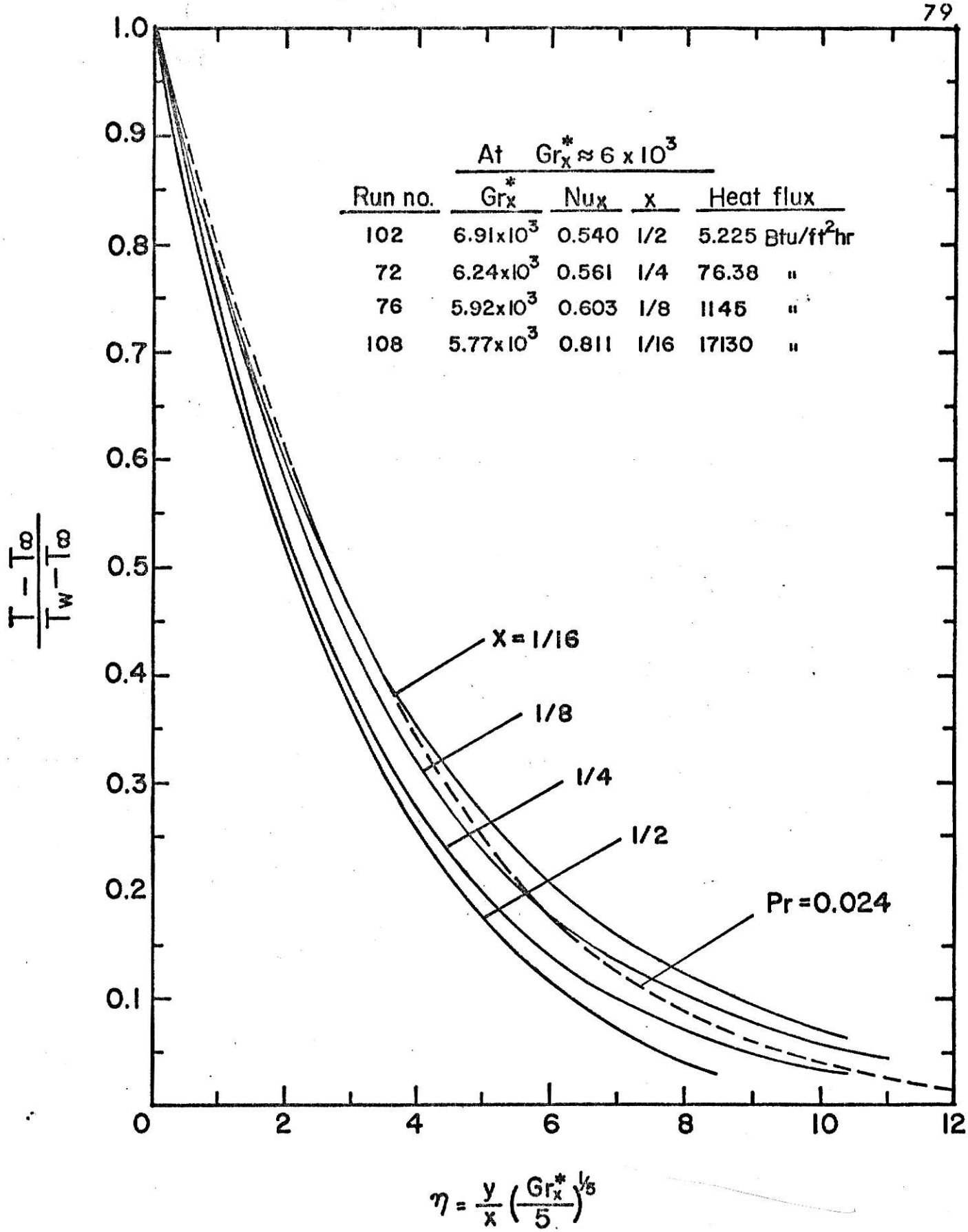


Figure 33. Effect of Vertical Position on the Dimensionless Temperature Profiles of Mercury at $Gr_x^* \approx 6 \times 10^3$.

The perturbation solutions are not available for this comparison.

(6.6) Heat Transfer Correlation

Sparrow and Gregg [63] using the boundary-layer theory obtained the following correlation:

$$\frac{Gr_x^{*\,1/5}}{Nu_x} = 5^{1/5}\theta(0)$$

where $\theta(0)$ depends on Prandtl number only. Mercury has Prandtl number approximate to 0.024, the above equation becomes:

$$\frac{Gr_x^{*\,0.20}}{Nu_x} = 6.3$$

Julian's [33] experimental results of mercury with the Grashof numbers ranging from 10^4 to 10^9 found a correlation of:

$$\frac{Gr_x^{*\,0.188}}{Nu_x} = 5.1$$

with the standard deviation of 0.021. Chang's [6] experimental data with the Grashof numbers ranging from 10 to 10^8 found a correlation of:

$$\frac{Gr_x^{*\,0.178}}{Nu_x} = 4.03$$

with the standard deviation of 0.033. Fifty data points were correlated for the present work. The correlation with the Grashof numbers ranging from 10^{-1} to 10^5 is:

$$\frac{Gr_x^{*\,0.204}}{Nu_x} = 9.70$$

with the standard deviation of 0.022. Four correlations are presented in

Figure 34 for comparison. The figure indicates that the Nusselt Numbers of present results are smaller than their theoretical values and are contrary to both Chang's [6] and Julian's [33] results, which had positive deviations from the theoretical values.

The explanations of this disagreement are that the Grashof numbers in the present experiment are extremely small and the temperature differences obtained experimentally are larger than the corresponding theoretical values. Though the deviations are negative, the correlation coefficient of 0.024 is approximate to the boundary-layer solution of 0.20, which means that the Nusselt number is proportional to one-fifth of the Grashof number.

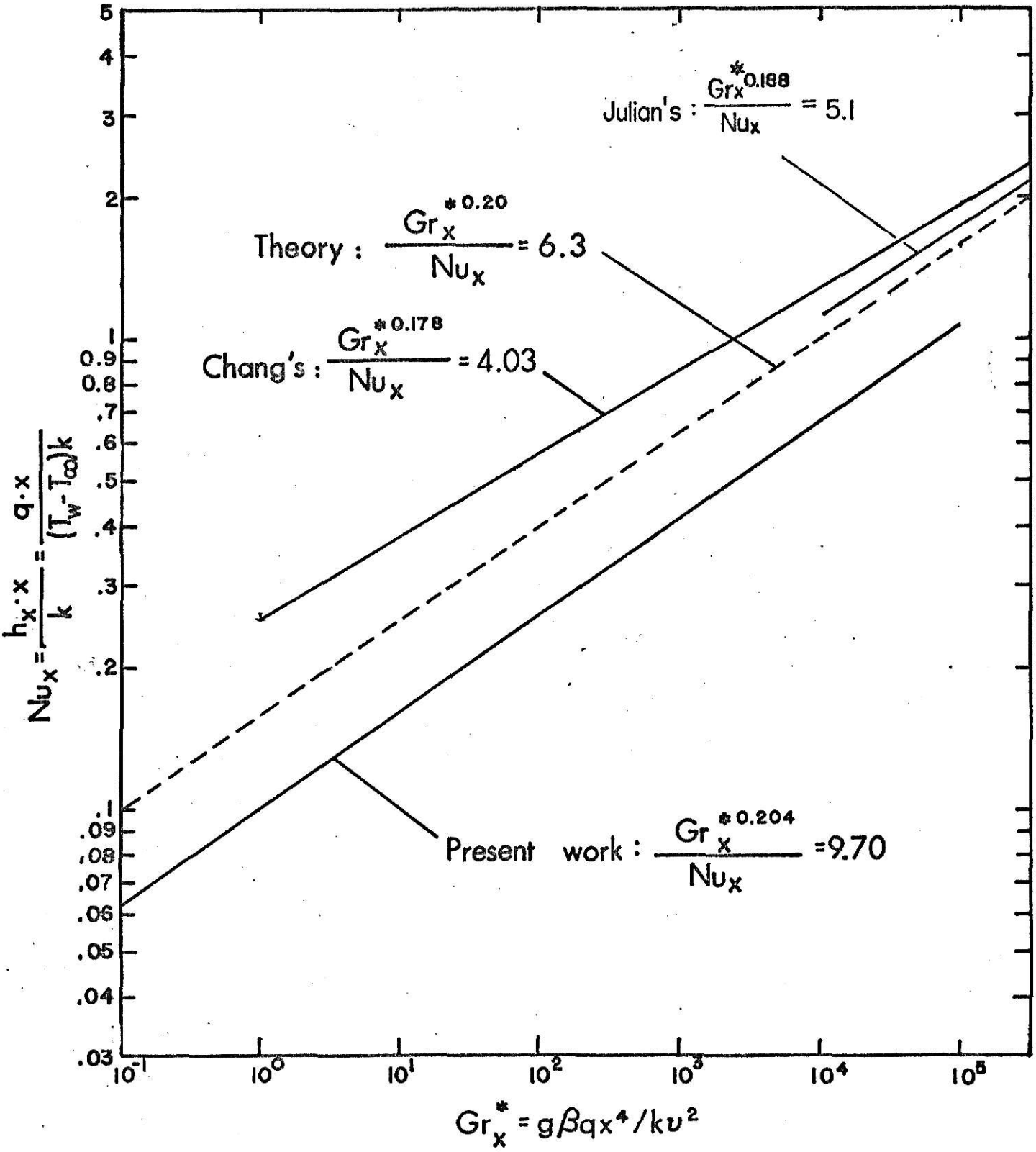


Figure 34. Correlations of Nusselt and Grashof Numbers.

7. Conclusions

Most of the free convection heat transfer analyses both theoretically and experimentally were based on the boundary-layer assumptions. The assumptions are invalid when the boundary-layer thickness is no longer negligible compared with the height of the plate. In 1967, Chang, et al. [7] obtained numerically the first-order perturbation solutions of free convection from a uniformly heated vertical plate for small Prandtl numbers. Almost no experimental investigations of free convection in liquid metal are done until recently. Julian [33] in 1967 and Chang [6] in 1970 did the free convection experiments of mercury in the moderate and small ranges of Grashof numbers respectively.

In the present work, free convection of water and mercury at extremely small Grashof numbers($10^{-1} < Gr_x^* < 10^5$) has been examined experimentally. The results showed significant deviations from the boundary-layer solutions in the dimensionless temperature-versus-distance plots for mercury and water due to small Grashof and Prandtl numbers. And the deviations for mercury were much more pronounced than those for water because the boundary-layer for mercury was about seven times thicker than that for water. The dependence of the dimensionless temperature profiles on the vertical position up the plate at a constant Grashof number (based on L) is such that the lower the position the higher the dimensionless temperature profile is, which is entirely contrary to that of the perturbation solutions obtained by Chang, et al. [7], and partially agrees with Chang's experimental results [6]. The dependence of the profiles on the Grashof number (based on L) at a fixed position up the plate is such that a smaller Grashof number gives a higher dimensionless temperature profile, and the dependence of the profiles on the position up the plate at a constant Grashof number (based on x) is such that

a lower vertical position gives a higher dimensionless temperature profile. Both dependences agree, in general, well with Chang's results [6], but no perturbation solutions are available for these two comparisons. The heat transfer correlation in terms of Nusselt and Grashof numbers has a coefficient of 0.204, which agrees well with the boundary-layer solution [63] but is greater than Chang's [6] and Julian's [33] experimental values.

NOMENCLATURE

C_p	heat capacity at constant pressure per unit mass, L^2/t^2T
C_v	heat capacity at constant volume per unit mass, L^2/t^2T
$F(\eta)$	zero-order velocity function, dimensionless
F', F'', F'''	derivatives of $F(\eta)$ with respect to η, dimensionless
$f_{oo}(\eta), F_m(\eta)$	first-order velocity functions, dimensionless
$f_{oo}', f_{oo}'', f_{oo}'''$	derivatives of $f_{oo}(\eta)$ with respect to η, dimensionless
f_m', f_m'', f_m'''	derivatives of $f_m(\eta)$ with respect to η, dimensionless
G	dimensionless gravitational acceleration defined by Eq. (30)
Gr_L^*	modified Grashof number based on L, $\frac{g\beta L^4 q}{k\nu^2}$, dimensionless
Gr_x^*	modified Grashof number based on x, $\frac{g\beta x^4 q}{k\nu^2}$, dimesnionless
g	gravitational acceleration, L/t^2
g_x	gravitational acceleration in x direction, L/t^2
g_y	gravitational acceleration in y direction, L/t^2
h_x	local heat transfer coefficient, M/t^3T
k	thermal conductivity, ML/t^3T
L	vertical length of plate, L
m	subscript for 0, 1, 2, . . .

Nu_x	local Nussel number, $\frac{h_x x}{k}$ or $\frac{qx}{k(T_w-T_\infty)}$, dimensionless
$0(\ )$	order of magnitude
P	dimensionless pressure defined by Eq. (29)
$P^{(0)}, P^{(1)}$	zero- and first-order pressure of P, dimensionless
P_X, P_Y	$\frac{\partial P}{\partial X}$, $\frac{\partial P}{\partial Y}$
Pr	Prandtl number, $\frac{\nu}{\alpha}$, dimensionless
p	pressure, M/Lt^2
p_∞	pressure at bulk, M/Lt^2
q	constant heat flux at plate, M/t^3
Ra_x	local Rayleigh number, $Gr_x Pr$, dimensionless
S	0.864806 . . .
T	temperature, T
T_R	reference temperature, T
T_W	wall temperature, T
T_∞	bulk temperature, T
t	time, t
u	vertical velocity component, ψ_y, L/t
$\bar{u}$	dimensionless vertical velocity component, $\bar{\psi}_{\bar{y}}$

v horizontal velocity component, $-\psi_x$, L/t

$\bar{v}$ dimensionless horizontal velocity component, $-\bar{\psi}_{\bar{x}}$

X transformed dimensionless vertical coordinate defined by Eq. (32)

x vertical coordinate, L

$\bar{x}$ dimensionless vertical coordinate, $\frac{x}{L}$, dimensionless

Y transformed dimensionless horizontal coordinate defined by Eq. (32)

y horizontal coordinate, L

$\bar{y}$ dimensionless horizontal coordinate, $\frac{y}{L}$, dimensionless

z rectangular coordinate, L

Greek Symbol

α thermal diffusivity, $\frac{k}{C_\rho \rho}$, $\frac{L^2}{t}$

β coefficient of thermal expansion, $-\frac{1}{\rho}\left(\frac{\partial \rho}{\partial T}\right)_p$, $\frac{1}{T}$

δ boundary layer thickness, L

ε constant parameter in series expansion, $Gr_L^{*-\frac{1}{5}}$, dimensionless

η similiarity variable, $\frac{Y}{(5X)^{1/5}}$ or $\frac{y}{x}\left(\frac{Gr_x^*}{5}\right)^{1/5}$, dimensionless

θ dimensionless temperature defined by Eq. (28)

$\theta^{(0)}, \theta^{(1)}$ zero- and first-order temperature of θ, dimensionless

$\theta_X, \theta_Y, \theta_{XX}, \cdots$	$\frac{\partial\theta}{\partial X}, \frac{\partial\theta}{\partial Y}, \frac{\partial^2\theta}{\partial X^2}, \cdots$
$\theta_{oo}(\eta), \theta_m(\eta)$	first-order temperature functions, dimensionless
$\theta_{oo}', \theta_{oo}''$	derivatives of $\theta_{oo}(\eta)$ with respect to η, dimensionless
θ_m', θ_m''	derivatives of $\theta_m(\eta)$ with respect to η, dimensionless
$\bar{\theta}$	dimensionless temperature defined by Eq. (16)
$\bar{\theta}', \bar{\theta}''$	derivatives of $\bar{\theta}(\eta)$ with respect to η, dimensionless
μ	viscosity, M/Lt
ν	kinematic viscosity, $\frac{\mu}{\rho}$, L^2/t
π	3.14159. . .
ρ	density, M/L^3
$\bar{\bar{\tau}}$	shear stress tensor, M/t^2L
ψ	stream function, L^2/t
ψ_x, ψ_y	$\frac{\partial\psi}{\partial x}, \frac{\partial\psi}{\partial y}$
$\bar{\psi}$	dimensionless stream function defined by Eq. (27)
$\bar{\psi}_{\bar{x}}, \bar{\psi}_{\bar{y}}$	$\frac{\partial\bar{\psi}}{\partial\bar{x}}, \frac{\partial\bar{\psi}}{\partial\bar{y}}$
Ψ	transformed dimensionless stream function defined by Eq. (33)
$\Psi^{(0)}, \Psi^{(1)}$	zero- and first-order Ψ, dimensionless
$\Psi_X, \Psi_Y, \Psi_{XY}, \cdots$	$\frac{\partial\Psi}{\partial X}, \frac{\partial\Psi}{\partial Y}, \frac{\partial\Psi}{\partial X\partial Y}, \cdots$

BIBLIOGRAPHY

1. Acrivos, A., "On the Solution of the Convection Equation in Laminar Boundary-layer Flows", Chemical Engineering Science, 17, pp. 457-465 (1962).

2. Bird, R. B., W. E. Stewart, and E. N. Lightfoot, "Transport Phenomena", pp. 297-300 and 330-333, John Wiley, New York (1962).

3. Bottemanne, F. A., "Theoretical Solution of Simultaneously Heat and Mass Transfer by Free Convection about a Vertical Flat Plate", Applied Scientific Research, 25, 1/2, pp. 137-149 (1971).

4. Brodowicz, K., "An Analysis of Laminar Free Convection around Isothermal Vertical Plate", Int. J. Heat Mass Transfer, 11, pp. 201-209 (1968).

5. Chang, B. H., "An Experimental Investigation of Natural Convection in Mercury at Low Grashof Numbers", Master Thesis, Kansas State University (1970).

6. Chang, B. H., and R. G. Akins, "An Experimental Investigation of Natural Convection in Mercury at Low Grashof Numbers", Int. J. Heat Mass Transfer, 15, pp. 513-525 (1972).

7. Chang. K. S., R. G. Akins, and S. G. Bankoff, "Free Convection of a Liquid Metal from a Uniformly Heated Vertical Plate", I & EC Fundamentals, 5, 1, pp. 26-37 (1966).

8. Cheesewright, R., "Natural Convection from a Vertical Plate Surface", Ph. D. Thesis, University of London (1966).

9. Cheesewright, R., "Natural Convection from a Vertical Plate Surface in Non-Isothermal Surroundings", Int. J. Heat Mass Transfer, 10, pp. 1847-1859 (1967).

10. Churchill, S. W., and H. H. S. Chu, "Correlating Equations for Laminar and Turbulent Free Convetion from a Vertical Plate", Int. J. Heat Mass Transfer, 18, 11, pp. 1323-1329 (1975).

11. Churchill, S. W., and H. Ozoe, "A Correlation for Laminar Free Convection from a Vertical Plate", J. Heat Transfer, Trans. ASME, 95, pp.540-541 (1973).

12. Churchill, S. W., and R. Usagi, "A General Expression for the Correlation of Rates of Transfer and Other Phenomena", A.I.Ch.E. Jl., 18, pp. 1121-1128 (1972).

13. Cygan, D. A., and P. D. Richardson, "A Transcendental Approximation for a Natural Convection at Small Prandtl Numbers", Can. J. Chem. Eng., 46 5, p. 321 (1968).

14. Dotson, J. P., "Heat Transfer from a Vertical Plate by Free Convection", Master Thesis, Purdue University (1954).

15. Eckert, E. R. G., and E. Soehngnen, "Studies on Heat Transfer in Laminar Free Convection with the Zehnder-Mach Interferometer", USAF Report 5747 (1948).

16. Eckert, E. R. G., and R. M. Drake, "Heat and Mass Transfer", McGraw-Hill, New York, Second Edition, pp. 311-333 (1959).

17. Eichhorn, R., "Measurement of Low Speed Gas Flows by Particle Trajectories: A New Determination of Free Convection Velocity Profiles", Int. J. Heat Mass Transfer, 5, p. 915 (1962).

18. Eichhorn, R., "Natural Convection in a Thermal Stratified Fluid", Prog. Heat Mass Transfer 2, 41, (1969).

19. Finston, M., "Free Convection past a Vertical Plate", ZAMP, 7, pp. 527-529 (1956).

20. Foote, J. R., "An Asymptotic Method for Free Convection past a Vertical Plate", ZAMP, 9, pp. 64-67 (1958).

21. Fujii, T., "Mathematical Analysis of Heat Transfer from a Vertical Flat Surface by Laminar Free Convection", Bul. of Japan Soc. of Mech. Eng., JSME, 2, 7, pp. 365-369 (1959).

22. Fujii, T., and H. Imura, "Natural-Convection Heat Transfer from a Plate with Arbitrary Inclination", Int. J. Heat Mass Transfer, 15, 4, pp. 755-768 (1972).

23. Gebhart, B., "Effects of Viscous Dissipation in Natural Convection", J. Fluid Mech., 14, pp. 225-232 (1962).

24. Godaux, F., and B. Gebhart, "An Experimental Study of the Transition of Natural Convection Flow Adjacent to a Vertical Surface", Int. J. Heat Mass Transfer, 17, 1, pp. 93-107 (1974).

25. Goldstein, R. J., and E. R. G. Eckert, "The Steady and Transient Free Convection Boundary Layer on a Uniformly Heated Vertical Plate", Int. J. Heat Mass Transfer, 1, 2/3, pp. 208-218 (1960).

26. Goren, S. L., "On Free Convection in Water at $4^{\circ}C$", Chem. Eng. Science, 21, pp. 515-518 (1966).

27. Gryzagoridis, J., "Natural Convection from a Vertical Flat Plate in the Low Grashof Number Range", Int. J. Heat Mass Transfer, 14, pp. 162-165 (1971).

28. Gryzagoridis, J., "Leading Edge Effect on the Nusselt Number for a Vertical Plate in Free Convection", Int. J. Heat Mass Transfer, 16, pp. 517-520 (1973).

29. Gryzagoridis, J., "Combined Free and Forced Convection from an Isothermal Vertical Plate", Int. J. Heat Mass Transfer, 18, 7/8, pp. 911-916 (1975).

30. Hardwick, N. E., and E. K. Levy, "Study of the Laminar Free-Convection Wake above an Isothermal Vertical Plate", J. Heat Transfer, Trans. ASME, 95, pp. 289-294 (1973).

31. Hayday, A. A., D. A. Bowlus, and R. A. McGraw, "Free Convection from a Vertical Flat Plate with Step Discontinuities in Surface Temperature", J. Heat Transfer, Trans. ASME, 89, 8, pp. 244-250 (1967).

32. Hieber, C. A., "Natural Convection around a Semi-Infinite Vertical Plate: Higher-Order Effects", Int. J. Heat Mass Transfer, 17, 7, pp. 785-791 (1974).

33. Julian, D. V., and R. G. Akins, "Experimental Investigation of Natural Convection Heat Transfer to Mercury", I & EC Fundamentals, 8, 4, pp. 641-646 (1969).

34. Kelleher, M., "Free Convection from a Vertical Plate with Discontinuous Wall Temperature", J. Heat Transfer, Trans. ASME, 93, pp. 346-356 (1971).

35. Kelleher, M., and K. T. Yang, "A Gortler-Type Series for Laminar Free Convection along a Non-Isothermal Vertical Plate", Quart. J. Mech. Applied Math., 25, part 4, pp. 447-458 (1972).

36. Kuiken, H. K., "Free Convection at Low Prandtl Numbers", J. Fluid Mech., 37, 4, pp. 785-789 (1969).

37. Kuiken, H. K., "General Series Solution for Free Convection past a Nonisothermal Vertical Flat Plate", Appl. Scient. Res., 20, 2-3, p. 205 (1969).

38. Kuo, Y. H., "On the Flow of an Incompressible Viscous Fluid past a Flat Plate at Moderate Reynolds Numbers", J. Math. Phys., 32, pp. 83-101 (1953).

39. Lienhard, J., R. Eichhorn, and V. Dhir, "Laminar Natural Convection under Uniform Gravity" J. Heat Transfer, Trans. ASME, 94, 1, pp. 80-86 (1972).

40. Lorenz, L., "Ueber das leitungsvermogen der metalle fur Warme und Electricitat", Wiedemanns Annelen, 13, p. 582 (1881).

41. Menold, E. R., and K. T. Yang, "Asymptotic Solutions for Unsteady Laminar Free Convection on a Vertical Plate", J. Appl. Mech., Trans. ASME, E29, pp. 124-126 (1962).

42. Merk, H. J., and J. A. Prins, "Thermal Convection in Laminar Boundary Layers", Appli. Sci. Res., 4, Section A, pp. 11-24 (1954).

43. Niuman, F., and K. Pohlhausen, Remark on the paper by M. Finston: "Free Convection past a Vertical Plate", ZAMP, 9, pp. 67-69 (1958).

44. Nishikawa, K., and R. Ito, "An Analysis of Free Convection Heat Transfer from an Isothermal Vertical Plate to Supercritical Fluids", Int. J. Heat Mass Transfer, 12, pp. 1449-1463 (1969).

45. Ostrach, S., "An Analysis of Laminar Free-Convection Flow and Hear Transfer about a Flat Plate Parallel to the Direction of the Generating Body Force", National Advisory Committee for Aeronautics, Report 1111, pp. 63-79 (1953).

46. Pohlhausen, E., "Der Warmeaustausch Zwischen festen Korpen und Flussigkeiten mit kleiner Reibung und kleiner Warmelietung", ZAMM, 1, pp. 115-121 (1921).

47. Prasad, K. K., and V. Ramanathan, "Heat Transfer by Free Convection from a Longitudinally Vibrating Vertical Plate", Int. J. Heat Mass Transfer, 15, 6, pp. 1213-1224 (1972).

48. Rajan, V. S. V., abd J. J. C. Picot, "Experimental Study of the Laminar Free Convection from a Vertical Plate", Ind. Eng. Chem. Funda., 10, 1, pp. 132-134 (1971).

49. Rich, B. R., "An Investigation of Heat Transfer from an Inclined Flat Plate in Free Convection", Trans. ASME, 75, p.489 (1953).

50. Saunders, O. A., "Natural Convection in Liquids", Proc. Roy. Society (London), A172, pp. 55-71 (1939).

51. Schechter, R. S., and H. S. Isbin, "Natural-Convection Heat Transfer in Regions of Maximum Fluid Density", A.I.Ch.E. Jl., 4, pp. 81-89 (1958).

52. Scherberg, M. G., "Natural Convection near and above Thermal Leading Edge on Vertical Walls", Int. J. Heat Mass Transfer, 5, pp. 1001-1010 (1962).

53. Scherberg, M. G., "Natural Convection at a Thermal Leading Edge on a Vertical Wall", Int. J. Heat Mass Transfer, 8, 10, pp. 1319-1331 (1965).

54. Scherberg, M. G., "Natural Convection from Wall Sections of Arbitrary Distribution by an Integral Method", Int. J. Heat Mass Transfer, 7, pp. 501-516 (1964).

55. Schetz, J. A., and R. Eichhorn, "Natural Convection with Discontinuous Wall Temperature Variations", J. Fluid Mech., 18, p. 167 (1964).

56. Schlichting, H., "Boundary Layer Theory", McGraw-Hill, New York, Fourth Edition, pp. 243-260 (1960).

57. Schmidt, E., and W. Beckmann, "Das Temperatur und Geschwindigkeitsfeld vor eimer Warme Abgebenden Senkrechten Platte bei Naturlicher Konvektion", Tech. Mech. Thermodynamik, Bd. 1, No.10, pp. 341-349 (1930), continued Bd. 1, 11, pp. 391-406 (1930).

58. Schuh, H., "Einige Probleme bei freier Stromung zaher Flussigkeiten", Gottinger Monographien, Bd. B, Grenzschichten (1946).

59. Siegel, R., "Transient Free Convection from a Vertical Flat Plate", Trans. ASME, 80, pp. 347-359 (1958).

60. Soundalgekar, V. M., "Laminar Free Convection Flow of Water at 4°C from a Vertical Plate with Variable Wall Temperature", Chem. Eng. Sci., 28, 1, pp. 307-309 (1973).

61. Sparrow, E. M., "Free Convection with Variable Properties and Variable Wall Temperatures", Ph.D. Thesis, Harvard University (1956).

62. Sparrow, E. M., "Laminar Free Convection on a Vertical Plate with Prescribed Nonuniform Wall Heat Flux or Prescribed Nonuniform Wall Temperature", NACA TN 3508 (1955).

63. Sparrow, E. M., and J. L. Gregg, "Laminar Free Convection from a Vertical Plate with Uniform Surface Heat Flux", Trans ASME, 78, pp. 435-440 (1956).

64. Sparrow, E. M., and J. L. Gregg, "Similar Solutions for Free Convection from a Nonisothermal Vertical Plate", Trans. ASME, 80, pp. 379-386 (1958).

65. Sparrow, E. M., and J. L. Gregg, "The Variable Fluid-Property Problem in Free Convection", Trans. ASME, 80, pp. 879-886 (1958).

66. Sparrow, E. M., F. K. Tsou, and E. F. Kurtz, Jr., "Stability of Laminar Free Convection Flow on a Vertical Plate", Physics Fluids, 8, 8, p. 1559 (1965).

67. Sparrow, E. M., and L. D. F. Guinle, "Deviations from Classical Free Convection Boundary Layer Theory at Low Prandtl Numbers", Int. J. Heat Mass Transfer, 11, 9, p. 1403 (1968).

68. Squire, H. B., in "Modern Developments in Fluid Dynamics", Oxford University Press, London and New York, pp. 638-645 (1938).

69. Squire, H. B., in "Modern Developments in Fluid Dynamics", Oxford University Press, London and New York, p. 641 (1957).

70. Sugawara, S., and I. Michiyoshi, Mem. Fac. Eng. Kyoto University 13, p. 149 (1951).

71. Sugawara, S., and I. Michiyoshi, "Effect of Prandtl Number on Heat Transfer by Natural Convection - The Cases where Prandtl Number is Comparatively Small", Proc. 3rd Japan National Congress for Applied Mechanics (1953).

72. Suriano, F. J., K. T. Yang, and J. A. Donlon, "Laminar Free Convection along a Vertical Plate at Extremely Small Grashof Numbers", Int. J. Heat Mass Transfer, 8, pp. 815-831 (1965).

73. Suriano, F. J., and K. T. Yang, "Laminar Free Convection about Vertical and Horizontal Plates at Small and Moderate Grashof Numbers", Int. J. Heat Mass Transfer, 11, 3, pp. 473-490 (1968).

74. Szewczyk, A. A., "Combined Forced and Free-Convection Laminar Flow", J. Heat Transfer, Trans. ASME, C86, 4, pp. 501-507 (1964).

75. Takhar, H. S., "Free Convection from a Flat Plate", J. Fluid Mech., 34, part 1, pp. 81-89 (1968).

76. Tien, C., "Laminar Natural Convection Heat Transfer from Vertical Plate to Power-Law Fluid", Appl. Sci. Res., 17, pp. 233-248 (1967).

77. Tien, C., and H. S. Tsuei, "Laminar Natural Convection Heat Transfer in Ellis Fluids", Appl. Sci. Res., 20, pp. 131-147 (1969).

78. Tritton, D. J., "Transition to Turbulence in the Free Convection Boundary Layers on an Inclined Heated Plate", J. Fluid Mech., 16, 3, p. 417 (1963).

79. Van Dyke, M., "Perturbation Method in Fluid Mechanics", Academic Press, New York (1964).

80. Vanier, C. R., and C. Tien, "Further Work on Free Convection in Water at 4°C", Chem. Eng. Sci., 22, 12, p. 1747 (1967).

81. Vliet, G. C., "Natural Convection Local Heat Transfer on Constant-Heat-Flux Inclined Surfaces", J. Heat Transfer, Trans. ASME, 91, 11, pp. 511-516 (1969).

82. Von Karman, T., Z. Angew. Math. Mech. 1, p. 233 (1921).

83. Wilks, G., "Combined Forced and Free Convection Flow on Vertical Surfaces", Int. J. Heat Mass Ttansfer, 16, 15, pp. 1958-1964 (1973).

84. Wilks, G., "The Flow of a Uniform Stream over a Semi-Infinite Vertical Flat Plate with Uniform Surface Heat Flux", Int. J. Heat Mass Transfer, 17, 7, pp. 743-753 (1974).

85. Yang, K. T., "Possible Similarity Solutions for Laminar Free Convection on Vertical Plates and Cylinders", J. Appl. Mech., Trans. ASME, E82, pp. 230-236 (1960).

86. Yang, K. T., "Laminar Free-Convection Wake above a Heated Vertical Plate", J. Appl. Mech., Trans. ASME, E31, 1, pp. 131-138 (1964).

87. Yang, K. T., and E. W. Jerger, "First-Order Perturbation of Laminar Free-Convection Boundary Layers on a Vertical Plate", J. Heat Transfer, Trans. ASME, C86, 1, pp. 107-115 (1964).

88. Yang, K. T., J. L. Novotny, and Y. S. Cheng, "Laminar Free Convection from a Nonisothermal Plate Immersed in a Temperature Stratified Medium", Int. J. Heat Mass Transfer, 15, 5, pp. 1097-1110 (1972).

89. Yung, S. C., and R. B. Oetting, "Free Convection Heat Transfer from an Inclined Heated Flat Plate in Air", J. Heat Transfer, Trans. ASME, 91, 2, pp. 192-194 (1969).

ACKNOWLEDGMENTS

The author gratefully expresses her sincere appreciation to:
the major professor, Dr. Richard G. Akins, for his constant guidance and discussions during the whole course of this work;
the members of the supervisory committee, Dr. L. T. Fan and Dr. J. C. Matthews, for their suggestions and comments;
her husband, Te-Yu Chen, for his advice and encouragement in writing this thesis;
and the National Science Fundation for its financial support under Grant Eng-7204086.

APPENDIX A

COMPUTER PROGRAM FOR DATA REDUCTION

```
      DIMENSION DIS(50),T(50),TTI(50),X(100)
 1001 FORMAT(3I10,A10,4F10.6)
01010 FORMAT(A5,I5,I2)
01020 FORMAT(4F10.6,I10)
01040 FORMAT(2F10.6)
01050 FORMAT(1H1,19X,15H RUN WITH WATER,15X,7H NUMBER,A6,35X,I2,2X,I2,2X
     1,I4)
01060 FORMAT(/10X,22H POSITION OF THE PLATE,F8.5,2H CM)
01080 FORMAT(10X,6H POWER,F8.3,6H WATTS,20X,6H SPEED,F4.0,7H MM/SEC)
01090 FORMAT(/10X,22H RAW EXPERIMENTAL DATA,6X,4H TW=,F8.4,3H MV,5X,6H
     1TINF=,F8.4,3H MV)
01100 FORMAT (41X,5H Y MM,18X,5H T MV, 20X,4HT MV)
01110 FORMAT(38X,F8.2,15X,F8.2,15X,F10.6)
01200 FORMAT(/50X,20H PHYSICAL PROPERTIES)
01210 FORMAT(10X,4H TF=,F8.2,2H C,21X,6H BETA=,E12.6,4H 1/C,13X,4H RR=,E
     112.6)
01220 FORMAT( 11X,8HDENSITY=,F12.6,6H GM/CC,8X,5H VIS=,E12.6,10H GM/CM S
     1EC,8X,6H COND=,E12.6,13H CAL/CM SEC C)
01300 FORMAT(/40X,32H CALCULATED EXPERIMENTAL RESULTS)
01310 FORMAT( 10X,4H TW=,F8.4,2H C,8X,6H TINF=,F8.4,2H C,8X,6H DTEM=,
     1F8.4,2H C)
01320 FORMAT(10X,5H GRX=,E12.6,5X,5H GRL=,E12.6,7X,5H ANU=,E12.6)
01330 FORMAT(10X,6H PAR1=,E12.6,4X,6H PAR2=,E12.6,6X,6H PAR3=,E12.6,5X,6
     1H PAR4=,E12.6)
01340 FORMAT( 10X,7H QFLUX=,E12.5,14H CAL/SC.CM.SEC,3X,7H POWER=,F10.4,
     16H WATTS,7X,8H XRATIO=,E12.5)
01350 FORMAT(10X,10H LOG(GRX)=,E12.6,9H LOG(NU)=,E12.5,3X,11H LOG(DTEM)=
     1,F12.5)
01400 FORMAT('-',T6,'DISTANCE FROM',T31,'DIMENSIONLESS',T57,'TEMPERATURE
     1',T82,'TEMPERATURE',T106,'DIMENSIONLESS',/,T8,'PLATE,CM',T34,'DIS
     1TANCE',T60,'DEG. C',T85,'RATIO',T107,'TEMPERATURE')
01410 FORMAT(T7, F9.6,T32,F10.5,T57,F10.6,T82, F9.6,T107, F9.6)
01420 FORMAT(2F10.6)
C       JRUN        RUN NUMBER
C       XX          DISTANCE FROM THE LEADING EDGE, IN
C       VOLT        VOLTAGE BETWEEN THE COPPER RODS
C       CURNT       CURRENT, AMPERE
C       TREF        REFERENCE TEMP OF THERMOCOUPLE, MV
C       TZERO       ZERO SUPRESSION  TEMP OF THE NANOVOLTMETER, MV
C       TW          TEMP AT THE PLATE RELATIVE TO THE ZERO SUPRESSION TEMP, MV
C       TINF1       TEMP AT INFINITE WHEN TOWARD THE PLATE RELATIVE TO THE ZERO, MV
C       TINF2       TEMP AT INFINITE WHEN AWAY FROM THE PLATE, MV
C       N           NUMBER OF DATA POINTS
C       N1          NUMBER OF DATA POINTS TOWARD THE PLATE
C       DIS(J)      LOCAL DISTANCE, MM FROM PLATE
C       T(J)        LOCAL TEMPERATURE, MM FROM ZERO POSITION
C       SPEED       SPEED OF CHART, MM/SEC
C       M           HIGHEST DEGREE POLYNOMIAL SPECIFIED
C       TINF        THE AVERAGE INFINITE TEMP OF TOWARD AND AWAY, MV
  100 READ(5,1001,END=500) MONTH,JDAY,JYEAR,RUN,JRUN,XX,VOLT,CURNT,TREF
      READ(5,1020)TZERO,TW,TINF1,TINF2,N
      READ(5,1040)(DIS(J),T(J),J=1,N)
      SPEED=1.0
      M=2
      XX=XX*2.54
      POWER=VOLT*CURNT
      TW=TW+TZERO+TREF
      TINF1=TINF1+TZERO+TREF
```

THIS BOOK CONTAINS NUMEROUS PAGES THAT ARE CUT OFF

THIS IS AS RECEIVED FROM THE CUSTOMER

```
      TINF2=TINF2+TZERO+TREF
      TINF=(TINF1+TINF2)/2.0
      WRITE(9,1010) RUN,N,M
      WRITE(6,1050) RUN,MONTH,JDAY,JYEAR
      WRITE(6,1060)XX
      WRITE(6,1080)POWER,SPEED
      WRITE(6,1090)TW,TINF
      N1=N/2
      DO 200 J=1, N1
  200 TTI(J)=TINF1+T(J)*(TW-TINF1)/T(1)
      N2=N1+1
      DO 201 J=N2,N
  201 TTI(J)=TINF2+T(J)*(TW-TINF2)/T(N2)
      WRITE(6,1100)
      WRITE(6,1110)(DIS(J),T(J),TTI(J),J=1,N)
C     CALCULATION OF WALL AND INFINITE TEMPERATURES
      A=TW
      TW=.184349E-01+(.259806E+02)*A-.793219*A*A+(.526949E-01)*A*A*A-(.2
     1240068E-02)*(A**4.)
      A=TINF
      TINF=.184349E-01+(.259806E+02)*A-.793219*A*A+(.526949E-01)*A*A*A-(
     1.2240068E-02)*(A**4)
C     REFERENCE TEMPERATURE FOR THE PHYSICAL PROPERTIES
      DTEM=TW-TINF
      TR=TW-.3*DTEM
C     COEFFICIENT OF THERMAL EXPANSION-WATER
      BETA=-(0.58744E-04)+(0.16983E-04)*TR-(0.23491E-06)*TR*TR+(0.26253E
     1-08)*TR*TR*TR-(0.10974E-10)*(TR**4.0)
C     PRANDTL NUMBER-WATER
      PR=(0.12220E+02)-(0.35230*TR)+(0.53521E-02)*TR*TR-(0.41941E-04) *T
     1R*TR*TR+(0.13217E-06)*(TR**4.0)
C     DENSITY-WATER
      RHO=(1.0002E+00)+(0.22345E-04)*TR-(0.66394E-05)*TR*TR+(0.31178E-07
     1)*TR*TR*TR-(0.88772E-10)*(TR**4.0)
C     VICOSITY-WATER
      VIS=1.0/(2.1482*((TR-8.435)+SQRT(3078.4+((TR-8.435)**2.0)))-120.0)
C     THERMAL CONDUCTIVITY-WATER
      COND=(0.1327E-02)+(0.59344E-05)*TR-(0.39312E-07)*TR*TR+(0.10154E-0
     19)*TR*TR*TR
      WRITE(6,1200)
      WRITE(6,1220)PRC,VIS,COND
      WRITE(6,1210)TR,BETA,PR
C     CALCULATION OF X RATIO,HEAT FLUX,GRASHOF NUMBER AND NUSSELT NUMBER
      XR=XX/5.08
      RESIS=(.703682E+02)+(.82593SE-01)*TW-(.751515E-04)*TW*TW
      RP=RESIS*.000197
      RT=VOLT/CURNT
      POWER=POWER*RP/RT
      Q=(POWER*.2390)/51.613
      Q=Q/2.0
      GRX=(980.665*BETA*RHO*RHO*Q*(XX**4))/(COND*VIS*VIS)
      GRL=(653754.4*BETA*RHO*RHO*Q)/(COND*VIS*VIS)
      ANU=(C*XX)/(COND*DTEM)
      WRITE(6,1300)
      WRITE(6,1310)TW,TINF,DTEM
      WRITE(6,1320)GRX,GRL,ANU
C     CALCULATION OF MISC MATERIAL
      AA=(ALOG(GRX))/2.30259
```

```
      AB=(ALOG(ANU))/2.30259
      AC=(ALOG(OTEM))/2.30259
      WRITE(6,1350)AA,AB,AC
C     CALCULATION OF THREE PARAMETERS OF INTEREST
      PAR1=ANU/EXP(.2*ALOG(GRX))
      PAR2=OTEM*EXP(.2*ALOG(GRX))*COND/(Q*XX)
      PAR3=.62*EXP(.2*ALOG(PR*PR*GRX/(.9+PR)))
      PAR4=(Q*XX)/(COND*OTEM)
      WRITE(6,1330)PAR1,PAR2,PAR3,PAR4
      WRITE(6,1340)C,POWER,XR
C     DISTANCE FROM PLATE
      WRITE(6,1400)
      L=N*M
C     TEMPERATURE PROFILE AND THE RATIO
      DO 300 I=L,M
      J=L+I
      DIST=2.54*DIS(I)/(16.*60.)*SPEED
      DDIST=DIST*EXP(.2*ALOG(GRX/5.))/XX
      A=TTI(I)
      TTJ=.184349E-01+(.259806E+02)*A-.793219*A*A+(.526949E-01)*A*A*A-(.
     1224068E-02)*(A**4)
      IF (I.GT.N1) GO TO 400
      TRATO=(TTJ-TINF1)/(TW-TINF1)
      THETA=(TTJ-TINF1)*COND*EXP(.2*ALOG(GRX/5.0))/(Q*XX)
      GO TO 401
  400 TRATO=(TTJ-TINF2)/(TW-TINF2)
      THETA=(TTJ-TINF2)*COND*EXP(.2*ALOG(GRX/5.0))/(Q*XX)
  401 WRITE(6,1410) DIST,DDIST,TTJ,TRATO,THETA
      X(I)=DDIST
      X(J)=TRATO
      WRITE(9,01420)  X(I),X(J)
  300 CONTINUE
      GO TO 100
  500 CONTINUE
      STOP
      END
```

APPENDIX B

COPPER-CONSTANTAN THERMOCOUPLE CALIBRATION

C	DEGREES CENTIGRADE .0	.1	.2	.3	.4	.5	REFERENCE JUNCTION 0 C. .6	.7	.8	.9
					MILLIVOLTS					
0	.0000	.0038	.0076	.0114	.0152	.0190	.0228	.0266	.0304	.0342
1	.0380	.0419	.0458	.0497	.0536	.0575	.0614	.0653	.0692	.0731
2	.0770	.0809	.0848	.0887	.0926	.0965	.1004	.1043	.1082	.1121
3	.1160	.1198	.1236	.1274	.1312	.1350	.1388	.1426	.1464	.1502
4	.1540	.1579	.1618	.1657	.1696	.1735	.1774	.1813	.1852	.1891
5	.1930	.1969	.2008	.2047	.2086	.2125	.2164	.2203	.2242	.2281
6	.2320	.2359	.2398	.2437	.2476	.2515	.2554	.2593	.2632	.2671
7	.2710	.2750	.2790	.2830	.2870	.2910	.2950	.2990	.3030	.3070
8	.3110	.3149	.3188	.3227	.3266	.3305	.3344	.3383	.3422	.3461
9	.3500	.3539	.3578	.3617	.3656	.3695	.3734	.3773	.3812	.3851
10	.3890	.3930	.3970	.4010	.4050	.4090	.4130	.4170	.4210	.4250
11	.4290	.4329	.4368	.4407	.4446	.4485	.4524	.4563	.4602	.4641
12	.4680	.4720	.4760	.4800	.4840	.4880	.4920	.4960	.5000	.5040
13	.5080	.5119	.5158	.5197	.5236	.5275	.5314	.5353	.5392	.5431
14	.5470	.5510	.5550	.5590	.5630	.5670	.5710	.5750	.5790	.5830
15	.5870	.5910	.5950	.5990	.6030	.6070	.6110	.6150	.6190	.6230
16	.6270	.6310	.6350	.6390	.6430	.6470	.6510	.6550	.6590	.6630
17	.6670	.6710	.6750	.6790	.6830	.6870	.6910	.6950	.6990	.7030
18	.7070	.7110	.7150	.7190	.7230	.7270	.7310	.7350	.7390	.7430
19	.7470	.7510	.7550	.7590	.7630	.7670	.7710	.7750	.7790	.7830
20	.7870	.7910	.7950	.7990	.8030	.8070	.8110	.8150	.8190	.8230
21	.8270	.8311	.8352	.8393	.8434	.8475	.8516	.8557	.8598	.8639
22	.8680	.8720	.8760	.8800	.8840	.8880	.8920	.8960	.9000	.9040
23	.9080	.9121	.9162	.9203	.9244	.9285	.9326	.9367	.9408	.9449
24	.9490	.9531	.9572	.9613	.9654	.9695	.9736	.9777	.9818	.9859
25	.9900	.9940	.9980	1.0020	1.0060	1.0100	1.0140	1.0180	1.0220	1.0260
26	1.0300	1.0341	1.0382	1.0423	1.0464	1.0505	1.0546	1.0587	1.0628	1.0669
27	1.0710	1.0751	1.0792	1.0833	1.0874	1.0915	1.0956	1.0997	1.1038	1.1079
28	1.1120	1.1161	1.1202	1.1243	1.1284	1.1325	1.1366	1.1407	1.1448	1.1489
29	1.1530	1.1571	1.1612	1.1653	1.1694	1.1735	1.1776	1.1817	1.1858	1.1899
30	1.1940	1.1981	1.2022	1.2063	1.2104	1.2145	1.2186	1.2227	1.2268	1.2309
31	1.2350	1.2392	1.2434	1.2476	1.2518	1.2560	1.2602	1.2644	1.2686	1.2728
32	1.2770	1.2811	1.2852	1.2893	1.2934	1.2975	1.3016	1.3057	1.3098	1.3139
33	1.3180	1.3222	1.3264	1.3306	1.3348	1.3390	1.3432	1.3474	1.3516	1.3558
34	1.3600	1.3641	1.3682	1.3723	1.3764	1.3805	1.3846	1.3887	1.3928	1.3969
35	1.4010	1.4052	1.4094	1.4136	1.4178	1.4220	1.4262	1.4304	1.4346	1.4388
36	1.4430	1.4472	1.4514	1.4556	1.4598	1.4640	1.4682	1.4724	1.4766	1.4808
37	1.4850	1.4891	1.4932	1.4973	1.5014	1.5055	1.5096	1.5137	1.5178	1.5219
38	1.5260	1.5302	1.5344	1.5386	1.5428	1.5470	1.5512	1.5554	1.5596	1.5638
39	1.5680	1.5722	1.5764	1.5806	1.5848	1.5890	1.5932	1.5974	1.6016	1.6058
40	1.6100	1.6142	1.6184	1.6226	1.6268	1.6310	1.6352	1.6394	1.6436	1.6478
41	1.6520	1.6562	1.6604	1.6646	1.6688	1.6730	1.6772	1.6814	1.6856	1.6898
42	1.6940	1.6983	1.7026	1.7069	1.7112	1.7155	1.7198	1.7241	1.7284	1.7327
43	1.7370	1.7412	1.7454	1.7496	1.7538	1.7580	1.7622	1.7664	1.7706	1.7748
44	1.7790	1.7832	1.7874	1.7916	1.7958	1.8000	1.8042	1.8084	1.8126	1.8168
45	1.8210	1.8253	1.8296	1.8339	1.8382	1.8425	1.8468	1.8511	1.8554	1.8597
46	1.8640	1.8683	1.8726	1.8769	1.8812	1.8855	1.8898	1.8941	1.8984	1.9027
47	1.9070	1.9112	1.9154	1.9196	1.9238	1.9280	1.9322	1.9364	1.9406	1.9448
48	1.9490	1.9533	1.9576	1.9619	1.9662	1.9705	1.9748	1.9791	1.9834	1.9877
49	1.9920	1.9963	2.0006	2.0049	2.0092	2.0135	2.0178	2.0221	2.0264	2.0307
50	2.0350	2.0393	2.0436	2.0479	2.0522	2.0565	2.0608	2.0651	2.0694	2.0737
51	2.0780	2.0823	2.0866	2.0909	2.0952	2.0995	2.1038	2.1081	2.1124	2.1167
52	2.1210	2.1253	2.1296	2.1339	2.1382	2.1425	2.1468	2.1511	2.1554	2.1597
53	2.1640	2.1683	2.1726	2.1769	2.1812	2.1855	2.1898	2.1941	2.1984	2.2027
54	2.2070	2.2113	2.2156	2.2199	2.2242	2.2285	2.2328	2.2371	2.2414	2.2457
55	2.2500	2.2543	2.2586	2.2629	2.2672	2.2715	2.2758	2.2801	2.2844	2.2887
56	2.2930	2.2973	2.3016	2.3059	2.3102	2.3145	2.3188	2.3231	2.3274	2.3317
57	2.3360	2.3404	2.3448	2.3492	2.3536	2.3580	2.3624	2.3668	2.3712	2.3756
58	2.3800	2.3843	2.3886	2.3929	2.3972	2.4015	2.4058	2.4101	2.4144	2.4187
59	2.4230	2.4274	2.4318	2.4362	2.4406	2.4450	2.4494	2.4538	2.4582	2.4626
60	2.4670	2.4714	2.4758	2.4802	2.4846	2.4890	2.4934	2.4978	2.5022	2.5066
61	2.5110	2.5154	2.5198	2.5242	2.5286	2.5330	2.5374	2.5418	2.5462	2.5506
62	2.5550	2.5594	2.5638	2.5682	2.5726	2.5770	2.5814	2.5858	2.5902	2.5946
63	2.5990	2.6034	2.6078	2.6122	2.6166	2.6210	2.6254	2.6298	2.6342	2.6386
64	2.6430	2.6474	2.6518	2.6562	2.6606	2.6650	2.6694	2.6738	2.6782	2.6826
65	2.6870	2.6914	2.6958	2.7002	2.7046	2.7090	2.7134	2.7178	2.7222	2.7266
66	2.7310	2.7354	2.7398	2.7442	2.7486	2.7530	2.7574	2.7618	2.7662	2.7706
67	2.7750	2.7795	2.7840	2.7885	2.7930	2.7975	2.8020	2.8065	2.8110	2.8155
68	2.8200	2.8244	2.8288	2.8332	2.8376	2.8420	2.8464	2.8509	2.8552	2.8596
69	2.8640	2.8684	2.8728	2.8772	2.8816	2.8860	2.8904	2.8948	2.8992	2.9036
70	2.9080	2.9125	2.9170	2.9215	2.9260	2.9305	2.9350	2.9395	2.9440	2.9485
71	2.9530	2.9574	2.9618	2.9662	2.9706	2.9750	2.9794	2.9838	2.9882	2.9926
72	2.9970	3.0015	3.0060	3.0105	3.0150	3.0195	3.0240	3.0285	3.0330	3.0375
73	3.0420	3.0465	3.0510	3.0555	3.0600	3.0645	3.0690	3.0735	3.0780	3.0825
74	3.0870	3.0915	3.0960	3.1005	3.1050	3.1095	3.1140	3.1185	3.1230	3.1275
75	3.1320	3.1365	3.1410	3.1455	3.1500	3.1545	3.1590	3.1635	3.1680	3.1725
76	3.1770	3.1815	3.1860	3.1905	3.1950	3.1995	3.2040	3.2085	3.2130	3.2175
77	3.2220	3.2265	3.2310	3.2355	3.2400	3.2445	3.2490	3.2535	3.2580	3.2625
78	3.2670	3.2715	3.2760	3.2805	3.2850	3.2895	3.2940	3.2985	3.3030	3.3075
79	3.3120	3.3165	3.3210	3.3255	3.3300	3.3345	3.3390	3.3435	3.3480	3.3525
80	3.3570	3.3615	3.3660	3.3705	3.3750	3.3795	3.3840	3.3885	3.3930	3.3975
81	3.4020	3.4066	3.4112	3.4158	3.4204	3.4250	3.4296	3.4342	3.4388	3.4434
82	3.4480	3.4525	3.4570	3.4615	3.4660	3.4705	3.4750	3.4795	3.4840	3.4885
83	3.4930	3.4976	3.5022	3.5068	3.5114	3.5160	3.5206	3.5252	3.5298	3.5344
84	3.5390	3.5435	3.5480	3.5525	3.5570	3.5615	3.5660	3.5705	3.5750	3.5795
85	3.5840	3.5886	3.5932	3.5978	3.6024	3.6070	3.6116	3.6162	3.6208	3.6254
86	3.6300	3.6346	3.6392	3.6438	3.6484	3.6530	3.6576	3.6622	3.6668	3.6714
87	3.6760	3.6806	3.6852	3.6898	3.6944	3.6990	3.7036	3.7082	3.7128	3.7174
88	3.7220	3.7265	3.7310	3.7355	3.7400	3.7445	3.7490	3.7535	3.7580	3.7625
89	3.7670	3.7716	3.7762	3.7808	3.7854	3.7900	3.7946	3.7992	3.8038	3.8084
90	3.8130	3.8176	3.8222	3.8268	3.8314	3.8360	3.8406	3.8452	3.8498	3.8544
91	3.8590	3.8637	3.8684	3.8731	3.8778	3.8825	3.8872	3.8919	3.8966	3.9013
92	3.9060	3.9106	3.9152	3.9198	3.9244	3.9290	3.9336	3.9382	3.9428	3.9474
93	3.9520	3.9566	3.9612	3.9658	3.9704	3.9750	3.9796	3.9842	3.9888	3.9934
94	3.9980	4.0026	4.0072	4.0118	4.0164	4.0210	4.0256	4.0302	4.0348	4.0394
95	4.0440	4.0487	4.0534	4.0581	4.0628	4.0675	4.0722	4.0769	4.0816	4.0863
96	4.0910	4.0957	4.1004	4.1051	4.1098	4.1145	4.1192	4.1239	4.1286	4.1333
97	4.1380	4.1426	4.1472	4.1518	4.1564	4.1610	4.1656	4.1702	4.1748	4.1794
98	4.1840	4.1886	4.1932	4.1978	4.2024	4.2070	4.2116	4.2162	4.2208	4.2254

E.M.F. (millivolts) vs. Temperature (^{o}C) for Copper-Constantan

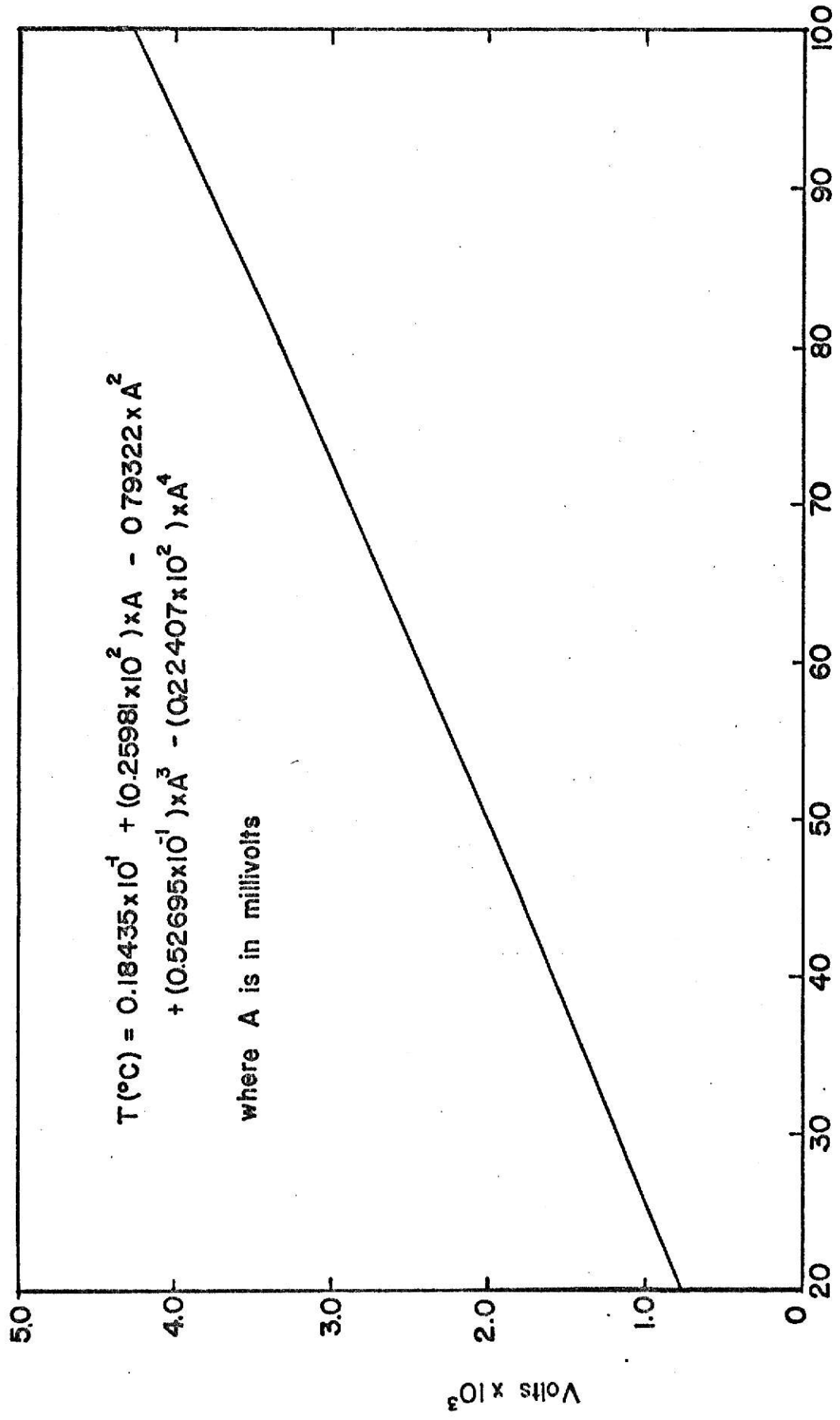


Figure 35. Copper-constantan thermocouple (reference junction 0°C).

APPENDIX C

SAMPLE CALCULATIONS

SAMPLE CALCULATIONS

Run with mercury No. 70 June 7, 1975

Voltage drop across the copper rod = 0.2185 volts

Current: 13.2 amperes

Position up the plate: $\frac{1}{16}$ inches = 0.15875 cm.

Reference temperature of the thermocouple cold junction: 24.38°C
= 0.9645 mV

Zero suppression of the Nanovoltmeter: 0.0042 mV

Temperature of the bulk with respect to the zero suppression of the Nanovoltmeter: 0.0032 mV

Temperature of the plate with respect to the zero suppression of the Nanovoltmeter: 0.0131 mV

Temperature at the plate

T_w(mv) = reference temperature of the thermocouple cold junction + zero suppression of the Nanovoltmeter + temperature at the plate with respect to the zero suppression of the Nanovoltmeter

= 0.9645 + 0.0042 + 0.0131

= 0.9818 mV

T_w(°C) = 24.8093 °C

Temperature at the bulk

T_∞(mV) = reference temperature of the thermocouple cold junction + zero suppression of the Nanovoltmeter + temperature at the plate with respect to the zero suppression of the Nanovoltmeter

= 0.9645 + 0.0042 + 0.0032

= 0.9719 mV

T_∞(°C) = 24.5661 °C

Reference temperature for physical properties

$T_R = 0.7\ T_w + 0.3\ T_\infty$

= 0.7 (24.8093) + 0.3 (24.5661)

= 24.7362 °C

Physical Properties at the reference temperature

Density, ρ	:	13.5342 gm/cm^3
Viscosity, μ	:	0.01525 gm/cm-sec
Prandtl number, Pr	:	0.02413
Thermal Conductivity, k	:	0.02104 cal/cm-sec-°C
Coefficient of thermal expansion, β	:	0.1818 x 10^{-3}/°C

Power dissipated at the plate

Total power dissipated in the equipment (P_T)

$$= \text{(Volts) (Current)}$$

$$= 0.2185 \times 13.2$$

$$= 2.884 \text{ watts}$$

Overall resistance (plate, copper rods, contact, etc.) (R_T)

$$= \frac{\text{Volts}}{\text{Current}}$$

$$= \frac{0.2185}{13.2}$$

$$= 0.01655 \text{ ohms}$$

Resistance of the plate (R_p) $= \dfrac{\text{(Resistivity)(length)}}{\text{area}}$

resistivity of the plate $= 7.2395 \times 10^{-5}$ ohm-cm

length of the plate $= 4 \text{ in} = 10.16 \text{ cm}$

plate cross sectional area $= 2 \text{ in} \times 0.004 \text{ in} \times 2.54^2 \left(\frac{\text{cm}}{\text{in}}\right)^2$

$$= 0.0516 \text{ cm}^2$$

$$R_p = \frac{7.2395 \times 10^{-5} \times 10.16}{0.0516} = 0.014255 \text{ ohms}$$

Power dissipated at the plate $= P_T \times \dfrac{R_p}{R_T}$

$$= 2.884 \times \frac{0.014255}{0.01655}$$

$$= 2.484 \text{ watts (86.13\% of total)}$$

Constant heat flux

Heat flux (q) $= \dfrac{\text{Power dissipated at the plate}}{\text{plate surface area}}$

$$= \frac{2.484 \text{ watts}}{2 \times 2 \times 4 \text{ in}^2} = 0.15525 \text{ watts/in}^2$$

$$= 0.15525 \left(\frac{\text{watts}}{\text{in}^2}\right) \times 492 \left(\frac{\text{Btu/ft}^2\text{-hr}}{\text{watts/in}^2}\right) = 76.38 \frac{\text{Btu}}{\text{ft}^2\text{-hr}}$$

$$= 0.15525 \left(\frac{\text{watts}}{\text{in}^2}\right) \times 0.0371 \left(\frac{\text{cal/cm}^2\text{-sec}}{\text{watts/in}^2}\right) = 0.0576 \frac{\text{cal}}{\text{cm}^2\text{-sec}}$$

Modified Grashof numbers

(1) Based on x

$$Gr_x^* = \frac{g\beta\rho^2 q x^4}{k\mu^2}$$

$$= \frac{980\left(\frac{\text{cm}}{\text{sec}^2}\right) \times 0.1818\times10^{-3}\left(\frac{1}{^\circ\text{C}}\right) \times 13.5342^2\left(\frac{\text{gm}}{\text{cm}^3}\right)^2 \times 0.00576\left(\frac{\text{cal}}{\text{cm}^2\text{-sec}}\right) \times 0.15875^4 (\text{cm})^4}{0.02104\left(\frac{\text{cal}}{\text{cm-sec-}^\circ\text{C}}\right) \times 0.01525^2\left(\frac{\text{gm}}{\text{cm-sec}}\right)^2}$$

$$= 2.558 \times 10^7$$

(2) Based on L

$$Gr_L^* = \frac{g\beta\rho^2 q L^4}{k\mu^2}$$

$$= 8.186 \times 10^{12}$$

Local Nusselt number

$$Nu_x = \frac{h_x x}{k} \quad \text{and} \quad q = h_x (T_w - T_\infty)$$

$$Nu_x = \frac{qx}{k(T_w - T_\infty)}$$

$$= \frac{(0.00575 \text{ cal/cm}^2\text{-sec}) \times (0.15875 \text{ cm})}{(0.02104 \text{ ca/cm-sec-}^\circ\text{C})(24.8093-24.5661)^\circ\text{C}}$$

$$= 0.1784$$

Dimensionless temperature at sample location

Sample location: temperature was 20 mm (chart scale) at a position of 31 mm (chart scale) away from the plate. The plate temperature was equal to 25.3 mm (chart scale). Therefore, by linear interpolation

$$T\ (°C) = T_\infty + \frac{T(mm)}{T_W(mm)}\ (T_W - T_\infty)$$

$$= 24.5661 + \frac{20}{25.3}\ (24.8093 - 24.5661)$$

$$= 24.7584\ °C$$

$$\text{Dimensionless temperature } \theta = \frac{T - T_\infty}{T_W - T_\infty}$$

$$= \frac{24.7584 - 24.5661}{24.8093 - 24.5661}$$

$$= 0.79055$$

Dimensionless distance at sample location

Motor : 2 rev/min

Pitch of screw : $\frac{1}{32}$ inches per turn

Chart speed : 1 mm/sec

$$\text{Factor} = \frac{2\ \text{rev}}{\text{min}} \times \frac{1\ \text{min}}{60\ \text{sec}} \times \frac{2.54\ \text{cm}}{\text{in}} \times \frac{\text{sec}}{1\ \text{mm}}$$

$$= 2.6458 \times 10^{-3}\ \frac{\text{cm}}{\text{mm}}$$

y(cm) = distance from the plate at sample location

$$= 2.6458 \times 10^{-3}\ \frac{\text{cm}}{\text{mm}} \times 31\ \text{mm}$$

$$= 0.08202\ \text{cm}$$

$$\text{Dimensionless distance } \eta = \frac{y}{x}\ \left[\frac{Gr_x^*}{5}\right]^{1/5}$$

$$= \frac{0.08202}{0.15875}\ \left[\frac{2.558 \times 10^7}{5}\right]^{1/5}$$

$$= 0.70923$$

APPENDIX D

COMPUTER PROGRAM FOR CURVE-FITTING

```
C                                                                       PLRG  10
C     ..................................................................PLRG  20
C                                                                       PLRG  30
C        SAMPLE MAIN PROGRAM FOR POLYNOMIAL REGRESSION - POLRG          PLRG  40
C                                                                       PLRG  50
C        PURPOSE                                                        PLRG  60
C           (1) READ THE PROBLEM PARAMETER CARD FOR A POLYNOMIAL REGRES-PLRG  70
C           SION, (2) CALL SUBROUTINES TO PERFORM THE ANALYSIS, (3)     PLRG  80
C           PRINT THE REGRESSION COEFFICIENTS AND ANALYSIS OF VARIANCE  PLRG  90
C           TABLE FOR POLYNOMIALS OF SUCCESSIVELY INCREASING DEGREES,   PLRG 100
C           AND (4) OPTIONALLY PRINT THE TABLE OF RESIDUALS AND A PLOT  PLRG 110
C           OF Y VALUES AND Y ESTIMATES.                                PLRG 120
C                                                                       PLRG 130
C        REMARKS                                                        PLRG 140
C           THE NUMBER OF OBSERVATIONS, N, MUST BE GREATER THAN M+1,    PLRG 150
C           WHERE M IS THE HIGHEST DEGREE POLYNOMIAL SPECIFIED.         PLRG 160
C           IF THERE IS NO REDUCTION IN THE RESIDUAL SUM OF SQUARES     PLRG 170
C           BETWEEN TWO SUCCESSIVE DEGREES OF THE POLYNOMIALS, THE      PLRG 180
C           PROGRAM TERMINATES THE PROBLEM BEFORE COMPLETING THE ANALY- PLRG 190
C           SIS FOR THE HIGHEST DEGREE POLYNOMIAL SPECIFIED.            PLRG 200
C                                                                       PLRG 210
C        SUBROUTINES AND FUNCTION SUBPROGRAMS REQUIRED                  PLRG 220
C           GDATA                                                       PLRG 230
C           ORDER                                                       PLRG 240
C           MINV                                                        PLRG 250
C           MULTR                                                       PLRG 260
C           PLOT   (A SPECIAL PLOT SUBROUTINE PROVIDED FOR THE SAMPLE   PLRG 270
C                  PROGRAM.)                                            PLRG 280
C                                                                       PLRG 290
C        METHOD                                                         PLRG 300
C           REFER TO B. OSTLE, 'STATISTICS IN RESEARCH', THE IOWA STATE PLRG 310
C           COLLEGE PRESS', 1954, CHAPTER 6.                            PLRG 320
C                                                                       PLRG 330
C     ..................................................................PLRG 340
C                                                                       PLRG 350
C     THE FOLLOWING DIMENSION MUST BE GREATER THAN OR EQUAL TO THE      PLRG 360
C     PRODUCT OF N*(M+1), WHERE N IS THE NUMBER OF OBSERVATIONS AND M   PLRG 370
C     IS THE HIGHEST DEGREE POLYNOMIAL SPECIFIED..                      PLRG 380
C                                                                       PLRG 390
C     THE FOLLOWING DIMENSION MUST BE GREATER THAN OR EQUAL TO THE      PLRG 420
C     PRODUCT OF M*M..                                                  PLRG 430
C                                                                       PLRG 440
C     THE FOLLOWING DIMENSION MUST BE GREATER THAN OR EQUAL TO          PLRG 470
C     (M+2)*(M+1)/2..                                                   PLRG 480
C                                                                       PLRG 490
C     Y(I) AND YEST(I) ADDED FOR CALCOM PLOTTING
      DIMENSION X(120),DI(90),D(90),Y(120),YEST(120)
C                                                                       PLRG 510
C     THE FOLLOWING DIMENSIONS MUST BE GREATER THAN OR EQUAL TO M..     PLRG 520
C                                                                       PLRG 530
      DIMENSION B(5),E(5),SP(5),T(5)
C                                                                       PLRG 550
C     THE FOLLOWING DIMENSIONS MUST BE GREATER THAN OR EQUAL TO (M+1).. PLRG 560
C                                                                       PLRG 570
      DIMENSION XBAR(6),STD(6),COE(6),SUMSQ(6),ISAVE(6)
C                                                                       PLRG 590
C     THE FOLLOWING DIMENSION MUST BE GREATER THAN OR EQUAL TO 10..     PLRG 600
C                                                                       PLRG 610
```

```
      DIMENSION ANS(10)
C                                                                       PLRG 630
C     THE FOLLOWING DIMENSION WILL BE USED IF THE PLOT OF OBSERVED DATA PLRG 640
C     AND ESTIMATES IS DESIRED.  THE SIZE OF THE DIMENSION, IN THIS     PLRG 650
C     CASE, MUST BE GREATER THAN OR EQUAL TO N*3.  OTHERWISE, THE SIZE  PLRG 660
C     OF DIMENSION MAY BE SET TO 1.                                     PLRG 670
C                                                                       PLRG 680
      DIMENSION P(90)
C                                                                       PLRG 700
C     .....PLRG 710
C                                                                       PLRG 720
C        IF A DOUBLE PRECISION VERSION OF THIS ROUTINE IS DESIRED, THE  PLRG 730
C        C IN COLUMN 1 SHOULD BE REMOVED FROM THE DOUBLE PRECISION      PLRG 740
C        STATEMENT WHICH FOLLOWS.                                       PLRG 750
C                                                                       PLRG 760
C     DOUBLE PRECISION X,XBAR,STD,D,SUMSQ,DI,E,B,SB,T,ANS,DET,COE       PLRG 770
C                                                                       PLRG 780
C        THE C MUST ALSO BE REMOVED FROM DOUBLE PRECISION STATEMENTS    PLRG 790
C        APPEARING IN OTHER ROUTINES USED IN CONJUNCTION WITH THIS      PLRG 800
C        ROUTINE.                                                       PLRG 810
C                                                                       PLRG 820
C        .....PLRG 830
C                                                                       PLRG 840
    1 FORMAT(I1)                                                        PLRG 850
    2 FORMAT(2F10.4)                                                    PLRG 860
    3 FORMAT(27H1POLYNOMIAL REGRESSION.....,A5//)
    4 FORMAT(23HONUMBER OF OBSERVATIONS,I5//)
    5 FORMAT(32HOPOLYNOMIAL REGRESSION OF DEGREE,I3)                    PLRG 890
    6 FORMAT(12HO  INTERCEPT,E20.7)                                     PLRG 900
    7 FORMAT(26HO  REGRESSION COEFFICIENTS/(6E20.7))                    PLRG 910
    8 FORMAT(1HO/24X,24HANALYSIS OF VARIANCE FOR,I4,19H  DEGREE POLYNOMIPLRG 920
     1AL/)                                                              PLRG 930
    9 FORMAT(1HO,5X,19HSOURCE OF VARIATION,7X,9HDEGREE OF,7X,6HSUM OF,9XPLRG 940
     1,4HMEAN,10X,1HF,9X,20HIMPROVEMENT IN TERMS/33X,7HFREEDOM,8X,7HSQUAPLRG 950
     2RES,7X,6HSQUARE,7X,5HVALUE,8X,17HOF SUM OF SQUARES)               PLRG 960
   10 FORMAT(20HO  DUE TO REGRESSION,12X,I6,F17.5,F14.5,F13.5,F20.5)    PLRG 970
   11 FORMAT(32H   DEVIATION ABOUT REGRESSION   ,I6,F17.5,F14.5)        PLRG 980
   12 FORMAT(8X,5HTOTAL,19X,I6,F17.5///)                                PLRG 990
   13 FORMAT(17HO  NO IMPROVEMENT)                                      PLRG1000
   14 FORMAT(1HO//27X,18HTABLE OF RESIDUALS//16H OBSERVATION NO.,5X,7HX PLRG1010
     1VALUE,7X,7HY VALUE,7X,10HY ESTIMATE,7X,8HRESIDUAL/)               PLRG1020
   15 FORMAT(1HO,3X,I6,F18.5,F14.5,F17.5,F15.5)                         PLRG1030
   16 FORMAT(A5,I5,I2)
C                                                                       PLRG1040
C     .....PLRG1050
C                                                                       PLRG1060
C     READ PROBLEM PARAMETER CARD                                       PLRG1070
C                                                                       PLRG1080
  100 READ(5,1,END=99) NPLOT
      READ(9,16) RUN,N,M
C                                                                       PLRG1100
C        N.....NUMBER OF OBSERVATIONS                                   PLRG1130
C        M.....HIGHEST DEGREE POLYNOMIAL SPECIFIED                      PLRG1140
C        NPLOT.OPTION CODE FOR PLOTTING                                 PLRG1150
C              0  IF PLOT IS NOT DESIRED.                               PLRG1160
C              1  IF PLOT IS DESIRED.                                   PLRG1170
C                                                                       PLRG1180
C     PRINT PROBLEM NUMBER AND N.                                       PLRG1190
```

```
C                                                                       PLRG1200
      WRITE (6,3) RUN
      WRITE (6,4) N                                                     PLRG1220
C                                                                       PLRG1230
C        RUN...PROBLEM NUMBER (MAY BE ALPHAMERIC)                       PLRG1110
C     READ INPUT DATA                                                   PLRG1240
C                                                                       PLRG1250
      L=N*M                                                             PLRG1260
      DO 110 I=1,N                                                      PLRG1270
      J=L+I                                                             PLRG1280
C                                                                       PLRG1290
C        X(I) IS THE INDEPENDENT VARIABLE, AND X(J) IS THE DEPENDENT    PLRG1300
C        VARIABLE.                                                      PLRG1310
C                                                                       PLRG1320
      READ (9,2) X(I),X(J)                                              PLRG1330
C    THE NEXT CARD WAS ADDED TO GIVE A POLYNOMIAL FIT OF THE FORM
C    LOG(X(I))=POLY(X(I))
  110 X(J)=ALOG10(X(J))
C                                                                       PLRG1340
      CALL CDATA (N,M,X,XBAR,STD,D,SUMSQ)                               PLRG1350
C                                                                       PLRG1360
      MM=M+1                                                            PLRG1370
      SUM=0.0                                                           PLRG1380
      NT=N-1                                                            PLRG1390
C                                                                       PLRG1400
      DO 200 I=1,M                                                      PLRG1410
      ISAVE(I)=I                                                        PLRG1420
C                                                                       PLRG1430
C     FORM SUBSET OF CORRELATION COEFFICIENT MATRIX                     PLRG1440
C                                                                       PLRG1450
      CALL ORDER (MM,D,MM,I,ISAVE,DI,E)                                 PLRG1460
C                                                                       PLRG1470
C     INVERT THE SUBMATRIX OF CORRELATION COEFFICIENTS                  PLRG1480
C                                                                       PLRG1490
      CALL MINV (DI,I,DET,B,T)                                          PLRG1500
C                                                                       PLRG1510
      CALL MULTR (N,I,XBAR,STD,SUMSQ,DI,E,ISAVE,D,SR,T,ANS)             PLRG1520
C                                                                       PLRG1530
C     PRINT THE RESULT OF CALCULATION                                   PLRG1540
C                                                                       PLRG1550
      WRITE (6,5) I                                                     PLRG1560
      IF(ANS(7)) 140,130,130                                            PLRG1570
  130 SUMIP=ANS(4)-SUM                                                  PLRG1580
      IF(SUMIP) 140, 140, 150                                           PLRG1590
  140 WRITE (6,13)                                                      PLRG1600
      GO TO 210                                                         PLRG1610
  150 WRITE (6,6) ANS(1)                                                PLRG1620
      WRITE (6,7) (B(J),J=1,I)                                          PLRG1630
      WRITE (6,8) I                                                     PLRG1640
      WRITE (6,9)                                                       PLRG1650
      SUM=ANS(4)                                                        PLRG1660
      WRITE (6,10) I,ANS(4),ANS(6),ANS(10),SUMIP                        PLRG1670
      NI=ANS(8)                                                         PLRG1680
      WRITE (6,11) NI,ANS(7),ANS(9)                                     PLRG1690
      WRITE (6,12) NT,SUMSQ(MM)                                         PLRG1700
C                                                                       PLRG1710
C     SAVE COEFFICIENTS FOR CALCULATION OF Y ESTIMATES                  PLRG1720
C                                                                       PLRG1730
```

```
      COE(1)=ANS(1)                                                    PLRG1740
      DO 160 J=1,I                                                     PLRG1750
  160 COE(J+1)=B(J)                                                    PLRG1760
      LA=I                                                             PLRG1770
  200 CONTINUE                                                         PLRG1780
C                                                                      PLRG1790
C     TEST WHETHER PLOT IS DESIRED                                     PLRG1800
C                                                                      PLRG1810
  210 IF(NPLOT) 100, 100, 220                                          PLRG1820
C                                                                      PLRG1830
C        CALCULATE ESTIMATES                                           PLRG1840
C                                                                      PLRG1850
  220 NP3=N+N                                                          PLRG1860
      DO 230 I=1,N                                                     PLRG1870
      NP3=NP3+1                                                        PLRG1880
      P(NP3)=COE(1)                                                    PLRG1890
      L=I                                                              PLRG1900
      DO 230 J=1,LA                                                    PLRG1910
      P(NP3)=P(NP3)+X(L)*COE(J+1)                                      PLRG1920
  230 L=L+N                                                            PLRG1930
C                                                                      PLRG1940
C        COPY OBSERVED DATA                                            PLRG1950
C                                                                      PLRG1960
      N2=N                                                             PLRG1970
      L=N*M                                                            PLRG1980
      DO 240 I=1,N                                                     PLRG1990
      P(I)=X(I)                                                        PLRG2000
      N2=N2+1                                                          PLRG2010
      L=L+1                                                            PLRG2020
  240 P(N2)=X(L)                                                       PLRG2030
C                                                                      PLRG2040
C     PRINT TABLE OF RESIDUALS                                         PLRG2050
C                                                                      PLRG2060
      WRITE (6,3) RUN                                                  PLRG2070
      WRITE (6,5) LA                                                   PLRG2080
      WRITE (6,14)                                                     PLRG2090
      NP2=N                                                            PLRG2100
      NP3=N+N                                                          PLRG2110
      DO 250 I=1,N                                                     PLRG2120
      NP2=NP2+1                                                        PLRG2130
      NP3=NP3+1                                                        PLRG2140
C  THE FOLLOWING TWO CARDS WERE ADDED SO THAT LOG(X(I)) WOULDN'T PRINT
      P(NP2)=10.**P(NP2)
      P(NP3)=10.**P(NP3)
      RESID=P(NP2)-P(NP3)                                              PLRG2150
C  THE FOLLOWING ARE ADDED TO PRODUCE THE ARRAYS NEEDED FOR THE CALCOM
      X(I)=P(I)*4.
      Y(I)=P(NP2)*(-10.)
      YEST(I)=P(NP3)*(-10.)
C
  250 WRITE (6,15) I,P(I),P(NP2),P(NP3),RESID                          PLRG2160
C                                                                      PLRG2170
C    FOR COMPUTER PLOT, ADD THE FOLLOWING HERE
C     CALL PLOT     (LA,P,N,3,0,1)
C     GO TO 100                                                        PLRG2200
C  99 STOP
C  THESE CARDS ARE ADDED FOR COMPUTER PLOT BECAUSE 'PLOT' HAS BEEN
C    CHANGED TO 'PLOTSUB'. PRINTING SHIFTED FROM CC1 TO CC10 FOR COMMENT
```

```
C          //LKED.CC DD DSN=SYS1.FORTRAN.SSP,DISP=SHR
C           CHANGE  PLOTSUB(PLOT)
C           INCLUDE DD(PLOTSUB)
C          //GO.FT13F001 DD UNIT=SYSDA,DCB=(RECFM=VBS,LRECL=200,BLKSIZE=200),
C          // SPACE=(TRK,(1,1))
C                                                                      PLRG2190
      DIMENSION IBUF(8000)
C  THE FOLLOWING 13 CARDS ARE ALLOWAY'S SIMPLE SORTING ROUTINE
C  THIS IS FOR SORTING THE X(I) INTO ASSENDING ORDER
      DO 400 I=1,NT
      K = I + 1
      DO 400 J=K,N
      IF (X(I).LT.X(J)) GOTO 400
      A=X(I)
      X(I)=X(J)
      X(J)=A
      A=Y(I)
      Y(I)=Y(J)
      Y(J)=A
      A=YEST(I)
      YEST(I)=YEST(J)
      YEST(J)=A
400   CONTINUE
C
      CALL PLOTS (IBUF,8000)
      CALL PLOT (0.,-11.,3)
      CALL PLOT (12.,-10.0,-3)
C  DEFINE NEW ORIGIN AT 1  INCHES FROM BOTTOM, 12 INCHES ALONG
C   DRAW AND LABEL X AXIS
      CALL DAXIS (0.,0.,3.,90.,.4,+5)
      CALL SAXIS(0.,.5,1,1,-5,'DIMENSIONLESS DISTANCE',-22)
C    DRAW AND LABEL Y AXIS
      CALL DAXIS (0.,0.,10.5,180.,.5,-2)
      CALL SAXIS(0.,.1,1,3,2,'DIMENSIONLESS TEMPERATURE',-25)
C   PRINT LEDGEND WITH RUN NUMBER
      CALL SYMBOL(-10.,3.,.14,'TEMPERATURE PROFILE FOR',90.,23)
      CALL SYMBOL(-9.5,3.,.14,'LAMINAR NATURAL CONVECTION',90.,26)
      CALL SYMBOL(-9.0,3.,.14,'IN WATER, RUN NO.',90.,17)
      CALL SYMBOL(999.,999.,.14,PR,90.,4)
      CALL SYMBOL(999.,999.,.14,'/',90.,1)
      CALL SYMBOL (999.,999.,.14,PR1,90.,2)
C   PLOT DATA POINTS
      DO 300 I=1,N
300   CALL SYMBOL (Y(I),X(I),.07,4,90.,-1)
C  MOVE TO FIRST POINT OF LINE WITH PEN UP
      CALL PLOT (YEST(1),X(1),3)
C   PLOT LEAST-SQUARES LINE
      DO 301 I=2,N
301   CALL PLOT (YEST(I),X(I),2)
C   MOVE 1  INCHES FOR NEXT PLOT
      CALL PLOT (1.0,0.,-3)
      GO TO 100
99    CALL PLOT(0.,0.,999)
      STOP
      END                                                              PLRG2210
```

EXPERIMENTAL INVESTIGATIONS OF NATURAL CONVECTION BOTH IN WATER AND IN MERCURY AT EXTREMELY LOW GRASHOF NUMBERS

by

SHU-CHEN YU

B. S., National Taiwan University, 1973

AN ABSTRACT OF A MASTER'S THESIS

submitted in partial fulfillment of the

requirements for the degree

MASTER OF SCIENCE

Department of Chemical Engineering

KANSAS STATE UNIVERSITY

Manhattan, Kansas

1976

Abstract

Laminar free convection from a uniformly heated vertical flat plate was investigated experimentally in very low Grashof number range both for water and mercury ($10^{-1} < Gr_x^* < 10^5$), the Prandtl numbers are about 7 and 0.03, respectively. The temperature profiles for the two fluids were measured with a copper-constantan thermocouple. The results are shown graphically in dimensionless plots, and are compared with the boundary layer solution, perturbation solution, and other experimental results. The experimental results show that the boundary layer thickness for mercury, which has the higher thermal conductivity (or low Prandtl number), was much thicker than that for water, the temperature profiles for mercury deviated considerably from the boundary layer solution, and the deviations were depedent upon the modified Grashof number and the vertical distance on the plate. These phenomena agreed, in general, well with previous experimental results, but were contrary to perturbation solutions.

VITA

Shu-Chen Yu, daughter of Mr. Yen-Chung Yu and Mrs. Wan-An King Yu, was born on July 19, 1951, in Taiwan.

With an excellent grade graduating from Chunghua girl's high school, she entered National Taiwan University in September 1969. In four-year's college education, she had been one of the top students in the class and obtained many honors and scholarships. In June 1973, she graduated with a Bachelor of Science Degree in Chemical Engineering.

Right after graduating from college, she came to the United States to continue her studies at Kansas State University and received the degree of Master of Science in Chemical Engineering in April 1976.

She was married to Mr. Te-Yu Chen in December 1974. Her husband is presently a candidate for the degree of Doctor of Philosophy also in Chemical Engineering.